

*The Moon Beyond 2002:
Next Steps in Lunar Science
and Exploration*

Taos, New Mexico
September 12-14, 2002

Abstract Volume



LPI

LPI Contribution No. 1128

The Moon Beyond 2002: Next Steps in Lunar Science and Exploration

September 12–14, 2002

Taos, New Mexico

Sponsors

Los Alamos National Laboratory
The University of California Institute of Geophysics and Planetary Physics (IGPP)
Los Alamos Center for Space Sciences and Exploration
Lunar and Planetary Institute

Meeting Organizer

David J. Lawrence (*Los Alamos National Laboratory*)

Scientific Organizing Committee

Mike Duke (*Colorado School of Mines*)
Sarah Dunkin (*Rutherford Appleton Laboratory*)
Rick Elphic (*Los Alamos National Laboratory*)
B. Ray Hawke (*University of Hawai'i*)
Lon Hood (*University of Arizona*)
Brad Jolliff (*Washington University*)
David Lawrence (*Los Alamos National Laboratory*)
Chip Schearer (*University of New Mexico*)
Harrison Schmitt (*University of Wisconsin*)

Lunar and Planetary Institute 3600 Bay Area Boulevard Houston TX 77058-1113

LPI Contribution No. 1128

Compiled in 2002 by
LUNAR AND PLANETARY INSTITUTE

The Institute is operated by the Universities Space Research Association under Contract No. NASW-4574 with the National Aeronautics and Space Administration.

Material in this volume may be copied without restraint for library, abstract service, education, or personal research purposes; however, republication of any paper or portion thereof requires the written permission of the authors as well as the appropriate acknowledgment of this publication.

Abstracts in this volume may be cited as

Author A. B. (2002) Title of abstract. In *The Moon Beyond 2002: Next Steps in Lunar Science and Exploration*, p. XX. LPI Contribution No. 1128, Lunar and Planetary Institute, Houston.

This volume is distributed by

ORDER DEPARTMENT
Lunar and Planetary Institute
3600 Bay Area Boulevard
Houston TX 77058-1113, USA
Phone: 281-486-2172
Fax: 281-486-2186
E-mail: order@lpi.usra.edu

Mail order requestors will be invoiced for the cost of shipping and handling.

ISSN No. 0161-5297

Preface

This volume contains abstracts that have been accepted for presentation at the conference on **The Moon Beyond 2002: Next Steps in Lunar Science and Exploration**, September 12–14, 2002, in Taos, New Mexico.

Administration and publications support for this meeting were provided by the staff of the **Publications and Program Services Departments** at the **Lunar and Planetary Institute**.

Contents

Lunar Geodetic Missions in SELENE (2005–2006) and SELENE2 <i>H. Araki, K. Matsumoto, K. Heki, H. Hanada, and N. Kawano</i>	1
The Moon: A Repository for Ancient Planetary Samples <i>J. C. Armstrong, L. E. Wells, M. E. Kress, and G. Gonzalez</i>	2
Admittance Computations from Lunar Gravity and Topography Data <i>S. W. Asmar and G. Schubert</i>	3
Sensitivity of Lunar Resource Economic Model to Lunar Ice Concentration <i>B. R. Blair and J. Diaz</i>	4
Permanent Shadow in Lunar Simple Craters <i>D. B. J. Bussey, M. S. Robinson, K. Edwards, P. D. Spudis, P. G. Lucey, and D. Steutel</i>	5
Volatiles at the Poles of the Moon <i>B. J. Butler</i>	6
A New Moon: Improved Lunar Orbiter Mosaics <i>C. J. Byrne</i>	7
Constraining the Material that Formed the Moon: The Origin of Lunar V, Cr, and Mn Depletions <i>N. L. Chabot and C. B. Agee</i>	8
New Approaches for Exploration Beyond Low Earth Orbit <i>D. R. Cooke</i>	9
Modeling the Stability of Volatile Deposits in Lunar Cold Traps <i>D. H. Crider and R. R. Vondrak</i>	10
Lunar Solar Power System and Lunar Exploration <i>D. R. Criswell</i>	11
Human Exploration of the Moon <i>M. B. Duke</i>	12
Sample Return from South Pole-Aitken Basin <i>M. B. Duke</i>	13

Contribution of Ion Sputtering to the Production of Na and K in the Lunar Atmosphere <i>C. A. Dukes and R. A. Baragiola</i>	14
Remote Sensing of Titanium in Mare Basalt Soils: Will the Real TiO ₂ Please Stand Up? <i>R. C. Elphic, D. J. Lawrence, T. H. Prettyman, W. C. Feldman, D. T. Vaniman, O. Gasnault, S. Maurice, J. J. Gillis, B. L. Jolliff, and P. G. Lucey</i>	15
North West Africa 773 (NWA773): Ar-Ar Studies of Breccia and Cumulate Lithologies <i>V. A. Fernandes, R. Burgess, and G. Turner</i>	16
Applying Strategic Visualization® to Lunar and Planetary Mission Design <i>J. R. Frassanito and D. R. Cooke</i>	17
An Analysis of Remotely Sensed Data of Mare Australe <i>J. J. Gillis and B. L. Jolliff</i>	18
Using Small Basaltic Lunar Clasts to Reconstruct the Early Magmatic History of the Moon <i>J. J. Hagerty, C. K. Shearer, and J. J. Papike</i>	19
Constraints on the Origin of Lunar Crustal Magnetism <i>J. S. Halekas, D. L. Mitchell, R. P. Lin, and L. L. Hood</i>	20
Expected Data by Lunar Imager/SpectroMeter (LISM) <i>J. Haruyama, M. Ohtake, T. Matsunaga, N. Hirata, H. Demura, R. Nakamura, and LISM Working Group</i>	21
Lunar Highlands Volcanism: The View from a New Millenium <i>B. R. Hawke, D. J. Lawrence, D. T. Blewett, P. G. Lucey, G. A. Smith, G. J. Taylor, and P. D. Spudis</i>	22
The Moon: Keystone to Understanding Planetary Geological Processes and History <i>J. W. Head III</i>	23
Ages, Thicknesses and Mineralogy of Lunar Mare Basalts <i>H. Hiesinger, J. W. Head III, U. Wolf, R. Jaumann, and G. Neukum</i>	24
Radar Speckle Displacement Interferometry to Study Moon's Polar Axis Behaviour in the Sky <i>I. V. Holin</i>	25
Next Steps in Understanding Lunar Paleomagnetism and Related Issues <i>L. L. Hood and N. C. Richmond</i>	26
Modeling the Degradation of Small Lunar Impact Craters: An Example Using a DEM <i>D. M. Hooper</i>	27

Global Lunar Gravity Mapping Using SELENE Sub-Satellites <i>T. Iwata, H. Hanada, N. Kawano, T. Takano, and N. Namiki</i>	28
Lunar Crustal and Bulk Composition: Th and Al Mass Balance <i>B. L. Jolliff and J. J. Gillis</i>	29
Systematics of Chromium and Titanium in Olivine from Lunar Mare Basalts Compared to Basalts from the Earth and Mars <i>J. M. Karner, J. J. Papike, and C. K. Shearer</i>	30
On the Age of the Nectaris Basin <i>R. L. Korotev, J. J. Gillis, L. A. Haskin, and B. L. Jolliff</i>	31
Identifying Locations for Future Lunar Sample Missions <i>D. J. Lawrence, R. C. Elphic, W. C. Feldman, O. Gasnault, T. H. Prettyman, and D. T. Vaniman</i>	32
Lunar Surface Outgassing and Alpha Particle Measurements <i>S. L. Lawson, W. C. Feldman, D. J. Lawrence, K. R. Moore, R. C. Elphic, S. Maurice, R. D. Belian, and A. B. Binder</i>	33
Anomalous Fading of Stimulated Luminescence (TL/OSL): Comparisons Between Lunar Materials and the JSC Mars-1 Simulant <i>K. Lepper</i>	34
Polar Night: A Mission to the Lunar Poles <i>P. G. Lucey</i>	35
A Complete First Order Model of the Near-Infrared Spectral Reflectance of the Moon <i>P. G. Lucey and D. Steutel</i>	36
Search for Correlations Between Crustal Magnetic Fields and Other Lunar Properties <i>D. L. Mitchell, J. S. Halekas, R. P. Lin, S. Frey, and L. L. Hood</i>	37
Mission Outline of Lunar-A <i>H. Mizutani, A. Fujimura, S. Tanaka, H. Shiraishi, S. Yoshida, and T. Nakajima</i>	38
Scientific Research in SELENE Mission <i>H. Mizutani, S. Sasaki, Y. Iijima, K. Tanaka, M. Kato, and Y. Takizawa</i>	39
Using the New Views of the Moon Initiative to Define Future Missions: The Lunar Seismic Network <i>C. R. Neal</i>	40

Siderophile Elements in Lunar Impact Melts: Implications for the Cataclysm, Impactor Sources, and Early Earth Environments <i>M. D. Norman and V. C. Bennett</i>	41
Crystallization Age and Impact Resetting of Ancient Lunar Crust from the Descartes Terrane <i>M. D. Norman, L. E. Borg, L. E. Nyquist, and D. D. Bogard</i>	42
DoD Technologies and Capabilities of Relevance to Future Lunar Science and Exploration Objectives <i>S. Nozette and S. P. Worden</i>	43
Capability and Data Analyses of the Multiband Imager for the SELENE Mission <i>M. Ohtake and H. Demura</i>	44
On Search and Identification of Super Heavy ($Z=110-114$) and Super Super Heavy ($Z\geq 160$) Cosmic Ray Nuclei Tracks in the Moon Olivine Crystals <i>V. P. Pereygin, I. G. Abdullaev, Yu. V. Bondar, Yu. T. Chuburkov, R. L. Fleischer, L. I. Kravets, and L. L. Kashkarov</i>	45
Compositional Units on the Moon: The Role of South Pole-Aitken Basin <i>C. A. Peterson, B. R. Hawke, D. T. Blewett, D. B. J. Bussey, P. G. Lucey, G. J. Taylor, and P. D. Spudis</i>	46
Reconstructing the Stratigraphy of the Ancient South Pole-Aitken Basin Interior <i>N. E. Petro and C. M. Pieters</i>	47
Lunar Science Missions in Context of the Decadal Solar System Exploration Survey <i>C. M. Pieters, M. Bullock, R. Greeley, B. Jolliff, A. Sprague, and E. Stofan</i>	48
Classification of Regolith Materials from Lunar Prospector Data Reveals a Magnesium-rich Highland Province <i>T. H. Prettyman, D. J. Lawrence, D. T. Vaniman, R. C. Elphic, and W. C. Feldman</i>	49
Did the Moon Come from the Impactor? Siderophile Element Constraints <i>K. Righter</i>	50
Topographic-Photometric Corrections Applied to Clementine Spectral Reflectance Data of the Apollo 17 Region <i>M. S. Robinson and B. L. Jolliff</i>	51
Lunar Radar Cross Section at Low Frequency <i>P. Rodriguez, E. J. Kennedy, P. Kossey, M. McCarrick, M. L. Kaiser, J.-L. Bougeret, and Yu. V. Tokarev</i>	52

A Miniature Mineralogical Instrument for In-Situ Characterization of Ices and Hydrated Minerals at the Lunar Poles <i>P. Sarrazin, D. Blake, D. Vaniman, D. Bish, S. Chipera, and S. A. Collins</i>	53
Future Lunar Sampling Missions. Big Returns on Small Samples <i>C. K. Shearer, J. J. Papike, and L. Borg</i>	54
An Imaging Laser Altimeter for Lunar Scientific Exploration <i>D. E. Smith, M. T. Zuber, and J. J. Degnan</i>	55
Searching for Antipodal Basin Ejecta on the Moon <i>P. D. Spudis and B. Fessler</i>	56
Lunar Core Dynamo Driven by Thermochemical Mantle Convection <i>D. R. Stegman, A. M. Jellinek, S. A. Zatman J. R. Baumgardner, and M. A. Richards</i>	57
Efficient Material Mapping Using Clementine Multispectral Data <i>D. Steutel, P. G. Lucey, M. E. Winter, and S. LeMouelic</i>	58
Call for Cooperation Between Lunar Scientists and Astronomers: Proposing Lunar Science Missions to Enable Astronomy from the Moon <i>Y. D. Takahashi</i>	59
Lunar Prospecting <i>G. J. Taylor and L. M. V. Martel</i>	60
Bulk Composition of the Moon: Importance, Uncertainties, and What We Need to Know <i>G. J. Taylor, B. R. Hawke, and P. D. Spudis</i>	61
Origin of Nanophase Fe ⁰ in Agglutinates: A Radical New Concept <i>L. A. Taylor</i>	62
Contoured Data from Lunar Prospector Indicate a Major Role for Minor Samples <i>D. T. Vaniman, T. H. Prettyman, D. J. Lawrence, R. C. Elphic, and W. C. Feldman</i>	63
Study Towards Human Aided Construction of Large Lunar Telescopes <i>P. J. van Susante</i>	64
A Manned Lunar Base for Determining the Three-Dimensional Make-Up of a Lunar Mare <i>J. L. Whitford-Stark</i>	65

Regolith Thickness, Distribution, and Processes Examined at Sub-Meter Resolution <i>B. B. Wilcox, M. S. Robinson, and P. C. Thomas</i>	66
Current and Future Lunar Science from Laser Ranging <i>J. G. Williams, D. H. Boggs, J. T. Ratcliff, J. O. Dickey, and T. W. Murphy</i>	67
Grand Observatory <i>E. W. Young</i>	68

Lunar geodetic missions in SELENE (2005-2006) and SELENE2. H. Araki, K. Matsumoto, K. Heki, H. Hanada, and N. Kawano. National Astronomical Observatory, Mizusawa, Iwate, 023-4501 (email arakih@miz.nao.ac.jp).

Introduction: Selenological and Engineering Explorer (SELENE) is to be launched in 2005 from Japan with the nominal mission period of one year. The main orbiter, with a circular/polar orbit as high as 100 km, is equipped with various instruments including a laser altimeter (LALT). Two subsatellites, with higher orbits, have very long baseline interferometry (VLBI) radio transmitters for three-dimensional tracking (VRAD), and Doppler signal relay equipments to enable direct farside gravimetry by high-low satellite-to-satellite radio tracking (RSAT). Details of the SELENE-B and SELENE2, two follow-on projects of SELENE, have not been determined yet, and we are proposing a polar telescope/PZT type optical telescope for accurate in-situ lunar orientation measurements (IOM).

SELENE: SELENE, to be launched in 2005 summer using an H-IIA launch vehicle, has three missions related to lunar geodesy, namely LALT for laser altimetry and RSAT/VRAD for lunar gravimetry:

Laser Altimetry. LALT, a laser range instrument [1], is one of fourteen instruments aboard the SELENE lunar orbiter. Its scientific objectives are, determination of global lunar figure, construction of precise topographic data base of the entire lunar surface including the polar region (much better accuracy/coverage than the Clementine LIDAR). The proto-type model of LALT, assembled in December 2000, passed various environmental tests, and its design refinement and manufacture of the flight model will be completed by the end of June 2003.

Two characteristics of lunar global figure, that is, the centers of mass/figure offset of about 2km, and triaxiality with elongation approximately toward the Earth, are the keys to clarify lunar origin, tidal evolution, and internal structure. In addition to this, selenocentric height determinations would also contribute to the refinement of the selenodetic control point network. Information on smaller scale topographic features, combined with lunar gravity data, is important in constraining lithospheric thickness, and lunar thermal evolution. Precise and accurate topographic mapping of the lunar polar region will have a crucial significance for the lunar ice deposit investigation.

Lunar Gravimetry. The lunar gravity field is one of the keys to research the lunar origin. Its lowest degree/order components will constrain the size and/or density of the core together with lunar libration data. Combining higher degree/order gravity coefficients with altimeter data provides information on lunar tectonics and thermal history. In spite of past lunar ex-

plorations, gravity field of the farside has never been measured directly. This situation will be overcome by employing a free-flying satellite (RSAT) that relays Doppler signals from the main orbiter on the lunar farside [2]. The data will mainly contribute to the improvement in the high-degree gravity coefficients, but an order of magnitude improvement in the low-degree gravity coefficients is also anticipated. Three-dimensional tracking of the two free-flying satellites with differential VLBI will improve the gravity field determination [3] especially near the lunar limb where line-of-sight gravity components do not provide much information on the mass distribution.

SELENE2: Luni-solar tidal torques for the Earth with an inclined spin axis let the axis change its direction with various periods (forced nutation). The motion of surface fluids such as ocean and atmosphere excites the Earth's free polar motion (Chandler wobble). Amplitudes and phases of these variations provide valuable information on the Earth's interior. Likewise, the Moon has physical (free and forced) libration, and their measurements are important to know the physical status of lunar core and lower mantle. In the lunar exploration project after the SELENE, soft landing onto the lunar surface is planned. We are proposing the IOM project [4], a lunar polar lander equipped with an optical telescope with diameter of 20 cm and focal length of 2 m. It is designed to enable accurate measurement of lunar rotational variation by analyzing the star trajectories associated with the lunar spin. This will greatly improve our knowledge of the lunar physical libration obtained by past lunar laser ranging (LLR) observations [5], and provide important information on the lunar interior.

References: [1] Araki H. et al. (1999) *Adv. Space Res.*, 23, 1813-1816. [2] Matsumoto K. et al. (1999) *Adv. Space Res.*, 23, 1809-1812. [3] Heki, K. et al. (1999) *Adv. Space Res.*, 23, 1821-1824. [4] Hanada, H. et al., (2000) *Proc. 22nd ISTS*, 1609-1614. [5] Dickey, J. et al. (1994) *Science*, 265, 482-490.

THE MOON: A REPOSITORY FOR ANCIENT PLANETARY SAMPLES. John C. Armstrong, Llyd E. Wells, Monika Kress, *Center for Astrobiology and Early Evolution, University of Washington, Box 351580, Seattle WA 98195, USA, (jca@astro.washington.edu)*, Guillermo Gonzalez, *Department of Physics and Astronomy, Iowa State University, Ames IA 50011-3160, USA.*

Searching the Moon for the Remains of Early Planetary Surfaces

The frequency of both lunar and Martian meteorites on the Earth indicates that the transfer of planetary material is common in the solar system. However, vigorous hydrologic or tectonic cycles, past or present, prevent most nearby planetary bodies from serving as long-term repositories of this material. The Moon is an important exception. Strategically located within the inner solar system, the Moon has theoretically collected material from all of the terrestrial planets since its formation. Lacking an atmosphere and widespread, long-lasting volcanism, the Moon has potentially preserved meteorites from Mercury through the asteroid belt. While the lack of an atmosphere prevents a soft landing on the lunar surface, its low gravity means objects with small velocities with respect to the Moon will experience relatively low impact velocities. Moreover, unlike on other terrestrial planets, Martian, Venusian and Terran meteorites, blasted off their respective planets 3.9 Ga during the late heavy bombardment, should still exist on the surface of the Moon.

Such meteorites are likely to contain uniquely preserved remains of these planets that are not available elsewhere in the Solar System. In particular, terran meteorites on the Moon may provide a substantive geological record for ancient Earth, corresponding to or predating the period for which the earliest evidence for life exists. The only attainable record of Venus' early surface geology, otherwise catastrophically erased 700 million years ago [1], is probably on the Moon. Similarly, a record of the type, characteristics and origins of the heavy bombardment impactors themselves may be available on the Moon. Such a record would clarify not only the geological history of Earth, but also its chemical and biological history – especially since these impactors were potentially major sources of biotic precursors on early Earth [2]. Mars is presently the focus of the search for early signs of life outside Earth. Ironically, the Moon may be the better place to search for the remains of both early Martian and early Terran life. The Moon is also a perfect testbed for targeted sample return.

Terran meteorites have the potential to extend and broaden Earth's geologic record for a time period that has otherwise left little or no physical evidence. The rocks' elemental composition and mineralogy (in particular, hydration) could be used to constrain characteristics of the early crust and mantle, the global oxidation state, the extent of planetary differentiation, and the availability of water. Volatile inclusions sampling noble gases, carbon dioxide and molecular nitrogen could clarify atmospheric origin and evolution and, along with the meteorite mineralogy, could provide substantive constraints on early atmospheric concentrations. Direct measurement of the timing, extent and planetary effects of the heavy bombardment by careful dating of Terran meteorites is also possible and would perhaps be the most robust and significant scientific reward of this project. In addition to the scientific benefits listed above,

which alone justify searching the Moon for Terran meteorites, a fraction of Earth-derived material on the Moon should contain geochemical and biological information, in the form of isotopic signatures, organic carbon, molecular fossils, biominerals or even, theoretically, microbial fossils. Terran meteorites should be examined for potentially novel evidence concerning early Earth life. Such evidence could substantiate or extend Earth's fossil record from 3.9 Ga to 3.5 Ga.

In a recent study [3], we find, for a well mixed regolith, that the median surface abundance of Terran material is roughly 7 ppm, corresponding to a mass of approximately 20,000 kg of Terran material over a 10x10 square km area. Over the same area, the amount of material transferred from Venus and Mars is 1 kg and 170 kg, respectively. The amount of Terran material is substantial, and we are embarking on an effort to identify and propose methods for retrieving it. In particular, probing existing stocks of Apollo lunar fines for hydrated, nickel-poor silicate grains may be the first step in proving the concept of this search. This will also provide necessary ground truth in our effort to distinguish terran material on the Moon.

Recovery and identification of Terran samples from the Moon represents a significant challenge. Still, returning a sample from the Moon bearing the remains of Earth life may be orders of magnitude easier than returning, say, Martian samples from Mars bearing the remains of Martian life. In this sense, lunar missions represent an interesting proving ground for these types of endeavors. The risk of contamination and relative scarcity of Terran material makes sample return missions difficult. Therefore, robotic missions need to be developed capable of finding Terran material, and advanced in-situ measuring devices will help identify such samples and largely drive the analysis on the Moon. We suggest using a rover to search near fresh craters for recently excavated material. In addition to searching for planetary meteorites, such a mission would provide the perfect vehicle for a number of other important lunar science instruments.

References

- [1] McKinnon, W. B., K. J. Zahnle, B. A. Ivanov, and H. J. Melosh 1997. Cratering on Venus: Models and Observations. in *Venus II*, edited by S. W. Bougher, D. M. Houten, and R. J. Phillips, University of Arizona Press, Tuscon, pp. 969-1014.
- [2] Pierazzo, E., and C. Chyba 1999. Amino acid survival in large cometary impacts. *Meteoritics and Planetary Science*, 34, 909-918.
- [3] Armstrong, John C., Llyd E. Wells, Guillermo Gonzalez 2002. Rummaging through Earth's attic for the remains of ancient life. *Submitted to Icarus*

ADMITTANCE COMPUTATIONS FROM LUNAR GRAVITY AND TOPOGRAPHY DATA. S. Asmar¹ and G. Schubert¹, ¹Department of Earth and Space Sciences, University of California, Los Angeles (SAsmar@ucla.edu).

The admittance transfer function, calculated from the gravity and topography data in the spectral domain, can be used to compute the elastic thickness of a terrestrial planet, the effective thickness of the part of the lithosphere that can support elastic stresses over long time scales. This has been applied extensively in recent years to Venus and Mars due to new datasets. The general form of the admittance at a wavenumber k ($k = \frac{2\pi}{\lambda}$, λ is the wavelength) is given by McKenzie (1994):

$$Z(k) = \frac{3g(\rho_c - \rho_w)}{2a\rho_p} \exp(-kz) \left[1 - \exp(-kt_c) \left(1 + \frac{ET_c^3 k^4}{2(1-\sigma^2)(\rho_m - \rho_c)g} \right)^{-1} \right]$$

where g is the gravitational acceleration at the surface, ρ_c is the density of the crust, ρ_w the density of the overlying fluid, ρ_m the density of the upper mantle, E Young's modulus and σ Poisson's ratio for the elastic layer of thickness T_c , z the height of the surface where the gravity measurements are made, t_c the mean crustal thickness, a is the radius of the planet and ρ_p its mean radius. Recent updates to the historical data set of lunar gravity from the Lunar Prospector data provides for a very rich dataset (Konopliv et al., 2001). Lunar topography from the Clementine lidar was augmented by radio occultations in the polar regions to provide a global field (Asmar and Schubert 2002). In the Cartesian Admittance approach, regions of interest on the moon, such as South Pole Aitken, are identified as rectangular section for the purpose of computations based on gravity data derived from either the spherical harmonic expansion of the line-of-sight accelerations.

The computations require assumptions about the properties of the moon and various signal processing techniques of windowing the data, to which the results are highly sensitive. Comparisons of these parameters will be presented along with applicable results. Geophysical interpretations will also be presented of the elastic thickness for selected regions of the moon.

References:

- [1] McKenzie, D. (1994) *Icarus*, 112, 55–88
- [2] Konopliv, A. S., S. W. Asmar, E. Carranza, D. N. Yuan, and W. L. Sjogren, (2001) *Icarus*, 150, 1–18.
- [3] Asmar, S., G. Schubert, W. Moore, A. Konopliv, D. Smith, & M. Zuber (2000) *EOS Trans. AGU* 81 (48), Fall Meet Suppl., Abstract G71A-04.
- [4] Asmar, S and G. Schubert, In Heather D. J. (ed) *New Views of the Moon, Europe: Future Lunar Exploration, Science Objectives, and Integration of Datasets*. ESTEC RSSD, Noordwijk.

SENSITIVITY OF LUNAR RESOURCE ECONOMIC MODEL TO LUNAR ICE CONCENTRATION Brad Blair¹ and Javier Diaz¹, ¹Colorado School of Mines, 1500 Illinois St., Golden, CO 80401, bblair@mines.edu

Lunar Prospector mission data [1] indicates sufficient concentration of hydrogen (presumed to be in the form of water ice) to form the basis for lunar *in-situ* mining activities to provide a source of propellant for near-Earth and solar system transport missions. A model being developed by JPL, Colorado School of Mines, and CSP, Inc. generates the necessary conditions under which a *commercial enterprise* could earn a sufficient rate of return to develop and operate a LEO propellant service for government and commercial customers. A combination of Lunar-derived propellants, L-1 staging, and orbital fuel depots could make commercial LEO/GEO development, inter-planetary missions and the human exploration and development of space more energy, cost, and mass efficient.

This paper presents preliminary model results for a commercial lunar-based propellant service, examining sensitivity of the model to ice concentration. The lunar Prospector results suggest an average ice concentration of 1.5%, but allow an interpretation that concentrations of as much as 10% exist [1]. While a profitable scenario may be possible at 1% ice concentrations, these variations can have a very large effect on the profitability of a lunar propellant production system. As concentrations rise, the amount of extraction and processing

equipment required on the Moon diminish and the time between initiation of the project and full production can be reduced. These physical changes in the architecture lead also to changes in the financial model. The results provide a strong incentive for lunar polar exploration to provide information both on typical occurrences of lunar ice as well as areas in which elevated concentrations may occur.

Acknowledgment: This work is supported by Contract #1237006 from the Jet Propulsion Laboratory to the Colorado School of Mines, M. Duke, Principal Investigator.

References:

- [1] Feldman W. C., Maurice S., Lawrence D. J., Little R. C., Lawson S. Gasnault L. O., Wiens R. C., Barraclough B. L., Elphic R. C., Prettyman T. H., Steinberg J. T., and Binder A. B. (2001) Evidence for Water Ice Near the Lunar Poles, *J. Geophys. Res., Planets*, 106, #E10, 23232 – 23252.

PERMANENT SHADOW IN LUNAR SIMPLE CRATERS. D. B. J. Bussey¹, M. S. Robinson², K. Edwards³, P. D. Spudis⁴, P. G. Lucey¹, and D. Steutel¹ ¹Hawaii Institute of Geophysics and Planetology, University of Hawaii at Manoa, 2525 Correa Road, Honolulu HI 96822 (bussey@higp.hawaii.edu), ²Northwestern University, Loy Hall 309, 1847 Sheridan Road, Evanston IL 60208, ³Q&D Programmers, PO Box 1002, Hearne, TX 77859, ⁴Lunar and Planetary Institute, 3600 Bay Area Blvd., Houston TX 77058,

Introduction: Simulation of illumination conditions for idealized simple lunar craters has increased our knowledge of the size and extent of permanently shadowed areas. We have conducted a comprehensive study of how the amount of permanent shadow in a simple crater varies as a function of crater size, location, and with season. We have used these results to determine the amount of permanent shadow, cold traps for water molecules, inside all fresh simple lunar craters between 1 and 20 km in size. These maps of permanent shadow provide more information on the locale of possible ice deposits.

Simulations: Key lunar simple crater quantities have been parameterized as a function of crater diameter [1]. Simple crater parameters (such as depth, rim height, flat floor diameter etc) can be expressed in the form $a=D^b$ where 'a' is a crater parameter, 'D' is crater diameter, and 'b' is a known constant. We have used this parameterization to produce digital elevation models (DEMs) of idealized simple craters. Simulation of illumination conditions for these craters permits the investigation of all possible illumination conditions, not just those for which images exist. We have conducted a comprehensive study [2] of simple craters 2.5 to 20 km in size, located from 70° to 90°. Seasonal variations have also been studied. Our results show that crater latitude is the dominant parameter in determining the amount of permanent shadow in a crater. Craters as far out as 20° from the pole can still have significant amounts (~27% for 20 km craters) of permanent shadow. At constant latitude, large craters have a slightly higher proportion of their interiors shaded than smaller craters, this effect is more pronounced at lower latitudes. Seasonal effects are independent of both crater size and location, the amount of darkness during a day in winter versus summer differs by about 15% of the crater area.

Darkness Maps: Results from the simulation study has permitted the production of an equation that predicts the amount of permanent shadow in a crater, given the diameter and latitude [3]. This equation has been used to produce maps of permanent shadow in simple craters in the polar regions.

North Pole. A detailed analysis of all fresh looking simple craters larger than 1 km within 12° of the pole was undertaken. The total number of craters mapped was 832. These craters have a total surface area of approximately 12,500 km² representing roughly 3% of the lunar surface poleward of 78°. The estimated amount of permanent shadow associated with these craters is 7500 km². This compares with previous estimates of 530 km² [4] & 2650 km² [5]. Our value of 7500 km² is a lower limit for the total amount of permanent shadow as it only represents shadow in simple craters between 1 and 20 km in diameter. The contribution of poleward facing walls of complex craters will also add large amounts of area to the overall permanent shadow budget. Additionally the highland area approximately defined by the boundaries 88-90°N, 90-180°W appears to contain copious

small shadowed areas that may be permanently shadowed [6].

South pole. A detailed analysis of all fresh looking simple craters larger than 1 km, within 12° of the pole identified 547 craters. These craters have a total area of 11,200 km² which represents just under 3% of the total lunar surface south of 78° S. The estimated amount of permanent shadow associated with these craters is 6500 km². This compares with 3300 km² [6], and 5100 km² [5]. As was stated for the north pole above, this number is a lower limit as it only reflects shadow in simple craters 1 to 20 km in diameter. A number of complex craters in the 20 – 35 km diameter range exist in the south polar that are likely to have large amounts of permanent shadow. Additionally for the south polar region, the combination of lack of image coverage together with the fact that it was winter in the southern hemisphere when the data were collected means that significant amounts of the surface are either in shadow or not imaged. These unimaged regions contain craters that have permanent shadow.

Conclusions: Illumination simulations of topography can greatly increase our knowledge of the amount and location of permanently shadowed regions near the pole. We have shown that latitude, rather than diameter, is the dominant parameter in determining the amount of permanent shadow in a simple crater. Craters as far out as 20° from a pole still contain significant amounts (22-27 %) of permanent shadow. An analysis of fresh simple craters in both polar regions produced new lower limits for the amount of permanent shadow, 7500 km² for the north pole and 6500 km² for the south pole, which represent significant increases compared to previous estimates. In addition to being large in total area, permanent shadowed regions are widely distributed and copious in number. There are therefore many potential cold traps, distributed over a large area, that could harbor water ice.

References: [1] Pike R. J. (1977) *Impact and Explosion Cratering*, 489-509., [2] Bussey D. B. J. et al., (2002) *LPSC XXXIII*, Abs. # 1819, [3] Bussey D. B. J. et al., (2002) *GRL* submitted, [4] Nozette S. et al., (1996) *Science*, 274, 1495-1498, [5] Margot J. L. et al., (1999) *Science*, 284, 1658-1660, [6] Vasavada A. R. et al., (1999) *Icarus*, 141, 179-193., [7] Bussey D. B. J. et al., (1999) *GRL*, 26, 1187-1190.

VOLATILES AT THE POLES OF THE MOON. B. J. Butler, *NRAO, Socorro NM 87801, USA, (bbutler@nrao.edu).*

Researchers in the early 1960's concluded that water ice could survive in permanently shaded regions in the lunar polar regions [1]. Results from the Apollo missions indicated that the lunar rock and soil samples were extremely dessicated, however, casting doubt on the possibility [2]. Later studies seemed to either support the idea or not [3], but no conclusive evidence was found either way.

In the summer of 1991, new radar maps of the surface of Mercury showed features in the polar regions which seemed to indicate the presence of large amounts of water ice, reinvigorating the discussion of water ice in the polar regions of the Moon [4]. Recent modelling has shown that there should be sufficient supply of water to the lunar surface, that transport should be efficient enough to form the deposits, and that the temperatures are low enough to keep the water ice stable [5]. So it certainly seems possible that water ice deposits could exist in the permanently shaded craters in the polar regions of the Moon.

High resolution radar images of the lunar polar regions were obtained in May and August of 1992 to try to address this question [6]. The Arecibo telescope was used in a manner similar to that used to obtain the Mercury images, and radar maps of the two polar regions were obtained, with a resolution of about 125 m. Detailed examination of these maps showed no regions similar to those seen on Mercury. Another result from this experiment was that it was much more likely that any such deposits, if they existed, would be located in the south polar regions rather than the north polar regions, because the amount of permanently shadowed terrain is much larger in the south than in the north. A similar conclusion was reached by examining images from the Clementine spacecraft. By combining together all of the photographs of the north and south polar regions, it could be seen which regions were never illuminated during the time in which the photos were taken. It was clear from these photos that there is much more area in the south polar region which remains in perpetual shadow than in the north polar region [7]. Subsequent studies have confirmed and more accurately quantified this result, showing that there is about twice as much permanently shadowed terrain in the south polar regions as in the north [8].

In April of 1994, the Clementine spacecraft was used to try to detect polar water ice deposits directly. During seven of its orbits, the transmitting antenna on the spacecraft was directed toward the polar regions, and the resulting reflected signal was received at one of the 70-m DSN antennas here on Earth. During one of the orbits which passed over the south pole, the data showed a signature which is vaguely similar to the polarization inversion seen in the Mercury radar data. This was interpreted as the signature of a small deposit of water ice (100-400 km²) [7]. However, detailed reanalysis of that data has shown that it does not support the existence of a water ice deposit, making the data consistent with the Earth-based radar data [9].

The Lunar Prospector mission, launched in 1998, was the next to provide insight into this issue. Prospector carried neutron and gamma ray spectrometers, allowing for the detection of excess hydrogen in the near surface (to a depth of roughly 50 cm). Indeed, the polar regions exhibited enhanced [H], which was roughly correlated with the positions of craters (and hence shadowed terrain) [10]. The amount of excess [H] is relatively small, however - if it were all in the form of water, it would be ~ 1.5% by mass in the south polar regions, and ~ 10% by mass in the north polar regions (though this second estimate is extremely uncertain because the features in the north were not resolved individually by the spectrometer [10]). There is still no conclusive evidence to indicate that this excess [H] signature is actually due to water ice, and, in fact, it has been argued that the excess [H] can be supplied solely by the solar wind [11]. In addition, it has recently been argued that water ice cannot migrate effectively to the polar cold traps, and hence should be an insignificant constituent in any polar volatile deposits [12].

While it is possible to find out more about these polar "deposits" on both the Moon via Earth-based observations, observations from spacecraft (and possibly landers/rovers) will really be needed to conclusively show what they are. There are currently three planned missions to the Moon: an ESA (European Space Agency) mission: SMART-1, scheduled for launch early in 2003; and two ISAS (Institute of Space and Astronautical Science of Japan) missions: LUNAR-A, scheduled for launch in 2003; and SELENE, scheduled for launch in 2004 (a joint mission with NASDA - National Space Development Agency of Japan). These three missions, while not explicitly designed to answer questions about the polar deposits, will certainly return data that will help constrain the possibilities regarding their composition. For example, LUNAR-A will carry heat probes which will help to measure the heat flow from the interior of the Moon - an important parameter in the models which determine the temperatures in the shaded polar craters.

[1] Watson et al. 1961, *JGR*, 66, 1598; Watson et al. 1961, *JGR*, 66, 3033; Pohn et al. 1962, *PASP*, 74, 93. [2] Estep et al. 1972, *PLPSC III*, 3047; Taylor et al. 1995, *LPSC XXVI*, 1399. [3] Arnold 1979, *JGR*, 84, 5659. Lanzerotti et al. 1981, *JGR*, 86, 3949; Hodges 1991, *GRL*, 18, 2113; Morgan and Shemansky 1991, *JGR*, 96, 1351. [4] Butler et al. 1993, *JGR*, 98, 15003; Harmon et al. 1994, 2001, *Nature*, 369, 213. [5] Butler 1997, *JGR*, 102, 19283; Moses et al. 1999, *Icarus*, 137, 197. Vasavada et al. 1999, *Icarus*, 141, 179. [6] Stacy et al. 1997, *Science*, 276, 1527. [7] Nozette et al. 1996, *Science*, 274, 1495. [8] Margot et al. 1999, *Science*, 284, 1658; Cook et al. 2000, *JGR*, 105, 12023; Bussey et al. 2002, *LPSC XXXIII*, 1819. [9] Simpson & Tyler 1999, *JGR*, 104, 3845. [10] Feldman et al. 2000, *JGR*, 105, 4175; Feldman et al. 2001, *JGR*, 106, 23231. [11] Starukhina & Shkuratov 2000, *Icarus*, 147, 585; Crider & Vondrak 2001, *JGR*, 105, 26773. [12] Hodges 2002, *JGR*, 107, 6-1.

A New Moon: Improved Lunar Orbiter Mosaics. Charles J. Byrne, Image Again, Middletown, New Jersey; cibyrene@monmouth.com.

Introduction: Photographs of the five Lunar Orbiter missions in 1965 and 1966 provide comprehensive coverage of the moon at resolutions in the range of about 1 meter to 300 meters. With a few exceptions, they are taken at a moderately low sun angle to clearly show the topography. These photos, especially the set edited by Bowker and Hughes [1], are still in active use in books, papers, and slide presentations and they are likely to be used in planning the missions of future lunar spacecraft. Scanning artifacts (sometimes called the "venetian blind effect") detract from the visual quality of the photographs, particularly when they are printed at high contrast to show albedo variations such as rays or subtle topology features such as the margins of lava flows. The author has written a program [2] to estimate and remove the artifacts from the pictures, greatly improving their cosmetic quality. The program detects lines between framelets of a mosaic, removes the lines caused by light leaking between framelets, estimates the systematic streaks caused by cathode ray tube scanning in the spacecraft and the Ground Reconstruction Equipment, and compensates for these streaks. Non-linearity introduced by contrast enhancement in the production of the input photos is considered in the compensation process. A comparison of a mosaic before and after processing is shown in Figure 1. Further information on the process is provided in Reference [2].

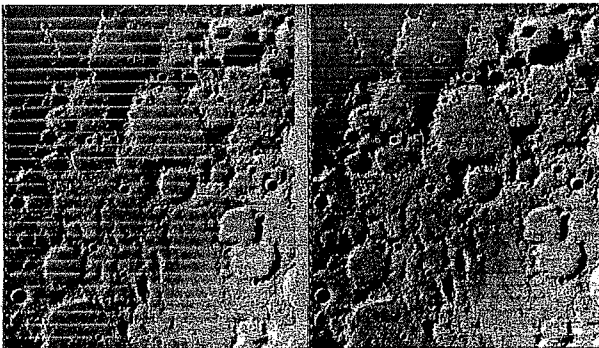


Figure 1: Lunar Orbiter subframe LO4-140H3 before and after processing.

Status of Processing: Currently, the photos being processed are selected from those of Bowker and Hughes [1]. The photos were digitized by staff of the Lunar and Planetary Institute with consultation and further processing by Jeff Gillis [3]. The processed photos from Lunar Orbiter missions 1, 2, 3, and 5 have

been provided to LPI for use in an annotated atlas, for release on electronic media. In the majority of cases, the images are strongly improved by processing.

Process Improvements: Experience in processing the pictures has led to improvements in the program and its operation. Some of these improvements increase the likelihood of successfully finding framelet edges, while others compensate for secondary artifacts; those that are only seen clearly after the primary artifacts are removed. For example, a feature has been added to compensate for an alternating pattern of darker and lighter framelets in some of the images. A spectral analysis program has been written to compare the spectra of the input and output images to provide a quantitative measure of improvement. Figure 2 shows the fine-scale normalized vertical spectral density of LO4-140H3 before and after processing.

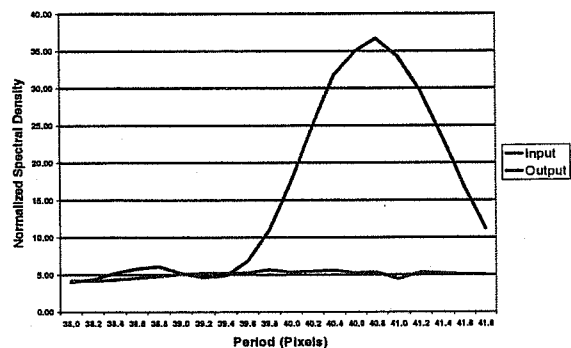


Figure 2: Spectral density of LO4-140H3 for periods near the framelet width (about 40 Pixels).

Future Plans: The author plans to complete the processing of digitized Lunar Orbiter 4 photographs. These photos form an extensive and orderly survey, primarily of the near side of the moon. Initial experiments indicate that the relative uniformity of the processed images can be used to produce larger mosaics of good quality.

References: [1] D. E. Bowker and J. K. Hughes (1971), *Lunar Orbiter Photographic Atlas of the Moon*, NASA SP 206. [2] C. J. Byrne (2002), *LPS XXXIII*, Abstract #1099, Lunar and Planetary Institute, Houston (CDROM). [3] J. Gillis (ed.), *Digital Lunar Orbiter Photographic Atlas of the Moon*, www.lpi.usra.edu/research/lunarorbiter, Lunar and Planetary Institute.

CONSTRAINING THE MATERIAL THAT FORMED THE MOON: THE ORIGIN OF LUNAR V, CR, AND MN DEPLETIONS. N. L. Chabot¹ and C. B. Agee², ¹Case Western Reserve University, Department of Geological Sciences, 112 A. W. Smith Bldg., Cleveland, OH, 44106-7216, USA, nlc9@po.cwru.edu, ²Institute of Meteoritics, Department of Earth and Planetary Sciences, University of New Mexico, Albuquerque, NM 87131, agee@unm.edu.

The mantles of the Earth and Moon are similarly depleted in V, Cr, and Mn relative to chondritic values [1, 2]. Core formation deep within the Earth was suggested by [1] as the origin of the depletions. Following Earth's core formation, the Moon was proposed to have inherited its mantle from the depleted mantle of the Earth by a giant impact event [3, 4]. This theory implied the Moon was primarily composed of material from the Earth's mantle.

Recent systematic metal-silicate experiments of V, Cr, and Mn evaluated the behavior of these elements during different core formation scenarios [5]. The study found that the V, Cr, and Mn depletions in the Earth could indeed be explained by core formation. The conditions of core formation necessary to deplete V, Cr, and Mn in the Earth's mantle were consistent with the deep magma ocean proposed to account for the Earth's mantle abundances of Ni and Co [6, 7].

Using the parameterizations of [5] for the metal-silicate partition coefficients (D) of V, Cr, and Mn, we investigate here the conditions needed to match the depletions in the silicate Moon and determine if such conditions could have been present on the giant impactor. Using a silicate composition consistent with the Moon and assuming a metallic core about 30% of the body with 6 wt% S and 3 wt% C, different core formation scenarios for the impactor were modeled. Figure 1 shows the modeling results, which indicate a high temperature (>3300 K) and reducing conditions ($IW < -2$) can match the lunar depletions of V and Cr, and nearly match the lunar depletion of Mn. The partitioning behavior of all three elements was not found to be significantly dependent on pressure [5], and thus, the core formation conditions from V, Cr, and Mn do not constrain the size of the planetary body.

These modeling results imply that the depletions of V, Cr, and Mn in the Moon are not necessarily inherited from the Earth but could have been inherited from the impacting body. Current estimates of the mass of the impactor place it at about two-thirds of an Earth mass [8], large enough to have formed a core at the hot and reducing conditions required in Fig. 1. Further, this result is consistent with recent modeling of the giant impact event, which suggests the majority of the material which formed the Moon was from the impacting body, not the proto-Earth [8].

This work was supported by NASA grants 344-31-20-25 to CBA and NAG5-11122 to R. P. Harvey.

References: [1] Ringwood A. E. (1966) *In Advances in Earth Science*, P. Hurley, Ed., MIT Press, Boston, 357-398. [2] Dreibus G. and Wanke H. (1979) *Lunar Planet. Sci.* 10, 315-317. [3] Ringwood A. E. (1986) *Nature* 322, 323-328. [4] Wanke H. and Dreibus G. (1986) *In Origin of the Moon*, W. K. Hartmann, R. J.

Phillips, G. J. Taylor, Eds., LPI, Houston, 649-672. [5] Chabot N. L. and Agee C. B. (2002) *GCA*, submitted. [6] Li J. and Agee C. B. (2001) *GCA* 65, 1821-1832. [7] Chabot N. L. and Agee C. B. (2002) *LPSC* 33, #1009. [8] Cameron A. G. W. (2000) *In Origin of the Earth and Moon*, R. M. Canup, K. Righter, Eds., U. of A. Press, Tucson, 133-144. [9] Walter M. J., Newsom H. E., Ertel W., and Holzheid A. (2000) *In Origin of the Earth and Moon*, R. M. Canup, K. Righter, Eds., U. of A. Press, Tucson, 265-289.

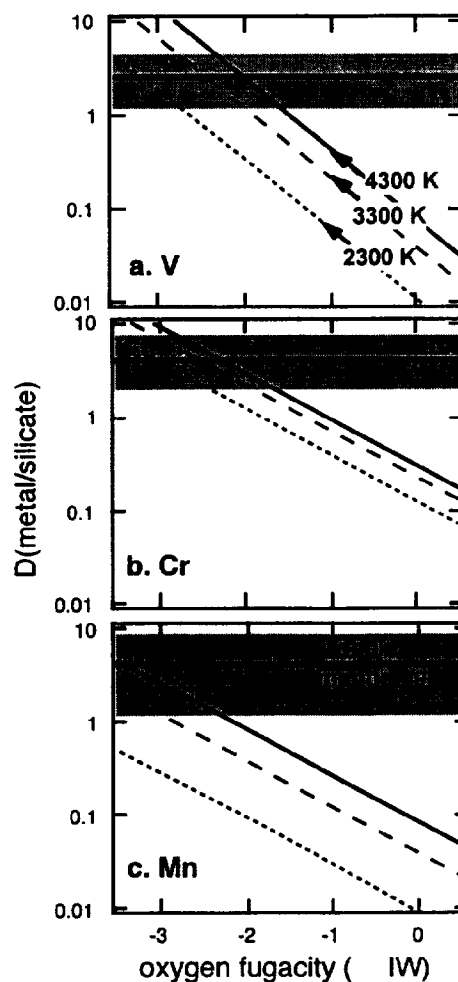
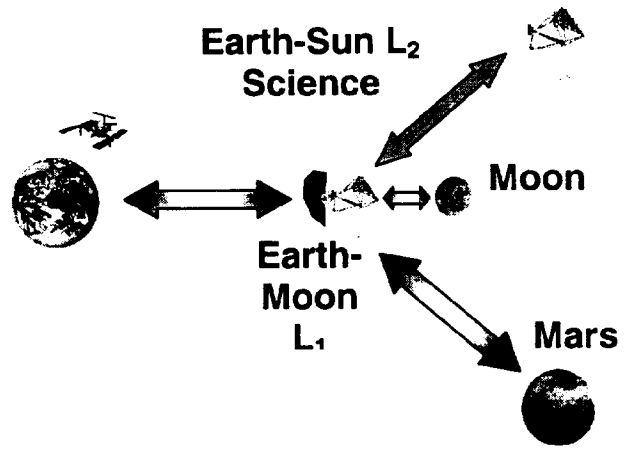


Fig. 1. The partition coefficients that are necessary to explain the depletions of a) V, b) Cr, and c) Mn in the silicate portion of the Moon are shown as shaded gray regions [9], with the preferred partitioning value shown as a thick black line. Each diagonal line indicates the modeled partition coefficients at different oxygen fugacities, expressed as log units below the iron-wüstite buffer (IW), and a constant temperature of either 2300, 3300, or 4300 K. The model lines cross into the gray areas at high temperatures and low oxygen fugacities, suggesting such conditions during core formation can explain the lunar V, Cr, and Mn depletions.

NEW APPROACHES FOR EXPLORATION BEYOND LOW EARTH ORBIT. D. R. Cooke, NASA Johnson Space Center, Houston, Texas, 77058

Introduction: Through the work of the NASA Exploration Team (NEXT), innovations in mission architectures have been developed. Missions beyond low Earth orbit have been dramatically simplified through new combinations in the application of advanced technologies and mission design. These concepts enable a stepping stone approach to discovery driven, technology enabled exploration. The architectures have evolved from the interest in easily reaching the poles of the moon, to take advantage of the water ice that is believed to exist in the permanently dark craters. The Polar Regions also have areas that are consistently sunlit, providing a constant source of power. By staging these missions from the Earth-Moon Lagrange point, L1, other sites on the lunar surface can be reached as easily as the polar sites. Through studying this approach to lunar exploration, and combining new trajectory approaches the staging of other missions from L1 has begun to look attractive. The possibilities of missions include the assembly and maintenance of arrays of telescopes for emplacement at the Earth-Sun L₂, and travel to Mars. The resulting numbers and masses of vehicles required are greatly reduced. Vehicle design concepts are developed for proof of concept, to validate mission approaches and understand the value of new technologies. The stepping stone approach employs an incremental buildup of capabilities; allowing for decision points on exploration objectives. It enables testing of technologies to achieve greater reliability and understanding of costs for the next steps in exploration.



MODELING THE STABILITY OF VOLATILE DEPOSITS IN LUNAR COLD TRAPS. D. H. Crider¹ and R. R. Vondrak², ¹200 Hannan Hall, Catholic University of America, Washington, DC 20064 (dcrider@lepvax.gsfc.nasa.gov); ²Code 690, NASA Goddard Space Flight Center, Greenbelt, MD 20771 (rvondrak@pop600.gsfc.nasa.gov).

Introduction: There are several mechanisms acting at the cold traps that can alter the inventory of volatiles there. Primarily, the lunar surface is bombarded by meteoroids which impact, melt, process, and redistribute the regolith [1]. Further, solar wind and magnetospheric ion fluxes are allowed limited access onto the regions in permanent shadow. Also, although cold traps are in the permanent shadow of the Sun, there is a small flux of radiation incident on the regions from interstellar sources. We investigate the effects of these space weathering processes on a deposit of volatiles in a lunar cold trap through simulations.

Like Arnold [2], we simulate the development of a column of material near the surface of the Moon resulting from space weathering. This simulation treats a column of material at a lunar cold trap and focuses on the hydrogen content of the column. We model space weathering processes on several time and spatial scales to simulate the constant rain of micrometeoroids as well as sporadic larger impactors occurring near the cold traps to determine the retention efficiency of the cold traps. We perform the Monte Carlo simulation over many columns of material to determine the expectation value for hydrogen content of the top few meters of soil for comparison with Lunar Prospector neutron data.

Each column is initialized with a random starting depth profile of hydrogen content assuming very immature soil. Time is allowed to run for 1 billion years and all changes to the column are calculated. An impactor flux from Gault et al. [3] is imposed to determine the timing and location of all nearby impacts. Nearby impacts excavate material from the column, exposing material from depth. More distant impacts cover the column with an ejecta blanket with a size and time dependent maturity value. In between impacts, the competing effects of sublimation, new deposition, and churning are simulated.

The constant modification of the lunar regolith from space weathering churns the lunar soil. As a result, continuous strata are not expected to be found if one were to take core samples in a cold trap. Space weathering processes act on several scale lengths in a non-unique way. However, we show how the hydrogen content would vary with depth following certain events. In the future event of core samples taken from lunar cold traps, this information is useful in determining the possible history of those columns.

Using the steady state delivery rate of water vapor to the lunar cold traps from Crider and Vondrak [4], we find that the removal rate from space weathering processes does not exceed the rate at which volatiles are delivered to the cold traps on average. Together with the steady migration of hydrogen released from the soil elsewhere on the Moon, the predicted hydrogen content of the topmost meter of regolith in cold traps is within a factor of 2 of the value measured by the LP Neutron Spectrometer [5]. Therefore, release of implanted solar wind hydrogen by sputtering and micrometeoroid bombardment is a sufficient source for the hydrogen at the lunar poles.

That the solar wind is a sufficient source for the cold trap hydrogen is puzzling because comets have impacted the Moon in its history and, thereby, delivered additional water to the Moon. However, this additional source of water is not required based on the current estimate. It is possible that cometary impacts produce a hot enough plume that the water quickly escapes from the system.

References: [1] Watson K. et al. (1961) *JGR* 66, 3033; Arnold J. R. (1979) *JGR* 84, 5659. [2] Arnold, JR (1975) *Proc. Lun. Sci Conf. 6th*, 2375. [3] Gault D. E. et al. (1972) *Geochim. Cosmochim. Acta.* 3, 2713 [4] Crider D. H. and Vondrak R. R. (2002) *Adv. Space. Res.* in press [5] Feldman W. C. et al. (2001) *JGR* 106, 23231.

LUNAR SOLAR POWER SYSTEM AND LUNAR EXPLORATION. D. R. Criswell¹, ¹Institute for Space Systems Operations, SR1, Suite 617, Mail Code 5506PHYS, University of Houston, TX, 77204-5506, dcriswell@uh.edu or dcriswell@houston.rr.com 281-486-5019 (phone and fax)

Global Power and the Moon: Five of the six billion people on Earth produce less than 2,500 \$/year-person of Gross World Product. GWP growth is severely limited by the high cost, low availability and reliability, environmental damages, and political uncertainties of conventional fossil, nuclear, and terrestrial renewable power systems. In 2000 the World Energy Council challenged all decision makers to enable the equivalent of 6.7 kWt/person of thermal power within two generations¹. This implies 67 TWt, or ~20 to 30 TWe, of sustainable electric power by 2050. Twenty-five power systems were reviewed to select which could:

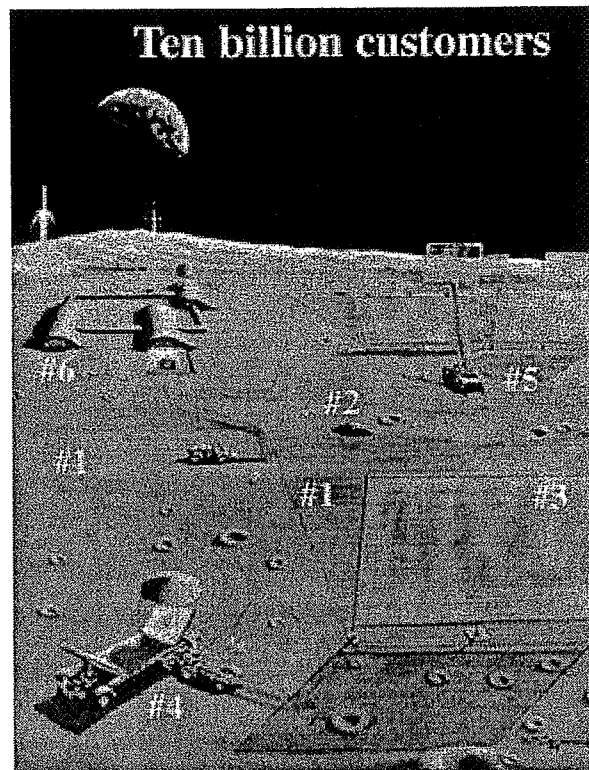
- sustainably provide 20 TWe to consumers;
- profitably sell electricity for < 0.01 \$/kWe-h;
- be environmentally neutral, even nurturing; and
- use understood technologies.

The analyses indicated that only the Lunar Solar Power (LSP) System could meet these requirements within the 21st Century.^{2,3}

LSP System: The Moon dependably receives 13,000 terawatts of solar power.^{3,4} Power stations on the east and west limbs of the Moon can convert a few percent of this dependable solar power into beams of microwaves. Those beams can dependably deliver more than 20 terawatts of the needed clean, safe, low-cost commercial electric power to receivers on Earth. Relay satellites in orbit about the Earth can supply load following power to receivers when the receivers cannot view the Moon. Each power station consists of tens of thousands of power plots.

The figure depicts several prototype power plots. A power plot consists of solar cells (#1), underground wiring (not shown), microwave generators (#2), and microwave reflective screens (#3). The microwave reflective screens (#3) of the power base overlap, as seen from Earth, to form a microwave lens that is 30 to 100 km in diameter. The cells, wiring, generators, and screens are made primarily from lunar materials and assembled by mobile (#4, #5) and fixed factories (#6) that are deployed from Earth. Making most of the plot components from lunar materials significantly reduces the need for transport from the Earth to the Moon. More versatile factories (#6) can make significant fractions of the production machinery (#4, #5, #6) from lunar materials. This further reduces the mass of components and machines that must be transported to the Moon.

Exploration: LSP establishes the Earth and the



Moon a two-planet economy. Lunar exploration can be conducted as a large-scale and long-term component of permanent human habitation of the Moon. Power, people, and resources will be available to support active seismology, deep drilling, systematic exploration of the surface, and long-term studies of the interaction of the Moon with the Earth and the solar system. Lunar geophysical laboratories can be free of terrestrial contamination. LSP industries can construct telescopes (radio, optical, UV, etc.) and powerful radars for probing the Earth, other bodies of the solar system, and performing experiments on space plasmas. Cis-lunar facilities and transport, combined with lunar power and materials, will enable large scale and safe exploration of the inner solar system.

References: [1] World Energy Council (2000) *Energy for Tomorrow's World – Acting Now!*, 175pp., see p. 2, Atalink Projects Ltd, London, [2] Criswell, D. R. (2002) *Energy Prosperity within the 21st Century and Beyond: Options and the Unique Roles of the Sun and the Moon*. Chapter 9: *Innovative Solutions To CO₂ Stabilization*, R. Watts (editor), Cambridge Un. Press, [3] Criswell, D. R. (2001) *Lunar Solar Power System: Industrial Research, Development, and Demonstration*, Session 1.2.2: 18th World Energy Congress <http://www.wec.co.uk/wec-geis/>, [4] Criswell, D. R. (2002, April/May) *Solar Power via the Moon*, *The Industrial Physicist*, 12–15, <http://www.tipmagazine.com>

HUMAN EXPLORATION OF THE MOON. Michael B. Duke, Colorado School of Mines, 1500 Illinois St., Golden, CO 80401. mikeduke@earthlink.com

The Earth's Moon is the only planetary body other than the Earth that has been explored directly by humans. The Apollo missions sent six crews of two astronauts to the lunar surface under conditions that were experimental, highly constrained and expensive. There are many scientific issues that would benefit from concerted human exploration that could be conducted from an outpost on the Moon. Among the interesting questions that can be posed, which have relevance for lunar and planetary origin and evolution, are:

1. How far back can impact basin stratigraphy be extended? Can pre-mare basin stratigraphy be resolved?
2. What were the processes of mare filling? How long did it take?
3. Can the early history of the sun be better determined? How far back can the history be extended?
4. Can the structure and composition of the lunar interior be determined more precisely and can better limits be placed on the timing of the Moon's geophysical evolution?
5. What are the characteristics of the permanently shadowed terrain near the lunar poles? Can their resources be developed?
6. Can the recent history of comets, asteroid and dust impact on the lunar (and therefore the Earth's) surface be established by systematic studies of impact craters at small scales?

Human exploration will be particularly effective on the Moon, due to the complex relationships between geological units and the Moon's impact history, which has stirred, mixed, and diluted rock abundances in the regolith and megaregolith. Humans can directly observe lunar structures exposed by tectonic and impact events and identify and classify major rock types in the field. They can assess very complex relationships that require identification, sample collection, and analysis of minor constituents within very large assemblages, such as clasts in impact breccias, barely initiated by Apollo astronauts, and collections of coarse particles from the regolith, requiring much more intensive separation and classification than the Apollo rake samples. Humans can conduct iterative sample collection and analysis as more understanding is gained of local and regional petrological relationships. They can supervise drilling through layered stratigraphy of the Maria, identifying possible subtle relations between basalt flows and intervening regolith units. They can guide robotic

systems into permanently shadowed areas where high-resolution images from orbit do not exist. And humans can emplace a new generation of sensitive geophysical instruments.

The number of important sites for exploration is quite large and distributed over the Moon. Global access is required, but is expensive with a series of independent missions (either robotic or human) to various locations, due to the overhead associated with landing on and leaving the lunar surface. A permanent outpost, from which long-distance surface vehicles are operated over extended periods of time, can be more effective, particularly if locally produced power and propellant sources are available. The development of solar power collection and conversion stations on the Moon and the production of hydrogen and oxygen from lunar polar ice are two technologies that can lead to a series of "gas stations" on the lunar surface, where the power and propulsion systems of surface exploration vehicles can be repeatedly replenished.

Technological developments that would bring benefits to human exploration include better spacesuits, better integrated robotic tools for human explorers, improved, light weight, effective laboratory analytical capability, long-range robotic mobility systems (robotic and crewed), and a range of crew support infrastructure needs such as regenerable life support systems, 100-500 kW power systems, and systems that support human health and performance. The development of power and propellant on the Moon and a reusable Earth/L1/Moon transportation system can reduce the cost of Earth-Moon transportation by approximately 75% in comparison to architectures in which all propellant must be brought from Earth.

Exploration of the Moon has benefits beyond additional understanding of lunar and planetary science. Opportunities exist on the Moon to extend astronomical, solar and magnetospheric observations to new scales. Scientific and commercial utilization of the reduced gravity and high vacuum conditions of the lunar surface have been suggested. Concepts for the use of lunar materials, particularly hydrogen or ice concentrations at the lunar poles, may have commercial significance. The production of Helium-3 and the collection of very large amounts of solar energy on the Moon for shipment to Earth have been suggested as the solution for the Earth's ultimate energy crisis. Any of these could be logical derivatives from the infrastructure and knowledge resulting from an intensive human lunar exploration program that could be carried out in the early years of the 21st Century.

SAMPLE RETURN FROM SOUTH POLE-AITKEN BASIN. M. B. Duke, Center for the Commercial Application of Combustion in Space, Colorado School of Mines, 1500 Illinois St., Golden, CO 80401, mikeduke@earthlink.com

The South Pole-Aitken Basin is the oldest and largest of the lunar impact basins that formed prior to 3.9 by ago. The impact may have penetrated several hundred kilometers through the crust and perhaps into an ancient mantle. The original crust was stripped off and emplaced as impact ejecta beyond the rim of the basin, while the interior of the basin was filled by subcrustal rocks, probably in the form of breccias and/or impact melts. Mare volcanism occurred locally within the Basin. The South Pole-Aitken event is significantly older than the oldest mare basalts that have been dated but it is not known whether the basin is significantly older than the front side mare basins. Several multi-ring impact basins formed within it, which redistributed rocks within the South Pole-Aitken Basin.

South Pole-Aitken Basin sample return has two major objectives: (1) determine the range of rock types that were excavated by the event and what classes of subcrustal rocks were involved. (2) determine the age of the basin. A cost-constrained mission was proposed to NASA's Discovery Program in 2000 with the objective of landing at a well-chosen site and collecting about 1 kg of material, mostly fragments between 1 mm and 1 cm, by sieving up to one hundred kilograms of regolith over a six day period [1]. A suite of fragments is anticipated that would contain primarily locally-derived rocks, with some fragments representing more distant sources. The mission fit into the scale, timing and cost constraints of the Discovery program, but was not selected for further study at that time.

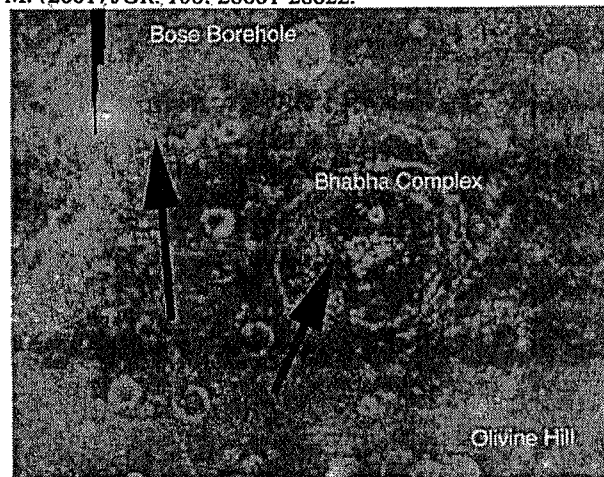
Is a "grab sample" adequate to address the important scientific issues represented by the South Pole Aitken Basin, considering the complexity of its formation and history? It is argued here that samples obtained from a limited area can be very effective because of the remote sensing data from Clementine and Lunar Prospector, which allow the selection of a site where the geological history is relatively simple (e.g. the center of a relatively recent large impact into the floor of the South Pole Aitken Basin) and the association of rock fragments in melt rocks and breccias to mapped nearby terrains. The image depicts the vicinity of the craters Bose and Bhabha (165W, 55S) described by Pieters et al [2]. The red and orange units in the image are believed to be noritic by and are interpreted as areas where Bose and Bhabha excavated either lower crust or the South Pole-Aitken breccia/melt suite. Areas depicted in green represent rocks of gabbroic composition and olivine-containing units. They appear to overly the norite and could represent later mare-type volcanism or perhaps differentiation of the melt sheet. In the region of Olivine Hill, the gabbroic unit appears to be thicker. Areas in blue most likely represent areas of mature regolith. Sampling at either of the locations indicated by arrows should provide unambiguous materials from both the noritic and gabbroic units excavated by Bose or Bhabha, which are relatively recent impacts. The excavated units should thus be free of influence from large post-South Pole-Aitken events such as Orientale and Imbrium. Alteration of the rocks of these units by the

Bose and Bhabha impacts is possible, which could make radiometric dating of the South Pole-Aitken event more difficult; however, the diversity of samples expected and the multiplicity of techniques that can be brought to bear on these samples in terrestrial laboratories should allow the history of this region to be unraveled.

Ultimately, several missions to diverse locations will be required to sample units within and outside of the Basin. However, a relatively simple sample return mission can be the first step in the intensive study of this region of the Moon, establishing the nature of the principal petrological units of the Basin, providing ground truth for more detailed interpretations of remote sensing data from Clementine, Lunar Prospector and SMART-1, and improving the characterization of landing sites for future sample returns.

References:

- [1] Duke M. B., Agee C., Bogard D., Carrier W. D., Coombs C., Head J., Jolliff B., Lofgren G., Papanastassiou D., Papike J. J., Pieters C. M. and Ryder G. (2000) South Pole-Aitken Basin Sample Return Mission, in ICEUM-4 Proc. Fourth Int. Conf. On the Exploration and Utilization of the Moon, ESA SP-462, pp. 137-140.
 [2] Pieters C. M., Head J. W., Gaddis L., Jolliff B. and Duke M. (2001) *JGR*, 106, 28001-28022.



CONTRIBUTION OF ION SPUTTERING TO THE PRODUCTION OF NA AND K IN THE LUNAR ATMOSPHERE. C. A. Dukes and R. A. Baragiola, University of Virginia, Laboratory for Space Physics, Charlottesville, VA 22904.

Neutral Na and K in the lunar atmosphere have been detected by a number of ground-based observations. To maintain their columnar densities in the Moon's tenuous exosphere, these atoms must be continually replenished by some mechanism(s). These processes include: electron-stimulated desorption, photon-stimulated desorption (primarily UV), thermal desorption, ion sputtering, and micro-meteoritic impact. We investigate the effect of solar wind bombardment on lunar-like minerals (albite, labradorite, and anortho-

clase – alkali containing feldspars similar to highland basalt), by measuring the cross section for ion-induced release of Na/K from feldspathic material. Measurements are made in an ultra-high vacuum chamber by irradiating a granular sample with 4 keV He⁺ ions and measuring the surface concentration of Na/K as a function of irradiation dose with x-ray photoelectron spectroscopy (XPS). We will discuss the astronomical implications of our measurements.

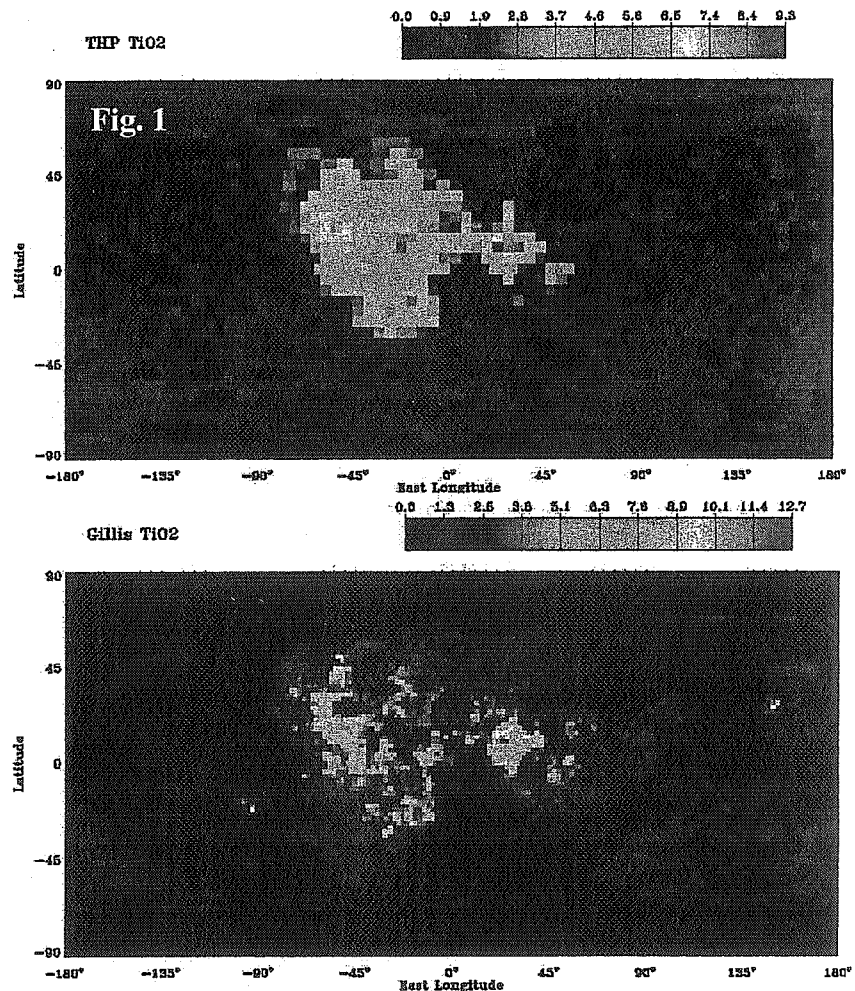
REMOTE SENSING OF TITANIUM IN MARE BASALT SOILS: WILL THE REAL TiO₂ PLEASE STAND UP? R. C. Elphic¹, D. J. Lawrence¹, T. H. Prettyman¹, W. C. Feldman¹, D. T. Vaniman¹, O. Gasnault², S. Maurice², J. J. Gillis³, B. L. Jolliff³, P. G. Lucey⁴, ¹Los Alamos National Laboratory, Los Alamos, NM, ²Observatoire Midi-Pyrénées, Toulouse, France; ³Dept. of Earth and Planetary Sciences, Washington University, St. Louis, MO; Hawai'i Institute of Geophysics and Planetology, University of Hawai'i, Manoa, HI.

Introduction: Lunar mare basalt classification schemes have relied on titanium content as a principal classifier owing to its considerable variability in returned samples [1]. Ti is an indicator of the mineral ilmenite, a potential lunar resource and a major player in mare basalt petrogenesis. Since lunar mare basalt samples (and associated soils) come from only a few nearside sites, it is important to determine if the sample collection accurately reflects the global distribution of titanium in mare basalts. Mare basalt soils in the sample suite suggest two fundamental populations of basalts, high-Ti and low-Ti, while global estimates based on spectral reflectance techniques reveal a continuous gradation of titanium abundance [2,3,4]. In addition, there have been disagreements between optical and nuclear remote sensing techniques used to estimate TiO₂ abundance [5]. Recent efforts to refine spectral reflectance techniques have provided better agreement with both samples and neutron-spectrometry techniques [6], but there are still differences in the estimates. Here we report on new results for TiO₂ obtained by the Lunar Prospector Gamma Ray Spectrometer data analysis, and compare them to estimates provided by other techniques.

LP GRS TiO₂: Figure 1 shows a 5° pixel resolution cylindrical projection map of TiO₂ from a recent LP GRS analysis [7]. The scale ranges from 0 to 9.3 wt%. The highest values of mare basalt soil titanium are found where they have been identified before using spectral reflectance techniques, namely in Mare Tranquillitatis and Oceanus Procellarum. The LP GRS abundance is generally in agreement with the neutron spectrometer values but are lower than has been previously estimated by spectral techniques [3].

CSR TiO₂ Hybrid Technique: Gillis et al. [5] have recently developed a hybrid UVVIS technique for estimating TiO₂ abundance. It makes use of not one but two regressions in UVVIS reflectance and spectral ratios, which essentially account for differences in plagioclase content of the Apollo and Luna mare basalt soil samples. Figure 2 shows the hybrid optical TiO₂ estimates (2° pixels, ranging up to 12.7 wt%). The agreement with the LP GRS titanium abundance is generally good, but there are still interesting differences which may point to locales where mare basalt mineralogy differs from that found in the sample suite.

References: [1] BVSP (1981) *Basaltic Volcanism on the Terrestrial Planets*, Pergamon Press; [2] Neal C. R., and Taylor L. A. (1992) *Geochim. Cosmochim. Acta*, 56; 2177; [3] Lucey, P.G., et al. (2000) *JGR-Planets*, 105, 20,297 [4] Giguere T. A., et al. (2000) *Meteor. Planet. Sci.*, 35(1), 193. [5] Elphic R. C. et al. (2002) *JGR-Planets*, 10.1029/2000JE001460 [6] Gillis, J. J. et al. (2002) *JGR-Planets*, in press. [7] Prettyman, T. H. et al. (2002) *33rd LPSC*, #2012, 2002.



NORTH WEST AFRICA 773 (NWA773): AR-AR STUDIES OF BRECCIA AND CUMULATE LITHOLOGIES

V. A. Fernandes, R. Burgess and G. Turner, Dept. Earth Sciences, Univ. of Manchester, Oxford Rd., Manchester, M13 9PL, UK (e-mail: vfernandes@fs1.ge.man.ac.uk)

Lunar meteorites may provide a more varied and less biased selection of lunar material. At present there are relatively few detailed age data available for the 26 lunar meteorites that have so far been discovered. As part of a wider study of Ar-Ar age determinations of lunar meteorites, we present data for North West Africa 773 (NWA773) a 633g lunar meteorite found in the Dchira, Western Sahara in 2000 [1]. It was initially defined as a regolith breccia with a cumulate olivine gabbro [2], however more recently [3] described it as having two distinct lithologies: a VLT basaltic composition and clastic components; and a Mg-rich, olivine-rich cumulate clast lithology with trace-elements and signature similar to KREEP.

Samples and method: The ^{40}Ar - ^{39}Ar dating technique has been applied to two different fragments in an attempt to determine the crystallisation age and timing of any shock events experienced by the meteorite. Sample NWA773-1 (3.203 mg) is comprised of only olivine-rich cumulate, while NWA773-5 (10.876 mg) has two lithologies: olivine-rich cumulate; and a dark clast (e.g. impact breccia component) containing small cumulate fragments. Both samples were analysed by conventional furnace step-heating over the temperature range 300-1600°C

Ar-Ar ages: The two fragments have different contents of non-radiogenic ^{40}Ar : NWA773-1 has a negligible content, while NWA773-5 has a relatively high trapped component with $^{40}\text{Ar}/^{36}\text{Ar}_i$ value of ~ 1.3 . Age spectra for NWA773 are shown in Fig. 1a. In NWA773-1 the apparent ages rise to a maximum of 2.9 Ga at 500°C but accounting for only 5% of the ^{39}Ar release. Apparent ages decline steadily to 2.1 Ga at intermediate release (12% ^{39}Ar release), before rising again to a maximum of 2.9 Ga at higher temperature (50% of K release). The total age obtained by summing data over all the temperature steps is 2.66 ± 0.03 Ga. Because NWA773-5 showed the presence of trapped $^{36}\text{Ar}/^{40}\text{Ar}$, both uncorrected (solid) and corrected (open) apparent age spectra are shown in Fig. 1a. The corrected age spectrum of NWA773-5 shows a similar pattern to NWA773-1; initially apparent ages increase from 2.6 Ga to 3.1 Ga at 500°C corresponding to 20% of the K release. The intermediate steps show a decrease in apparent age to 2.5 Ga, followed by an increase to a maximum of 3.1 Ga at high temperature. The

total age for NWA773-5 is 2.94 ± 0.04 Ga, broadly consistent with the age obtained for the breccia.

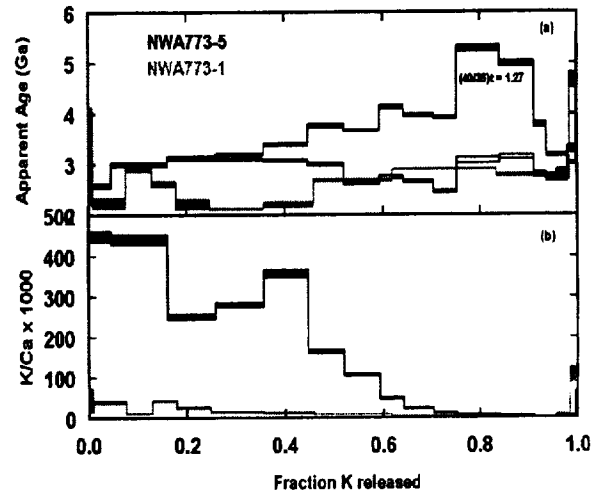


Fig. 1 Ar-Ar step-heating results for samples NWA773-1 and NWA773-5: (a) Apparent ages and (b) K/Ca molar, vs Fraction K released.

There is a marked difference in K content between the samples with the cumulate fragment having a K content (404 ppm) three times lower than that of the breccia (1214 ppm) this is also reflected in the different K/Ca release patterns (Fig. 1b). The Ca content of the two samples are similar NWA773-1=5.1wt%; NWA773-5=7.4wt%.

CRE-ages: Using the method of [4], we calculate cosmic-ray exposure ages of 91 ± 2 Ma and 177 ± 3 Ma for NWA773-1 and NWA773-5 respectively, where errors are analytical precision and do not account for uncertainties in production rate. The lower CRE age of NWA773-1 suggests a deeper burial history of this component and is consistent with it containing negligible trapped Ar.

Summary. The Ar-Ar age of the cumulate lithology in NWA-773 is ~ 2.7 Ga; the breccia component age is slightly higher, but this may not be significant because of the uncertainties introduced by correction for trapped Ar in this sample. It is noted that the age of NWA773 is similar to the Ar-Ar age of NWA032 (a mare basalt lunar meteorite) of 2.8 Ga [5].

Acknowledgements: This work was supported by the European Commission via a TMR fellowship to VAF and Fundação para a Ciência e a Tecnologia, Portugal.

[1] Grossman and Zipfel (2001) MAPS, 36, A293-322; [2] Fagan et al., (2001), MAPS 35, A55; [3] Korotev et al. (2002) MAPS 37, asbt# 5145; [4] Eugster and Michel (1995), GCA 58, 177-199; [5] Fagan et al. (2002) MAPS 37, 371-394

APPLYING STRATEGIC VISUALIZATION® TO LUNAR AND PLANETARY MISSION DESIGN.

By J. R. Frassanito¹ and D. R. Cooke², President, John Frassanito & Associates Inc. 1350 Nasa Rd. One, Houston, Texas 77058, jack@frassanito.com, Douglas R. Cooke, Advanced Development Office, Johnson Space Center, Houston, Texas 77058 douglas.r.cooke@jsc.nasa.gov

Abstract: NASA teams, such as the NASA Exploration Team (NEXT), utilize advanced computational visualization processes to develop mission designs and architectures for lunar and planetary missions. One such process, STRATEGIC VISUALIZATION® [1], is a tool used extensively to help mission designers visualize various design alternatives and present them to other participants of their team. The participants, which may include NASA, industry, and the academic community, are distributed within a virtual network. Consequently, computer animation and other digital techniques provide an efficient means to communicate top-level technical information among team members.

Furthermore, once the team has developed a sound mission design, STRATEGIC VISUALIZATION® is used to communicate that concept to the general public. This is a vital step that Dr. Wernher von Braun used to enhance public support for space exploration. In 1952, for example, Chestly Bonestell and others working under the direction of Dr. von Braun, created the *Collier's Magazine* series of eight articles known as "the *Collier's* space program." Unlike previous works of science fiction, these articles were based on rigorous science and technology. Virtually every aspect of space flight was considered: astronaut training, space stations, lunar expeditions and missions to Mars. [2] Space exploration was greatly advanced as a national priority when *Collier's* presented the American public with a bold and feasible vision of excursions to Moon and other planets.

Today, STRATEGIC VISUALIZATION® is used extensively both in the mission design process within the technical community, and to communicate the value of space exploration to the general public. Movies and digital images have been generated and shown on nationally broadcast television and the Internet, as well as in magazines and digital media.

In our presentation will show excerpts of a computer-generated animation depicting the reference Earth/Moon L1 Libration Point Gateway architecture. The Gateway serves as a staging corridor for human expeditions to the lunar poles and other surface locations. Also shown are crew transfer systems and current reference lunar excursion vehicles as well as the Human and robotic construction of an inflatable telescope array for deployment to the Sun/Earth Libration Point.

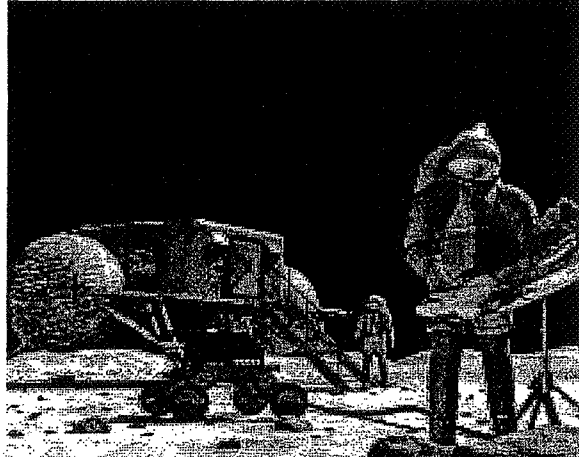


Figure 1. Computer generated illustration showing astronauts deploying a communication satellite link.

References:

- [1] J. Zukowsky. *Space Architecture, The Work of John Frassanito & Associates for NASA*
- [2] R. Miller. (2002) *American Heritage of Invention & Technology* summer 2002

AN ANALYSIS OF REMOTELY SENSED DATA OF MARE AUSTRALE. J. J. Gillis, B. L. Jolliff, Washington University, Dept. Earth & Planetary Science, Saint Louis, MO 63130 (gillis@levee.wustl.edu).

Introduction: In a continuing study of mare basalts and factors affecting their composition, volume, and eruption duration (e.g., incorporation of K-U-Th), we examine the compositions of mare basalts and nonmare units on the floor of Australe Basin. This pre-Nectarian basin is located on the southeastern limb of the Moon (52°S, 95°E) [1], far removed from Th-enriched proximal and possible antipodal Imbrium ejecta.

Australe, although one of the oldest basins, lacks younger superposed basins like those found in South Pole-Aitken Basin. Structurally, Australe exhibits two poorly preserved ring structures, an interior ring ~550 km and an exterior rim ~880 [1, 2]. Lacking well-defined ring structures, the Australe Basin is most readily apparent because of its quasi-circular collection of numerous separate basalt deposits. Basalt deposits within the Australe Basin cover about one-third of the basin surface area inside the main topographic rim.

Mare Australe: The basin floor is a collection of partly coalescing basalt deposits. This collection of disjointed mare deposits occurs in some cases within craters, but mostly, within intercrater regions of the basin floor. If volcanism had continued within the basin, it might have looked more like near-side maria. The lack of volcanic fill within the Australe Basin provides clues to the early stages of basin-filling volcanism that have been lost due to more extensive volcanism elsewhere.

Basalt Composition: Using 0.5° resolution data [3, 4], Th concentrations for 56 of the basalt ponds within Mare Australe average 0.7 ± 0.1 ppm. This is similar to most Apollo and Luna basaltic soils. Clementine derived TiO₂ concentrations (250 m resolution [5]) span the lower end of the sample range, from very low to moderate, with most basalt ponds containing <1 wt.% TiO₂. The basalt ponds are compositionally different from the Apollo and Luna soils with respect to FeO. The average FeO content of regolith on the surfaces of basalt ponds within the Australe Basin is 11.5 wt.% (Fig. 1; 250 m resolution [6]). Ejecta deposits surrounding young, small craters, which have excavated fresh mare material, exhibit FeO concentrations slightly higher than the basalt surfaces themselves (14-16 wt.% FeO).

Basin Floor Composition: On the basis of its size, Australe would have excavated deep into the lunar crust and possibly exposed mid-crustal materials. The nonmare component of the Australe Basin contains 6.4 ± 2.5 wt.% FeO, 0.4 ± 0.3 wt.% TiO₂, and 0.6 ± 0.3 ppm Th. The FeO content is slightly elevated with respect to the Feldspathic Highlands Terrane materials, whereas TiO₂ and

Th contents are similar [7].

Observations: The original compositions of the basalt deposits in Australe have been contaminated by impact mixing with nonmare material. This is evident in Fig. 1 where iron increases from the edge to the center of a basalt pond and parallel to the basalt/highland contact. The original composition is estimated by measuring the FeO content of young craters that have excavated less-contaminated material. The basalt deposits with the highest Th content have the highest FeO and TiO₂ concentrations. These basalt deposits are found along the outer parts of the basin, tend to be the youngest mare deposits in the basin, and erupted into the topographically lowest parts of the basin.

Interpretations: The absolute difference in composition between basalts of Imbrium and Australe reflects the overall compositional difference of the mantle source regions. We suggest that the low concentration of Th in basalt deposits of Mare Australe is related to the low volume of volcanism that has occurred in the basin. Interestingly, the basalt ponds of Mare Australe exhibit a compositional trend whereby the youngest basalts erupted within the basin exhibit the highest TiO₂, FeO, and Th contents, a trend also observed in Mare Imbrium, reflecting similar dynamic processes that occurred within the mantle source region.

References: [1] Wilhelms, *U. S. Geol. Surv. Prof. Paper 1348*, 1987; [2] Spudis, *The geology of multi-ring impact basins: The moon and other planets*, 1993; [3] Lawrence et al., LPSC XXXIII, abstract #1970, 2002; [4] Gillis et al., LPSC XXXI, abstract #2058, 2000; [5] Gillis et al., *JGR*, in press; [6] Lucey et al. *JGR*, 105, 20,297, 2000; [7] Jolliff et al., *JGR*, 105, 4197, 2000.

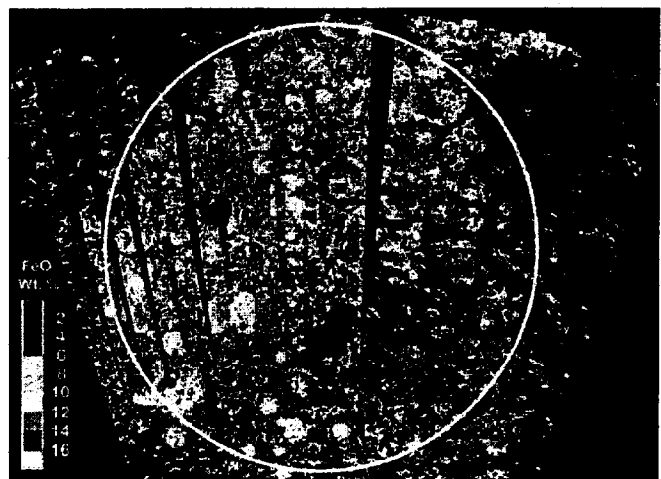


Fig. 1. Clementine derived FeO image of the Australe Basin. The white circle represents the 880 km topographic rim of Australe.

USING SMALL BASALTIC LUNAR CLASTS TO RECONSTRUCT THE EARLY MAGMATIC HISTORY OF THE MOON. J. J. Hagerty, C. K. Shearer, and J. J. Papike. University of New Mexico, Institute of Meteoritics, Dept. of Earth & Planetary Sciences, Albuquerque, NM 87131 U.S.A. e-mail: jh2713@unm.edu.

Introduction: Intense study of lunar samples represented by the Apollo, Luna, and meteorite collections has led to a substantial understanding of the Moon's magmatic and impact history [1]. The majority of the samples representing lunar magmatism prior to ~ 3.9 Ga, commonly occur in the form of soils or brecciated rocks, which means that these samples are essentially amalgamations of small, genetically unrelated fragments. One way to reconstruct the magmatic history represented in these samples is to resolve the compositional differences between the various fragments via microbeam techniques. The information derived from such analytical techniques can be used to decipher the chemical evolution of the Moon. For instance, the small Apollo 14 high-Al basalt fragments have been suggested to represent the earliest stages of basaltic magmatism on the Moon [2,3,4]. Trace element information from minerals in these samples can be used to make implications for the mechanisms of formation, as will be discussed below.

Scientific Rationale and Analytical Approach: The Apollo 14 high-Al basalt fragments have similar petrography, mineral compositions, and bulk major element compositions, yet there is an 8 to 10 fold increase in REE and other incompatible elements [2, 3]. It should be noted that these fragmented Apollo-14 basalts are quite small (< 1 to 3 mm in size) and contain variable amounts of mesostasis. These samples, therefore, may be unrepresentative of the bulk basalts from which they were derived. To better understand the source of the compositional variability previously observed in these fragments, we have chosen to analyze the trace elements of specific mineral phases in these fragments. Trace elements in olivine, plagioclase, pyroxene, and glass were measured using the Cameca ims 4f operated on the University of New Mexico campus by the Institute of Meteoritics.

Data and Discussion: REE data obtained from analyses of plagioclase phenocrysts in the high-Al basalts confirms that there is a wide range (8-10 fold increase) in overall REE content [4]. The Ce/Yb ratios of these fragments are distinctly different (ranging from 5 to 19), thus suggesting that these samples were not derived from the same parent magma and may actually represent individual pulses of magmatic activity [4]. It should also be noted that each of these fragments have distinct Ni-Co signatures, with the cores of the olivine grains being more enriched in Ni and Co than are the rims [4]. The Ni content in the olivine grains ranges from 50 – 375 ppm, while the Co content remains rela-

tively constant at 140 ppm [4]. This information can be used to discuss the potential mechanisms of formation. For example, the data from this study have been used to calculate the degree of fractional crystallization that would be necessary to produce the given chemical signatures (see figure 1). In order to produce the observed REE data, one would need ~85% fractional crystallization (figure 1), whereas to produce the Ni-Co trends, one would need ~15% crystallization (figure 1). These results suggest that the basalts cannot be related through a simple fractional crystallization scenario and instead may be indicative of cyclical assimilation of KREEP or melting of a hybridized source.

Conclusions: This study shows that SIMS trace element analyses can be used to investigate small lunar fragments, such that comparisons can be made between a variety of lunar lithologies. This type of comparison in turn will provide information about the formation mechanisms for these samples. For example, it should be possible to determine if these samples formed as a result of igneous or impact processes.

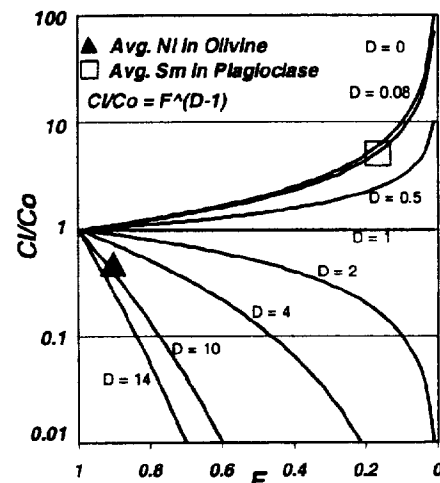


Figure 1. Fractional crystallization diagram showing the average Ni and Sm values in the Apollo 14 high-Al basalts. C_i=Concentration of element in liquid. C₀=Concentration of element in parental magma. D=distribution coefficient. F = fraction of melt remaining (increasing crystallization to the right).

References: [1] Papike J. J., et al. (1998) *Min. Soc. Am. Rev. Min.*, 36, 5-1 to 5-234; [2] Dickinson et al. (1985) *JGR*, 90, C365-C374; [3] Shervais et al. (1985) *JGR*, 90, D3-D18; [4] Hagerty J. J., et al (2002) *LPSC XXXIII*, CD-ROM#1574.

CONSTRAINTS ON THE ORIGIN OF LUNAR CRUSTAL MAGNETISM. J. S. Halekas, (*jazzman@ssl.berkeley.edu*), D. L. Mitchell, R. P. Lin, *Space Sciences Laboratory, University of California, Berkeley CA 94720, USA*, L. L. Hood, *Lunar and Planetary Laboratory, University of Arizona, Tucson AZ 85721, USA*.

The fundamental questions in lunar magnetism research remain much the same as they have since the Apollo days. What is the origin of the strong fields antipodal to young large impact basins? How were non-antipodal fields created? Was there ever an active lunar dynamo? How can paleointensity evidence from returned samples be reconciled with orbital magnetometer and electron reflectometer measurements? With the new data from Lunar Prospector (LP), we find ourselves in a better position to address these questions. However, many of the answers remain unclear.

Data from the Apollo subsatellites showed that the largest regions of strong fields surveyed (Apollo data covers a band of about ± 30 degrees about the equator) lay antipodal to the Orientale, Imbrium, Serenitatis, and Crisium basins [1]. The completely global LP data set has confirmed this association, showing that the largest strongly magnetized regions on the Moon are centered antipodal to these four young large basins and roughly fill the antipodes. Furthermore, there is a slight magnetic enhancement antipodal to Nectaris, a basin just older than the other four. This fits with an overall decline in average antipodal field with increasing age. Monte Carlo simulations show that the probability of achieving such high average antipodal fields (10-40 nT) for the youngest large impact basins by chance is on the order of 10^{-5} . It is unclear how the antipodal magnetic enhancements were produced, though the theory of Hood and Huang [2], which states that the antipodal fields were generated by shock remanent magnetization (SRM) associated with transient antipodal amplification of ambient magnetic fields and antipodal focussing of seismic energy and/or solid ejecta, is currently the best option.

The rest of the Moon is covered by randomly jumbled magnetic fields which are, on average, an order of magnitude weaker than the average antipodal fields. These magnetic fields have proven difficult to associate with geologic features. Many impact craters and basins have been shown to correlate with regions of low fields (extending to several crater or basin radii, suggesting impact demagnetization) [3], but local magnetic field maxima are in general more difficult to associate with specific geologic terranes [4,5]. Statistical studies have, however, proven somewhat successful in distinguishing the average magnetic properties of different terranes [4].

New statistical results for the entire Moon (excluding the magnetized antipodal regions) show consistent patterns. Impact craters and basins are weakly magnetic compared to other terranes of the same age, though the distinction is greatest for younger craters and basins. Crater and basin ejecta materials are some of the more strongly magnetic terranes in each age range. Light plains and terra materials, probably containing a large component of primary and/or secondary basin ejecta, are also relatively strongly magnetic. An overall average age history is seen, which also holds for most individual types of terranes. Average fields are weak over Copernican and Eratos-

thenian terranes (ranging from 1.4-2.6 nT). Imbrian terranes also show weak fields (0.5-3.2 nT), but the spread between the most weakly magnetic and the most strongly magnetic terranes is greater than for other age ranges. Nectarian and pre-Nectarian terranes are more strongly magnetic (2.5-4.0 nT).

At first glance, these various results seem contradictory. Strongly magnetic antipodal regions show a decline in field with increasing age (over a small age range), while non-antipodal terranes show an increase in average fields. To make matters worse, we must also reconcile these data with paleointensity results from returned lunar samples [6], which show evidence of a "magnetic era" in Nectarian and early Imbrian times, possibly due to a lunar dynamo. One can argue that the decline in antipodal fields with age also shows the early edge of this "magnetic era", but the observed age profile of non-antipodal magnetism seems to contradict the sample results.

One solution to this conundrum is to postulate that the paleointensity decline from Imbrian times to the present is real, but the decline in pre-Nectarian times is not. The lack of strong antipodal signatures for older basins, and the weak paleointensities found for older samples, may be the result of impact demagnetization. Samples which show petrographic evidence of high shock pressures generally give very low paleointensities [6], and shock pressures lower than those necessary to visibly affect rocks can affect their magnetic remanence [7,8]. Meanwhile, depending on the depth to which antipodal magnetization extends, the cumulative effect of impact demagnetization could be responsible for erasing older antipodal signatures.

Another solution is to hypothesize that there was no "magnetic era" at all. Instead, the strongly magnetic antipodes and the peak in paleointensity estimates could both be due to impact magnetization effects related to the end of the late heavy bombardment. Meanwhile, the cumulative effects of impact demagnetization could again be responsible for any apparent decline in fields before this time. This theory has the problem that, while transient magnetic field amplifications due to impacts may explain the antipodal fields, it is difficult to explain the remanence seen in lunar samples solely by SRM.

Whatever the resolution of this puzzle, we must reconcile the magnetic field age histories implied by the antipodal fields and the non-antipodal fields, and the paleointensity history implied by returned samples, if we hope to answer the fundamental questions of lunar magnetism.

REFERENCES: [1] Lin *et al.*, *Icarus*, 74, 529-541, 1988. [2] Hood and Huang *J. Geophys. Res.*, 96, 9837-9846, 1991. [3] Halekas *et al.*, *Geophys. Res. Lett.*, in press, 2002. [4] Halekas *et al.*, *J. Geophys. Res.*, 106, 27841-27852, 2001. [5] Hood *et al.*, *J. Geophys. Res.*, 106, 27825-27840, 2001. [6] Cisowski *et al.*, *J. Geophys. Res.*, *supp.*, 88, A691-A704, 1983. [7] Pohl *et al.*, *J. Geophys.*, 41, 23-41, 1975. [8] Cisowski and Fuller, *J. Geophys. Res.*, 83, 3441-3458, 1978.

EXPECTED DATA BY LUNAR IMAGER/SPECTROMETER (LISM). J. Haruyama¹, M. Ohtake¹, T. Matsunaga², N. Hirata¹, H. Demura¹, R. Nakamura¹, and LISM Working Group, ¹Lunar Mission Research Center, National Space Development Agency of Japan (NASDA), 2-1 Sengen, Tsukuba City, Ibaraki 305-8505, Japan. Haruyama.Juncihi@nasda.go.jp ²The Social and Environmental Systems Division, National Institute for Environmental Studies (NIES), 16-2 Ogawa, Tsukuba City, Ibaraki 305-8506, Japan

Introduction: The Moon is the nearest celestial body to the Earth. The Moon has keys to understand the origin and evolution of planets and their moons and our solar system. The Moon is the most important target of space explorations. Since 1960's, numerous unmanned and manned explorations have been carried out. The data by these explorations has been a huge amount and includes much information. However, there is still lack in data collected so far to understand the Moon. [e.g., 1]

National Space Development Agency of Japan (NASDA) and Institute of Space and Astronautical Science (ISAS) are developing a Moon explorer the SELENE and Engineering Explorer (SELENE) that will be launched in 2005 by an H-2A rocket. The purpose of this explorer is to accumulate data for scientific knowledge and to determine the possible availability of the Moon.

Understanding the surface morphology and the surface material and its distribution of the planets and their moons is fundamental for planetary explorations. By the investigation of the Moon surface, we can presume the history of the surface and can often realize when and how the surface was formed and even internal activity of the Moon. The information of the surface is also indispensable for the future activity of human being on the Moon.

Optical sensors are common and effective tools to investigate the Moon surface. We are planning to install the Lunar Imager / SpectroMeter (LISM) is a mission instrument on SELENE. The LISM consists of three subsystems: the Terrain Camera (TC), the Multiband Imager (MI) and the Spectral Profiler (SP). LISM was outlined in our past paper [2,3,4,5]. We completed the LISM Prototype Model (PM) phase in 2001, and have finished the Flight Model (FM) design phase recently. We are now in FM fabrication phase. We introduce the status of LISM development and discuss the LISM FM performance in this presentation.

LISM Outline

The Terrain Camera (TC) is a high-resolution camera. TC will map the entire surface of the Moon at 10m/pixel resolution from SELENE's 100km altitude orbit by TC. TC takes stereo pairs with two slant optical heads. The height resolution of the Digital Terrain Model produced by the stereo pairs will be ideally a few 10m.

The Multiband Imager (MI) is a high spatial resolution band imager. The detailed geological units of the entire of the Moon will be distinguished by using the MI's 5-band visible (415, 750, 900, 950, 1000nm) and 4-band near-infrared (1000,1050, 1250, 1550nm) range images. The spatial resolutions of MI are 20m/pixel for visible range and 62m/pixel for near-infrared range.

The Spectral profiler (SP) is a grating spectrometer that covers 500-2600nm spectral regions with 6-8 nm sampling interval. The footprint of SP is 500m. The TC or MI data and SP data will be combined to determine SP observation areas. The SP data will contribute to identify the surface mineral composition.

Development Status: We designed LISM considering research topics and given resources (development period, money, manpower, mass, electronic power, data amount, data rate, and so on). Before developing the LISM FM, we confirmed the feasibility and problems of LISM by making and testing one TC optical head as a PM and a whole SP as a Proto-Flight Model (PFM). We started LISM FM design in FY 2001, and finished in early 2002. The fabrication and various tests of LISM FM have been started and will be almost completed until the First fitting test scheduled in May, 2003.

- [1]Matsunaga, T. et al. (2000) , Proc. of SPIE vol. 4151.
- [2]Haruyama, J. et al. (2000), LPS XXXI 1317.pdf. [3] Hirata, N. et al. (2002), Abst. New Views of the Moon, Europe. [4] Haruyama, J. et al. (2002), Abst. New Views of the Moon, Europe. [5] Ohtake, M. et al. (2002), Abst. New Views of the Moon, Europe.

LUNAR HIGHLANDS VOLCANISM: THE VIEW FROM A NEW MILLENNIUM. B. R. Hawke¹, D. J. Lawrence², D. T. Blewett³, P. G. Lucey¹, G. A. Smith¹, G. J. Taylor¹, and P. D. Spudis⁴, ¹Planetary Geosciences, Hawaii Institute of Geophysics and Planetology University of Hawaii, Honolulu, HI 96822, ²Los Alamos National Laboratory, MS D466, Los Alamos, NM 87545, ³NovSol, 1100 Alakea Street, Honolulu, HI 96813, ⁴Lunar and Planetary Institute, Houston TX 77058.

Introduction: Since the Apollo era, the search for highlands volcanism has focused on selected light plains deposits as well as a class of spectral anomalies known as Red Spots. These spectral anomalies have spectra that are characterized by very strong ultraviolet absorptions. UV-IR color difference photographs were used by Whitaker [1] to identify and characterize Red Spots on the lunar nearside. He suggested that these anomalously red areas may have compositions that are substantially different from those of typical highlands. In the immediate post-Apollo era, several workers [2,3,4] presented evidence that at least some Red Spots were produced by highlands volcanism and suggested a connection with KREEP basalts (Medium-K Fra Mauro basalt) or even more evolved highlands compositions (e.g., High-K Fra Mauro basalt, dacite, rhyolite).

Method: Both Earth-based and spacecraft remote sensing data were used to investigate the chemistry and mineralogy of lunar Red Spots and selected light plains deposits. Calibrated Clementine UVVIS images were utilized to produce FeO, TiO₂, and maturity images using the spectral algorithms of Lucey *et al.* [5,6]. The 2° x 2° thorium data from the low-altitude portion of the Lunar Prospector mission [7] were reprojected and merged with shaded relief maps of the Red Spot regions. Telescopic near-IR spectra were analyzed and interpreted for selected Red Spots and light plains units.

Results and Discussion: We have completed a preliminary investigation of the following Red Spots: Darney Chi and Tau, Helmet, Southern Montes Rhiphaeus, Hansteen Alpha, Lassell K, G, and C, Mons La Hire, and the Gruithuisen domes [8,9]. Strong evidence of a highlands volcanic origin has been found only for Hansteen Alpha and the Gruithuisen domes [4,8,9,10].

Hansteen Alpha: This arrowhead-shaped highlands feature is located in southern Oceanus Procellarum just north of the crater Billy. Wood and Head [3] noted that this rough textured triangular mound (~25 km on a side) appeared distinctive in its surface texture, color, and albedo from nearby highlands and is embayed by adjacent mare deposits. The 0.5° x 0.5° Th map indicates that Th abundances range from ~4.5 ppm to ~8 ppm in the Arrowhead region. The Arrowhead itself exhibits Th values of ~6 ppm. Slightly higher values (6.0 – 6.5 ppm) are associated with the eastern portion of Hansteen crater and its adjacent ejecta deposits. Based on these preliminary results, it does not appear that the Arrowhead is composed of highly evolved highlands lithologies that are extremely rich in Th. The central portion of Hansteen Alpha has an FeO content of 5% to 8% and a TiO₂ abundance of <1%. Nearby highlands units are much richer in FeO and TiO₂. For example, the ejecta deposits of Billy and Hansteen craters exhibit FeO values that range between 11% and 15%. If the Arrowhead was present prior to the Billy and Hansteen impact events, it should have been cov-

ered by FeO-rich ejecta from both craters. Since it was not, the Arrowhead was formed after these Imbrian-aged craters. This Red Spot was emplaced by highlands volcanism. Two near-IR spectra were obtained for Hansteen Alpha. Both have relatively shallow (3.7% - 4.1%) "1 μm" bands centered shortward of 0.95 μm.

Gruithuisen Domes: Wood and Head [3] noted that Gruithuisen Gamma and Delta were distinctive red domical features 15 to 25 km in diameter that occur at the western edge of Mare Imbrium, south of Sinus Iridum. Head and McCord [4] identified a third spectrally distinct dome just northwest of Gruithuisen Gamma as well as three red domes just west of Mairan crater. They concluded that the Gruithuisen and Marian domes represent morphologically and spectrally distinct nonmare extrusive volcanic features of Imbrian age. Support for this interpretation was recently provided by Chevrel *et al.* [10].

The 0.5° x 0.5° Th map indicates that the Gruithuisen domes have Th values of about 8 ppm. Even higher Th values (10 to 12 ppm) are exhibited by highlands units northwest of the domes. Gamma and Delta exhibit FeO values between 6% and 10% and TiO₂ values <1%. The core portions of these domes have FeO abundances of 6% to 8% and very low (<0.5%) TiO₂ values. Near-IR spectra were collected for Gruithuisen Gamma and Delta. These spectra differ from those collected for typical highland areas in that they exhibit relatively broad bands centered at or longward of 1 μm.

Light Plains Deposits: Some light plains units for which a highlands volcanic origin had been proposed have now been demonstrated to be cryptomaria [e.g., 11, 12]. The best candidate for a light plains deposit that was emplaced by nonmare volcanism is the Apennine Bench Fm. Recent remote sensing studies have demonstrated that the chemistry and mineralogy of the Apennine Bench is consistent with KREEP basalt [e.g., 13].

References: [1] Whitaker, E.A. (1972), *Moon*, 4, 348. [2] Malin, M.C. (1974), *Earth Planet. Sci. Lett.*, 21, 331. [3] Wood, C.A. and Head, J.W. (1975) *Origins of Mare Basalts* (LSI), 189. [4] Head, J.W. and McCord, T.B. (1978) *Science*, 199, 1433. [5] Lucey, P. *et al.* (2000), *JGR*, 105, no. E8, 20,297. [6] Lucey, P. *et al.* (2000), *JGR*, 105, no. E8, 20,377. [7] Lawrence, D.J. *et al.* (2000), *JGR*, 105, no. E8, 20,307. [8] Hawke, B.R. *et al.* (2001), *LPS XXXII*, #1241. [9] Hawke, B.R. *et al.* (2002), *LPS XXXIII*, #1598. [10] Chevrel, S.D. *et al.* (1999), *JGR*, 104, no. E7, 16,515. [11] Blewett, D.T. *et al.* (1995), *JGR*, 100, 16,959. [12] Antonenko, I. *et al.* (1995), *E.M.P.*, 69, 141. [13] Blewett, D.T. and Hawke, B.R. (2001), *M.P.S.*, 36, 701.

THE MOON: KEYSTONE TO UNDERSTANDING PLANETARY GEOLOGICAL PROCESSES AND HISTORY. James W. Head, III¹, ¹Department of Geological Sciences, Brown University, Providence, RI 02912 USA (James_Head_III@Brown.edu).

Introduction: Extensive and intensive exploration of the Earth's Moon by astronauts and an international array of automated spacecraft has provided an unequaled data set that has provided deep insight into geology, geochemistry, mineralogy, petrology, chronology, geophysics and internal structure. This level of insight is unequaled except for Earth. Analysis of these data sets over the last 35 years has proven fundamental to understanding planetary surface processes and evolution, and is essential to linking surface processes with internal and thermal evolution. Much of the understanding that we presently have of other terrestrial planets and outer planet satellites derives from the foundation of these data. On the basis of these data, the Moon is a laboratory for understanding of planetary processes and a keystone for providing evolutionary perspective. Important comparative planetology issues being addressed by lunar studies include impact cratering, magmatic activity and tectonism. Future planetary exploration plans should keep in mind the importance of further lunar exploration in continuing to build solid underpinnings in this keystone to planetary evolution. Examples of these insights and applications to other planets are cited below.

Impact cratering: New information has become available about virtually every aspect of the nature of the cratering process, including depth of excavation, the role of oblique impact, the nature of the modification stage, the production of impact melt, the nature of ejecta emplacement dynamics, the role of volatile emplacement and fate, particularly at the poles, and the establishment of crater size-frequency distribution chronology.

Magmatic activity: Recent lunar studies have provided new insight into plutonism (intrusion) and volcanism (extrusion), and their role as major crustal building and resurfacing processes throughout planetary history. In addition, much new insight has been gained as to the distribution of mantle melting processes in space and time. Further appreciated has been the role of the evolution of density and thermal instabilities dating from early lunar history and effects that these have had on subsequent evolution of lunar magmatism. New remote sensing data have permitted an improved view of the nature of magmatic activity during heavy bombardment (intrusion, extrusion, cryptomaria) and in later lunar history, in terms of the mare

stratigraphic record, the distribution of basalt types, the distribution of melting in space and time, and volume and flux information. Also documented have been the full range of eruption styles and their petrogenetic significance.

Tectonic activity: The Moon is the type location for tectonics on a one-plate planet which can be understood in the context of the complete lunar data set and extended to other planetary bodies. Issues include distinguishing magmatic and tectonic graben, establishing the three-dimensional structure and chronology of wrinkle ridges and arches, determining the internal structure of mountain ranges and linking these events to lunar thermal evolution.

Summary and Conclusions: Upcoming missions by ESA and Japan will provide important additional insight into a host of comparative planetological problems, including: 1) Deconvolution of the complex record of early lunar crustal formation and evolution, 2) Relation of geological processes to the thermal evolution of the Moon and one-plate planets, 3) Establishment of a key planetary perspective on the first half of Solar System history, and 4) Extrapolation of these results to the nature and evolution of terrestrial planetary bodies including Earth.

In order to maximize the usefulness of the Moon as a keystone to understanding planetary geological processes and history, three major steps are required: 1) Compilation of the existing information and data sets into a readily available and easily understood synthesis for other members of the space science and exploration community (such as the New Views of the Moon synthesis); 2) Identification of existing gaps in our knowledge about the Moon that will contribute to the Moon as a keystone for planetary exploration; and 3) Acquisition of data that will address these questions and fill existing gaps in our knowledge. Among the data needed are higher resolution global altimetric data, comprehensive higher resolution multispectral morphological, and stereo image data, higher spatial and spectral resolution mineralogy data, comprehensive and high resolution seismic data, additional heat flow measurements, and sample return from key landing sites selected on the basis of these improved data sets.

AGES, THICKNESSES AND MINERALOGY OF LUNAR MARE BASALTS H. Hiesinger¹, J. W. Head¹, U. Wolf², R. Jaumann², and G. Neukum², ¹Brown University, Dept of Geological Sciences, Box 1846, Providence, RI 02912, Harald_Hiesinger@brown.edu, ²DLR-Inst. of Space Sensor Technology and Planetary Exploration, Rutherfordstr. 2, 12489 Berlin, Germany.

Introduction:

About 17% of the lunar surface are covered with lunar mare basalts [1]. Mare basalts occur preferentially on the lunar nearside and their presence on planetary surfaces is indicative of the thermal activity and volcanic evolution of the body [e.g., 2, 3, 4]. In order to place constraints on the thermal/volcanic evolution and petrogenetic models for the formation of lunar mare basalts, we dated basalts exposed on the lunar nearside. Over the last 6 years we performed crater counts for Oceanus Procellarum, Mare Nubium, Cognitum, Insularum, Humorum, Imbrium, Serenitatis, Tranquillitatis, Humboldtianum, and Australe [e.g., 5, 6, 7]. Currently we are extending our crater counts to basalt areas in Mare Frigoris, Nectaris, Vaporum, Smythii, and Marginis. We are also in the progress of dating some lava-filled impact craters such as Schickard, Crüger, and Grimaldi. Crater counts not only allow one to determine the age of a basalt unit but also provide important information about the thickness, the volume, and the temporal separation of individual basalt flow units [8]. In addition, age data in combination with Clementine [e.g., 9] and Lunar Prospector data [e.g., 10, 11, 12, 13] allow one to investigate changes in mineralogy with time [e.g., 6, 14].

Results and Conclusions:

Ages: Based on our crater counts of ~220 basalt units in 10 different nearside mare regions we found that lunar volcanism in these areas started at ~4 b.y. ago and ended at ~1.1 b.y. Most of the investigated basalts on the lunar nearside erupted during the Late Imbrian Period between ~3.3 and ~3.7 b.y. We see evidence for a significantly decreased flux of basalts during the Eratosthenian Period. The spatial distribution of basalt ages indicates that the youngest basalts are exposed within central parts Oceanus Procellarum and Mare Imbrium; often in the vicinity or associated with volcanic centers such as the Aristarchus Plateau. The youngest basalts are exposed within the Procellarum KREEP terrane, which is characterized by elevated concentrations of thorium, one of the major heat producing elements.

Thicknesses: We refined the technique of using the shape of crater size-frequency distribution (CSFD) curves to estimate the thickness of individual lunar mare flow units [8, 15]. We find that a characteristic knee often observed in CSFD curves is reasonably interpreted to represent the presence of two lava flow units separated in time, and that the diameter at which this knee occurs is related to the thickness of the overlying flow unit. Examination of 58 curves with this characteristic knee in several lunar nearside basins allowed us to identify flow units that have not been detected in low-sun images. We found that the range of flow unit thickness is ~20-200 m and the average is ~30-60 m [8]. These estimates are in good agreement with estimates based on shadow measurements [e.g., 16, 17, 18, 19].

Volumes: On the basis of the known area of exposure of each of our 58 flow units, and their minimum and maximum average thickness, we estimated their volumes [8].

We found that the range of volumes is 30-7700 km³. The minimum average volume of all investigated flow units is ~590 km³ and the maximum average volume is ~940 km³ [8]. *Yingst and Head* [1997, 1998] investigated individual isolated lava ponds in Mare Smythii, Marginis, Orientale/Mendel-Rydberg, and South Pole-Aitken [20, 21]. From a comparison with their volumes of lava ponds in these areas, we conclude that our volume estimates are comparable to volumes of lava ponds that were interpreted to have been filled during a single eruptive episode [20, 21].

Mineralogy: Investigating age data and mineralogy data (Ti, Fe, Th, Sm) from Clementine and Lunar Prospector [e.g., 9-13], we found that some of our units showed mineralogies that are unusual for mare basalts, that is, very low titanium and iron contents. Li [22] used Clementine data to perform multiple endmember mixing models, which allowed them to estimate the amount of highland contamination in mare basalts. Based on their map we identified units that are contaminated with more than 25% highland material and excluded them from our study. Units with less than 25% highland contamination exhibit a more or less constant range in Ti, Fe, Th, and Sm values over the covered time period, that is from ~4 b.y. to ~1.1 b.y. Our study did not reveal any correlation between the titanium content and the age of a basalt. Titanium-poor basalts can erupt at the same time as titanium-rich basalts and there is no evidence that older basalts are systematically more titanium-rich than younger basalts. These results are consistent with previous results, which were based on a Galileo UV/VIS ratio in order to derive the titanium content. Similar results were obtained for Fe, Th, and Sm.

References:

- [1] Head, (1976), *Rev. of Geophys. Space Phys.* 14, 265-300; [2] Solomon and Head (1984), *JGR* 89, 6885-6897; [3] Solomon and Head (1980), *Rev. Geophys. and Space Phys.* 18, 107-141; [4] Head and Solomon (1981), *Science* 213, 62-76; [5] Hiesinger et al. (2000), *JGR* 105, 29239-29275; [6] Hiesinger et al. (2001), *LPSC XXXII*, 1826; [7] Hiesinger et al. (2001), *LPSC XXXII*, 1815; [8] Hiesinger et al. (2002), *GRL* 29, 10.1029/2002GL014847; [9] Lucey et al. (2000), *JGR* 105, 20297-20305; [10] Lawrence et al. (2000), *JGR* 105, 20307-20331; [11] Elphic et al. (2000), *JGR* 105, 20333-20345; [12] Feldman et al. (2000), *JGR* 105, 20347-20363; [13] Prettyman et al. (2002), *LPSC XXXIII*, 2012; [14] Hiesinger et al. (2002), *New Views of the Moon, Europe*; [15] Neukum, and Horn (1976), *The Moon* 15, 205-222; [16] Gifford and El-Baz (1981), *Moon and Planets* 24, 391-398; [17] Howard et al. (1972) *Proc. Lunar Planet. Sci. Conf.* 3rd, 1-14; [18] Schaber (1973), *Proc. Lunar Planet. Sci. Conf.* 4th, 73-92; [19] Schaber et al. (1976), *Proc. Lunar Planet. Sci. Conf.* 7th, 2783-2800; [20] Yingst and Head (1997), *J. Geophys. Res.* 102, 10909-10931; [21] Yingst and Head (1998), *J. Geophys. Res.* 103, 11135-11158; [22] Li (2002), Ph.D. thesis, Brown Univ.

RADAR SPECKLE DISPLACEMENT INTERFEROMETRY TO STUDY MOON'S POLAR AXIS BEHAVIOUR IN THE SKY. I. V. Holin, Space research institute, Moscow, Russia, holin@mail.cnt.ru

Introduction: Radar Speckle Displacement Interferometry (RSDI) is a new on principle Earth-based radar technique which allows precise measurement of instantaneous rotational-progressive motion components of distant bodies [1...8]. It is based on the effect of speckle displacement or far coherence of speckled radar fields scattered by rough surfaces of moving objects. RSDI examinations in practice of radar astronomy have been successfully initiated in 2001...2002 both in Europe [7] and in the USA [9]. In particular, RSDI is considered as one of most promising ground-based techniques to solve the problem of Mercury's obliquity and librations [10]. It was proposed in [11] how Moon's physical librations can be measured. Below RSDI possibilities are discussed as applied to estimation of Moon's instantaneous spin axis orientation in the sky and its variation with time.

RSDI: The essentials and theory of RSDI were developed mainly in [12...14] (see also references in [12,14]). Due to its rough surface the Moon can be considered as a reflecting antenna with a random speckled backscattering pattern. When the Moon-antenna rotates with respect to Earth its speckle pattern rotates as well and sweeps across the Earth surface remaining "frozen" for a rather long time. If two or more receiving antennas are placed along this speckle pattern displacement direction it will be possible to measure vector components of Moon's instantaneous spin-vector which are orthogonal to the Earth-Moon line-of-sight. In case with the Moon the Earth rotation is substantial as well.

Accuracy: In fig. 1 speckle velocity vectors are shown which contribute to the resulting velocity v speckle displacement as projected onto a plane orthogonal to the line-of-sight. The component caused by the orbital motion is $v_v = 2V \sim 2 \text{ km s}^{-1}$, where V is the orbital velocity of Moon. The component $v_E \sim 700...800 \text{ m s}^{-1}$ is related to the Earth rotation and is orthogonal to the Earth's spin-vector Ω_E . The component of interest $v_\Omega = 2\Omega_M(R-R_E) \sim 2 \text{ km s}^{-1}$ (where R is the Earth-Moon distance, R_E is less than or equal to the Earth radius, so the difference $v_M = v_v - v_\Omega \sim 40 \text{ m s}^{-1}$) can vary both in length and direction (shaded area 1 in fig. 1). Because of this the resultant speckle vector v will vary as well (shaded area 2). It follows from fig. 1 that Moon's polar axis variations of ~ 10 arcmin (and the same value for v_Ω) will lead to variations in the resultant speckle vector v direction of ~ 20 arcmin.

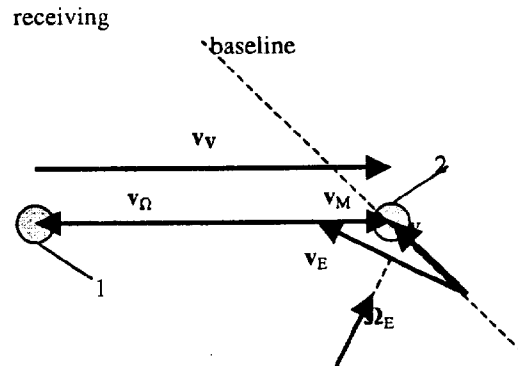


Fig. 1. Speckle displacement geometry as projected onto the Earth's surface.

The direction of v can be measured by a two element radar interferometer as discussed in [1-8, 11-14]. For the Goldstone – VLA radar interferometer (Goldstone transmits, two of 27 VLA's 25m-dishes receive the echo) the one-look accuracy as shown in [11] will be limited by a random refraction in the Earth atmosphere and will be of an order of one arcsecond or better. This means that the Moon's instantaneous spin-vector orientation in the sky can be estimated by Earth-based RSDI with accuracy better than one arcsecond and polar axis variations can be measured with the relative accuracy better than 1%. Both regular and random (if present) walk of the polar axis in the sky can be studied by this approach.

References: [1] Holin I. V. (1999) *Uspekhi Sovr. Radioel.*, 7, 16-28 (in russian). [2] Holin I. V. (2001) Mercury conference (abstract # 8038). [3] Holin I. V. (2002) *LPS XXXIII*, 1387+. [4] Holin I. V. (2002) *Solar System Res.* 36, 226-233. [5] Holin I. V. (2002) *Meteorit. Planet. Sci.* 37, No. 9 (submitted). [6] Holin I. V. (2002) Proceedings of the IEE Radar 2002 conf. (in press). [7] Holin I. V. (2002) *Met. Soc.* 65, 5131+. [8] Holin I.V. (2002) *Met. Soc.* 65, 5041+. [9] Peale S. J., Margot J-l. (2001, 2002) private communications. [10] Peale S. J. et al. (2002) *Meteorit. Planet. Sci.* 37, No. 9 (in press). [11] Holin I. V. (2002) *LPS XXXIII*, 1393+. [12] Holin I. V. (1988) *Radiophys. Quant. Electron.* 31, 515-518. [13] Holin I. V. (1992) *Radio-phys. Quant. Electron.* 35, 433-439. [14] Holin I. V. (1998) *Uspekhi Sovr Radioel.*, 4, 3-15 (in russian).

NEXT STEPS IN UNDERSTANDING LUNAR PALEOMAGNETISM AND RELATED ISSUES. L. L. Hood, N. C. Richmond, *Lunar and Planetary Laboratory, University of Arizona, Tucson, AZ 85721-0092, USA, (lon@lpl.arizona.edu).*

Current unresolved issues relating to the origin and interpretation of lunar paleomagnetism include: (a) the existence and size of a lunar metallic core; (b) the existence and temporal duration of a former core dynamo; (c) the role of impact plasmas in generating and/or modifying lunar magnetizing fields; (d) the origin of swirl-like albedo markings that correlate with the strongest individual orbital anomalies; and (e) the sources of magnetic anomalies on the far side in regions antipodal to major impact basins.

A prerequisite for a former lunar core dynamo field is a metallic core. Conversely, if a former core dynamo is shown to be required by lunar paleomagnetic data, then the existence of a metallic core would be assured, with important implications for lunar origin and evolution models. At present, a number of geophysical constraints strongly suggest, but do not absolutely require, a metallic core with a radius in the range of 300 to 400 km (for a review, see ref. 1). The most direct method for resolving the core issue is to analyze new seismic data such as that which may be obtained by the Lunar A mission (2). However, we emphasize here the possibility of analyzing orbital paleomagnetic data to investigate the existence of a former core dynamo and, indirectly, the existence of a metallic core. Specifically, modeling studies of relatively isolated orbital anomalies can yield estimates for bulk directions of magnetization for major anomaly sources. These directions of magnetization can be used to test the hypothesis that the lunar magnetizing field was dipolar and centered in the Moon, as expected for a core dynamo (issue (b) above). At the same time, inferred directions of magnetization for ejecta units such as the Cayley Formation, which are associated with a single basin-forming impact, can be used to investigate the role of impact plasmas in modifying or generating transient magnetizing fields (issue (c) above). Finally, correlative studies of orbital anomalies with surface geology can investigate the time period when lunar magnetizing fields were strongest.

An unexpected result of the mapping of lunar crustal magnetic fields by instruments on both the Apollo subsatellites and Lunar Prospector (LP) was the discovery that the strongest individual anomalies correlate with unusual, curvilinear albedo markings (hereafter referred to as "swirls") (3,4). This correlation is especially clear for the case of the prototypical nearside swirl marking known as Reiner Gamma. The Reiner Gamma swirls are most easily visible because of their superposition on darker mare basalt flows of western Oceanus Procellarum. One model for the origin of the lunar swirls hypothesizes that these represent surface regions that are depleted in solar wind hydrogen owing to deflection of solar wind ions by strong local lunar magnetic fields (5). This model assumes that the presence of solar wind hydrogen is a secondary catalytic agent for the darkening with time ("optical maturation") of lunar surface materials by micrometeoroid impacts. Future missions can

help to resolve the mystery of the lunar swirls (issue (d) above) in several ways. First, a sample return from Reiner Gamma would establish whether the surface composition of this region is anomalous or whether an altered reflectance spectrum is the only distinguishing characteristic. Second, emplacement of one or more solar wind spectrometers on the lunar surface at Reiner Gamma would establish whether the solar wind fluence is measurably reduced because of deflection by the associated anomalous magnetic field. Finally, a surface traverse by a robotic lander equipped with a portable magnetometer would assist in establishing the location and identity of the anomaly source (near-surface rocks or basin ejecta materials buried by subsequent mare basalt flows).

Issue (e) above can be addressed observationally using existing data by carrying out more detailed correlative studies and by detailed modeling of individual anomalies (see, e.g., ref. 4 and ref. 6). Previous work strongly indicates that unusual, modified ("grooved and pitted" or "hilly and lineated") terrain in basin antipode regions are the most probable sources of the farside anomalies. However, the origin of this terrain, which is most clearly seen near the antipodes of the Imbrium, Serenitatis, and Orientale basins, is not yet clear. Possible origins include (i) surface modification by ejecta from the respective basin-forming impacts converging at the antipode (7); and (ii) surface modification by converging seismic pressure and surface waves from the respective impacts (8). Future sample return missions would allow a more definitive determination of the origin of this terrain and, hence, the nature of the magnetic anomaly sources in these regions. Surface traverses by robotic landers equipped with portable magnetometers would also more strongly constrain the nature and origin of anomaly sources in these regions. Finally, higher resolution orbital photography and multi-spectral remote sensing in basin antipode zones would allow improved studies of the origin and nature of the modified terrain.

REFERENCES. (1) Hood, L. and M. Zuber, in *Origin of the Earth and Moon* (K. Righter and R. Canup, eds.), Lunar and Planetary Institute, pp. 397-412, 2000; (2) Mizutani, H., A. Fujimura, S. Tanaka, H. Shiraishi, S. Yoshida, and T. Nakajima, paper presented at New Views of the Moon Europe, Berlin, Germany, January, 2002; (3) Hood, L. et al., *Science*, 204, 53-57, 1979; (4) Hood, L. and C. Williams, in *Proc. Lunar Planet. Sci. Conf. 19th*, LPI, Houston, 99-113, 1989; (5) Hood, L. and G. Schubert, *Science*, 208, p. 49, 1980; (6) Richmond, N. C., L. L. Hood, J. Halekas, D. Mitchell, R. Lin, M. Acuña, and A. Binder, poster paper presented at 27th EGS meeting, Nice France, April, 2002; (7) Moore, H. J., C. Hodges, and D. Scott, *Proc. Lunar Sci. Conf. 5th*, p. 71-100, 1974; (8) Schultz, P. and D. Gault, *The Moon*, 12, 159-177, 1975.

Modeling the Degradation of Small Lunar Impact Craters: an Example Using a DEM.
 Donald M. Hooper, Department of Geology, One University Plaza, Youngstown State University, Youngstown, OH 44555, e-mail: dmhooperdm@cc.ysu.edu and dmhooper@ysu.edu after 15 August 2002.

Introduction: A numerical model has been formulated to simulate the degradational evolution of lunar impact craters, specifically those with a rim-crest diameter range of 1 to 15 km. Meteoritic bombardment is generally considered to be the primary source of erosion on the lunar surface [1]. This repetitive bombardment by small particles and secondary fragments produces individual effects that are small compared to topographic scale and this steady erosional process modifies crater shape as a function of time. The net result of this impact erosion is a smoothing of the lunar surface in a linearly-diffusive manner of degradation [2].

Description and Morphometry: The computer-simulation approach comprises a linear diffusion-equation algorithm expressed in finite-difference form that operates upon a grid of elevation values depicting the three-dimensional topography of an idealized lunar impact crater. Morphometry for this model crater was derived from the detailed geometric relations of lunar impact craters cataloged by Pike [3]. Using this classification scheme for craters within the diameter range of 1 to 15 km, class 1 craters are the freshest in appearance, while class 2 examples are more degraded. For class 1 craters (n=131), mean rim-crest diameter was 8.01 km, mean d/D (depth/diameter ratio) was 0.202, and mean of the average slope of the interior wall was 23.9 degrees. These morphometric and geometric parameters, combined with digitization and rasterization, were utilized to construct the digital elevation model (DEM) of a typical, fresh lunar impact crater that was employed in the modeling.

Simulation Results: Simulation results demonstrate the progressive erosional modifi-

cations of the classic bowl-shaped craterform: rounding of the crater rim, decrease of crater rim height, gradual crater infilling, decrease in crater depth, and decline of the slope angle of the interior crater wall. Topographic profiles extracted at key time steps display this degradational evolution. The older, more degraded class 2 craters can be correlated with numerical model results. Class 2 craters (n=17) have a mean d/D of 0.172 and a mean of the average slope of the interior wall of 20.3 degrees. This correlation between changing d/D value, crater age, and computer time step can be used to calculate diffusion coefficient values. For example, simulation runs using a 40 m cell size yield a linear diffusion coefficient ranging between 0.5 and 3.0 m²/kyr, depending upon the estimated mean age of the degraded impact craters (class 2). This calibration provides a rough estimate of the rate of transport or erosion. Relative chronologies obtained from crater morphometry can contribute toward an understanding of lunar surface processes as well as toward reconstructing an accurate sequence of geologic events.

References: [1] Ross H. P. (1968) *JGR*, 73, 1343-1354. [2] Soderblom L. A. (1970) *JGR*, 75, 2655-2661. [3] Pike R. J. (1980) U.S.G.S. Prof. Paper 1046-C, 77 p.

GLOBAL LUNAR GRAVITY MAPPING USING SELENE SUB-SATELLITES. T. Iwata¹, H. Hanada², N. Kawano², T. Takano³, and N. Namiki⁴, ¹National Space Development Agency of Japan (2-1-1 Sengen, Tsukuba, Ibaraki 305-8505, Japan; iwata.takahiro@nasda.go.jp), ²National Astronomical Observatory of Japan (2-12 Hoshigaoka-machi, Mizusawa, Iwate 023-0861, Japan), ³Institute of Space and Astronautical Science, 3-1-1 Yoshinodai, Sagami-hara, Kanagawa 229-8510, Japan), ⁴Dept. Earth Planet. Sci., Kyushu University (6-10-1 Hakozaki, Higashi-ku, Fukuoka 812-8581, Japan).

Introduction: The spatial distributions of the lunar gravity field have been investigated from the orbit perturbations which had been observed by two-way range and range rate (RARR) measurements for the spacecrafts in lunar orbits. The orbital determination data till Lunar Prospector have produced and improved the models of the lunar gravity field [1]. The gravity data above the lunar far side were, however, less accurate than those above the near side, because they were observed from higher orbits or estimated from the near side data which were affected with accumulated acceleration by the far side gravity.

SELENE is under development by National Space Development Agency of Japan (NASDA) and Institute of Space and Astronautical Science (ISAS), and will be launched in 2005 to elucidate lunar origin and evolution. SELENE is composed of Main Orbiter, and two micro sub-satellites; the Relay Satellite (Rstar) and the VLBI Radio Satellite (Vstar) which will be used for selenodesy experiments [2]. Rstar and Vstar will be injected into the initial elliptical orbit of 2,400-100 km and 800-100 km in altitude, respectively. Main Orbiter will be controlled to keep the circular orbit of 100 km in altitude. These satellites will be used to obtain selenodetic data of higher accuracy by four-way Doppler measurements and differential VLBI observations.

RSAT : Relay Satellite Transponder: The Orbit of SELENE Main Orbiter above the lunar far side will be directly determined by the four-way Doppler measurements relayed by Rstar (Fig.1). The orbit of Rstar will be simultaneously measured by two-way ranging and ranging rate (RARR). Relay Satellite Transponder, RSAT-1 on Rstar and RSAT-2 on Main Orbiter, relay two-way ranging signals and four-way carrier signals at S or X-band transmitted from 64-m antenna at Usuda Deep Space Center (UDSC). Four-way Doppler measurements derive the first direct orbit determination of low lunar orbiter above the lunar far side, which will produce the first global gravity map of the moon. Analysis of the coverage considering the four-way links shows that our method derives fully covered gravity map.

VRAD : Differential VLBI Radio Sources: Orbits of Rstar and Vstar will be determined with the highest accuracy by differential VLBI observation toward S and X-band radio sources on Rstar and Vstar (Fig.1). Differential VLBI Radio Sources, VRAD-1 on Rstar and VRAD-2 on Vstar, transmit three pairs of S-band and a pair of X-band carrier signals to VLBI radio telescopes at seven ground stations. The distribution of frequencies are determined to calibrate the delay by the terrestrial ionosphere and to solve uncertainties of the delay over one wave length. The accuracy of the satellite positions determination by VRAD are estimated to be about 20cm, which are more precise by three orders than those obtained by hitherto two-way RARR methods. Because neither Rstar nor Vstar have orbital and active attitude control, the longest arc of orbits are analyzed to produce the highest sensitivity for the lower degrees of lunar gravity coefficients.

References: [1] Konopliv, A. S., Asmar, S. W. Carranza, E., Sjogren, W. L., and Yuan, D. N. (2001), *Icarus*, 150, 1-18. [2] Iwata, T., Takahashi, M., Namiki, N., Hanada, H., Kawano, N., Heki, K., Matsumoto, K., and Takano, (2001), *J. Geod. Soc. Japan.*, 47, 558-563.

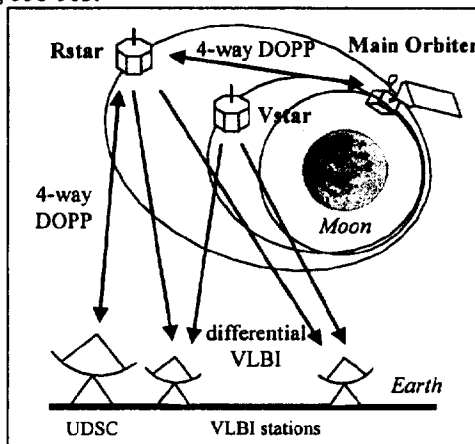


Fig. 1 The concept of the gravity field measurements by SELENE

LUNAR CRUSTAL AND BULK COMPOSITION: TH AND AL MASS BALANCE. B. L. Jolliff and J. J. Gillis, Washington University, St. Louis MO 63130. (blj@levee.wustl.edu)

Introduction: Global compositional remote sensing of the Moon, coupled with accurate correlation of results to Apollo and Luna samples and lunar meteorites, has led to new efforts to estimate crustal and bulk Moon compositions. Global data permit delineation of broad geochemical terranes on the Moon and extrapolation of compositions to depth on the basis of material excavated from the middle and perhaps lower crust by basin impacts [1,2]. Crustal compositions inferred from surface data and mantle compositions inferred from mare basalts permit estimation of lunar bulk composition. Here, we discuss results for Th and Al, two elements that have been extracted from the mantle and concentrated strongly into the crust during global lunar differentiation. Assessment of Th content is important for determining the thermal evolution of the Moon resulting from heat of radioactive decay. Our model follows the general model described by [1], but here we consider the implications of thinner crust, suggested by recent re-evaluation of Apollo seismic data [3,4].

Model: As a framework for assigning regional compositions, we use the "terrane" model of [1]. The anorthositic central region of the Feldspathic Highlands Terrane (FHT), located from about the equator to the north pole on the lunar far side, represents the feldspathic upper crust of early lunar differentiation. We take its composition to be essentially that of the average of feldspathic lunar meteorites [5,6]. The composition of the Procellarum KREEP Terrane (PKT) is noritic and is taken to be Th-rich (avg. 5 ppm) throughout its depth. We use a thickness of crust in the PKT of 45 km [3] and adjust other regions to yield a 52 km average, globally [see 4].

Mid- and lower-crustal compositions of the FHT are inferred from basin ejecta deposits. South Pole-Aitken basin (SPA) provides a sample of lower crustal composition in its interior regions and of mid-level crust in its ejecta deposits. In terms of Th concentrations, the interior averages ~2 ppm, excluding localized highs that may be associated with Imbrium antipodal deposits. Deposits exterior to SPA and surrounding basins of the "Eastern Basin Terrane" [7] indicate mid-crustal compositions of ~1 ppm Th. We adopt a two-layer model for the FHT (essentially all crust except for the PKT and SPA) in which the upper crust is 20–35 km thick (thickest in the northern far side) and has 0.3 ppm Th and the lower crust is 30 km thick and has 1.2 ppm Th, on average. The crustal mass-balance model incorporates a minor mare-basalt component and a correction for a global veneer of Th-rich Imbrium ejecta.

Results: A significantly thinner crust has little effect on the average Th and Al concentrations in the lunar crust. Our calculation yields an average crustal

concentration of ~0.9–1.0 ppm, in close agreement with the estimates of [8,9] and slightly less than our previous estimate of 1.05 [1]. The main reason for the lower average concentration is the significant reduction of PKT crustal thickness from 60 to 45 km. We obtain an average Al₂O₃ concentration of ~25 wt%. A thinner crust, however, has a significant effect on the bulk-Moon content of Th and Al. The crustal thicknesses used in this model amount to only about 75% of the volume of crust in our previous model.

Discussion: For whole-Moon mass balance, the main problem now lies in mantle compositions. Concentrations of Th and Al in mare basalt source regions are not well constrained, and they are even less well constrained in the deep mantle (below 400–500 km). Most models take the upper mantle to be an ultramafic cumulate series derived from solidification of a magma ocean some 400–500 km deep. However, geochemical and thermodynamic reasoning provide compelling arguments that melting should occur early in terrestrial planets and moons, initiating at the center of a body reaching a 500 km accreting diameter [10]. Vigorous convection and intense early impact bombardment allow core formation during accretion and ensure planetary-scale differentiation, i.e., a fully differentiated mantle. If the lower mantle is "depleted" similarly to the upper mantle, then the bulk Moon may be enriched in Al and Th only ~1.5× relative to CI. If on the other hand the lower mantle is undifferentiated or contains a significant amount of garnet as a host for Al and Th, then bulk Moon concentrations could be > 2 × CI.

Concentrations of Th and Al in different regions of the mantle depend in part on cumulate mineralogy ($D^{\text{min}/\text{melt}} \text{Oliv} < \text{Opx} \ll \text{Gar, Cpx}$) and the amount of entrained or admixed residual melt. For Th, most sampled mare basalts have < 2 ppm [11], but some have up to 4 ppm, and remote sensing of the western PKT supports the occurrence of basalts with 3–5 ppm [2,12]. Thus, mantle Th contents in different regions could range from < 0.001 to 0.1 ppm. We will explore the implications of non-uniform Th enrichment in the lunar mantle for global mass balance as well as the consequences for localized heat production in basalt source regions.

References: [1] Jolliff et al. (2000) *J. Geophys. Res.* 105, 4197; [2] Haskin et al. (2000) *J. Geophys. Res.*, 105, 20,403; [3] Khan et al. (2000) *GRL* 27, 1591; [4] Taylor and Khan (2002) abst. #5027, 65th Ann. Mtg., Meteoritical Soc.; [5] Korotev (1999) *LPS* 30, #1303; [6] Gillis et al. (2000) *LPS* 30, #1699; [7] Jolliff et al. (2002) *LPS* 33, #1157; [8] Taylor (1982) *Planetary Science, A Lunar Perspective*. LPI, Houston; [9] Warren (2000) *LPS* 31, #1756. [10] Hofmeister & Criss (2002) Unpub. Man.; [11] Korotev (1998) *J. Geophys. Res.* 103, 1691; [12] Gillis et al. (2002) *LPS* 33, #1934.

SYSTEMATICS OF CHROMIUM AND TITANIUM IN OLIVINE FROM LUNAR MARE BASALTS COMPARED TO BASALTS FROM THE EARTH AND MARS. J.M. Karner, J.J. Papike, and C.K. Shearer, Institute of Meteoritics, Department of Earth and Planetary Sciences, University of New Mexico, Albuquerque, NM 87131-1126, USA. e-mail: jkarn@unm.edu.

Introduction: Trace element analysis of olivine from the Earth, Moon and Mars has allowed for the comparison of planetary basalts at a mineralogical scale [1-3]. We continue this approach by exploring the behavior of Cr and Ti in planetary olivine, relating the similarities and differences in element partitioning to planetary basalt origin, setting, and process.

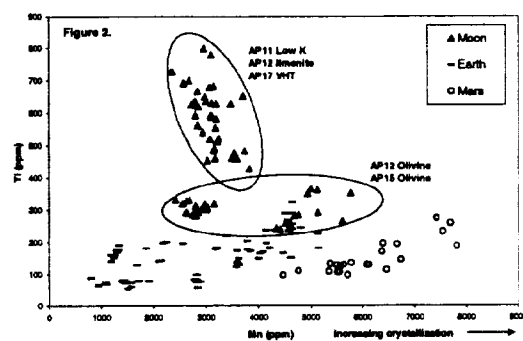
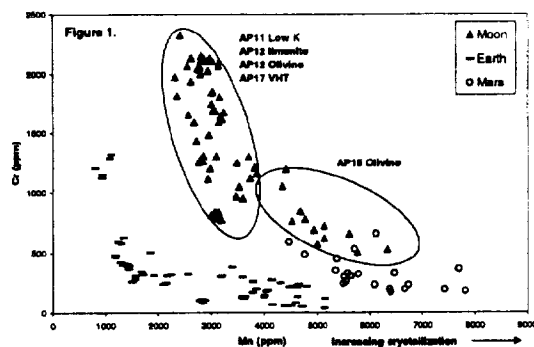
Analytical method: Analysis of olivine grains was performed using a Cameca IMS 4f ion microprobe at the University of New Mexico. A primary beam of O^+ ions was used with an accelerating voltage of 10 kV, a current of 20 nA, and a spot size of $\sim 20 \mu m$. Absolute concentrations of the trace elements were obtained by the use of calibration curves of known olivine standards.

Results and Discussion Figure 1 is a plot of Cr in olivine from the three planets. The plot shows that Cr is more abundant in lunar olivine than martian and terrestrial olivine, a trend that is also seen in the bulk compositions of the magmas [4]. The reason for the Cr enrichment in lunar melts could be that the low fO_2 on the Moon results in a significant reduction of Cr^{3+} to Cr^{2+} , and this, in turn, affects the partition coefficients such that Cr^{2+} favors the melt relative to Cr^{3+} [4]. Figure 1 also highlights the differing behavior of Cr in olivine from specific lunar basalt suites. Olivine from the AP11, AP17, AP12 Olivine and AP12 Ilmenite suites shows high Cr concentrations that decrease significantly with crystallization. The AP15 Olivine suite has olivine with slightly lower Cr concentrations that decrease only slightly with crystallization. The difference between the lunar suites is likely due to different bulk compositions, where the suites with high Cr in the olivine have higher Mg# and are less evolved than the AP15 Olivine suite. Crystallization of spinel, pyroxene, and olivine from the former group deplete the melt rapidly in Cr.

The behavior of Ti in olivine from the three planetary bodies is shown in Figure 2. The plot generally shows that lunar olivine contains more Ti than terrestrial and martian olivine. The high concentration of Ti in lunar olivine reflects the Ti-enriched nature of the melts and basalt source regions on the Moon compared to the Earth and Mars. Figure 2 also shows that Ti concentration in martian and terrestrial olivine increases with increasing crystallization. Lunar olivine shows two trends: in olivine from high-Ti suites (AP11, 17, 12 Ilmenite) Ti decreases rapidly with crystallization. In olivine from low-Ti suites, (AP12, 15 Olivine) Ti increases with crystallization. These contrasting Ti behaviors are a consequence of melt composition and crystallization sequence. In Ti-rich suites, Ti decreases rapidly in olivine with

crystallization because early crystallizing armalcolite and ilmenite deplete the melt in Ti. In suites with low Ti, olivine is slightly enriched in Ti content with crystallization because Ti is not compatible in any of the early crystallizing phases.

Conclusions The systematics of Cr and Ti in olivine from the Moon differs greatly from olivine from the Earth and Mars. This is the result of two main factors: 1) the much lower fO_2 on the Moon relative to the Earth and Mars and 2) the more compositionally diverse source regions on the Moon (e.g. high Ti). The diverse source regions occur because the lunar magma ocean concentrated Ti, KREEP and the heat producing elements (Th, U) in the late crystallizing melts. This enabled melting of ilmenite-rich refractory cumulates.

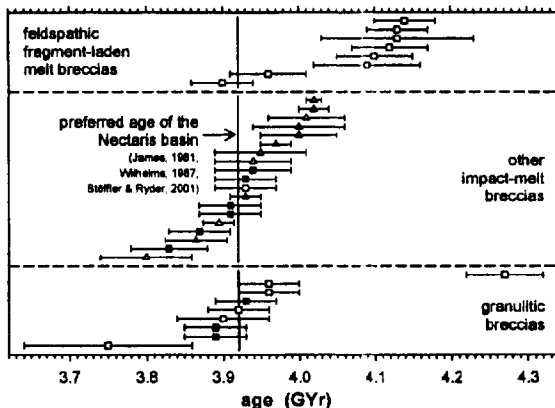


References [1] Papike J.J. et al. (1999) *Am Min* 84, 329-399 [2] Herd, C.D.K. et al. (2001) *LPSC* 32, #1390. [3] Karner et al. (2001) *LPSC* 32 #1017. [4] Papike J.J. and Bence.A.E. (1978) *Geophys. Res Lett*, 803-806.

ON THE AGE OF THE NECTARIS BASIN. R. L. Korotev, J. J. Gillis, L. A. Haskin, and B. L. Jolliff, Department of Earth and Planetary Sciences, Washington University, Saint Louis MO 63130 (rlk@levee.wustl.edu)

We do not know which, if any, rocks of the Apollo collection record the age of the Nectaris impact. However, the age of Nectaris is generally accepted (e.g., [1,2]) to be 3.92 Gyr on the basis of the careful analysis of breccia ages by James (1981, [3]). In essence, the argument is based on the following observations and assumptions, among others. Of the Apollo sites, Apollo 16 lies closest to the Nectaris basin, but Imbrium is bigger and its deposits overlie some Nectaris deposits because it's older. Nevertheless, from ejecta deposit modeling, "most of the material at the Apollo 16 site should have Nectarian or pre-Nectarian ages" [3], i.e., it would predate Imbrium. Granulitic breccias are common at the site. Although it is not known in which basin or crater they formed, they are not likely products of the Imbrium impact, and their measured ages would not likely be affected by the Imbrium impact. They are also not likely products of post-Nectarian, pre-Imbrian impacts that formed local craters. Their ages, therefore, provide an upper limit to the Nectaris age. Most granulitic breccias, and most materials of the Apollo 16 site, have 3.9 Gyr ages (Fig. 1), so this age likely corresponds to a basin, probably Nectaris. Because of certain textural features, the apparent old ages of the feldspathic fragment-laden melt breccias (Fig. 1) "may not have any chronologic significance" [3].

We review some recent data, observations, hypotheses, models, and opinions. (1) It is not self-evident that the geochronologic data provide a precise date for any event (Fig. 1). (2) New ejecta deposit modeling suggests that Serenitatis, which also post-dates Nectaris, strongly influenced the site [4]. Thus, Apollo 16 granulitic breccias are as likely to record the age of Serenitatis as Nectaris. (3) Although most Th-rich Apollo 16 rocks have 3.85–4.0-Gyr ages, there is no evidence from Lunar Prospector data [5] that Th-rich material was encountered or excavated by the Nectaris impactor. All or most of the Th-rich breccias of the Apollo 16 site likely derive from the Procellarum KREEP Terrane



[6,7]. (4) In a popular model of the Apollo 16 site geology, an Imbrium ejecta deposit, the Cayley Formation, overlies a Nectaris ejecta deposit, the Descartes Formation, and the North Ray Crater (NRC) impactor penetrated the Cayley to exhume and deposit Descartes material at the surface [e.g., 2]. However, our preliminary inspection of data from Lunar Prospector [5] and Clementine [9] indicate that in the vicinity of the Apollo 16 site there is no significant compositional distinction at the surface between the Descartes and Cayley Formations. (5) Feldspathic fragmental breccias, a characteristic lithology of NRC, are identified as a likely Descartes component [8]. In addition to clasts of granulitic breccia, they contain clasts of Th-rich impact-melt breccia; the only such clast measured is 3.9 Gyr in age [10]. Thus, the feldspathic fragmental breccias of NRC may be constituents of a heterogeneous ejecta deposit from Imbrium, not Nectaris. (6) There is no evidence in the Ar isotopic data for Apollo 16 impact-melt breccias ("other..." Fig. 1) that the Cayley Plains and NRC ejecta sampled basin deposits of a different ages or that KREEP-rich and non-KREEP-rich breccias sampled basin deposits of different ages.

In combination, these issues suggest that the NRC impactor did not penetrate the Cayley Formation and excavate Descartes Formation and that few if any Apollo 16 rocks record the age of Nectaris. Thus, Nectaris may have formed earlier than 3.9 Gyr ago, perhaps at 4.1 Gy [11,12]. Ages of ~3.9 Gyr may approximate the age of Imbrium or Serenitatis or "may not have any chronologic significance."

References: [1] Wilhelms (1987) *The Geologic History of the Moon*, USGS Prof. Paper 1348; [2] Stoffler & Ryder (2001) *Space Sci. Rev.* 96, 9–54; [3] James (1981) *PLPSCI2B*, 209–233; [4] Haskin et al. (2002) *L&PS* 33, #1364; [5] Lawrence et al. (2000) *J. Geophys. Res.* 105, 20,307–20,331; [6] Haskin et al. (1998) *Meteorit. Planet. Sci.* 33, 959–975; [7] Korotev (2000) *J. Geophys. Res.* 105, 4317–4345; [8] Stoffler (1985) *PLPSCI5*, C449–C506; [9] Lucey et al. (1995) *Science* 268, 1150–1153; [10] Marvin et al. (1987) *PLPSC* 17, E471–E490; [11] Schaeffer & Schaeffer (1977) *PLSC* 8, 2253–2300; [12] Wetherill (1981) In *Multi-Ring Basins, PLPSCI24*, 1–18; [13] Steiger & Jäger (1977). *Earth Planet. Sci. Lett.* 36, 359–362.

Figure 1. Whole-rock ^{40}Ar - ^{39}Ar ages of Apollo 16 breccias with ages >3.6 Gyr. Squares represent samples from stations 11 and 13 (North Ray Crater); triangles represent all other stations (Cayley Plains). Filled symbols represent samples with compositions like melt groups 1 and 2 of [6] and which, consequently, are likely to be mafic and contain a large proportion of KREEP (>3 $\mu\text{g/g}$ Th). Unfilled symbols represent samples with like melt groups 3 and 4 of [6] and which are likely to be feldspathic with little or no KREEP. Data are from the compilations of [2] and [3], which include only ages derived from "good" plateaus and which have been corrected to decay constant of [13]. For data from the lab of O. Schaeffer, we assume correction procedure of [3] to be more valid than that of [2]. For the few samples for which more than one age is available, the error-weighted mean is plotted. Each point represents a different sample.

IDENTIFYING LOCATIONS FOR FUTURE LUNAR SAMPLE MISSIONS. D. J. Lawrence¹, R. C. Elphic¹, W. C. Feldman¹, O. Gasnault², T. H. Prettyman¹, D. T. Vaniman¹, ¹Los Alamos National Laboratory, Los Alamos, NM; ²Observatoire Midi-Pyrénées, Toulouse, France.

Introduction: With global composition data in hand from the Clementine [1] and Lunar Prospector (LP) [2] missions, one of the goals for using these data is to delineate the full range of lunar elemental and compositions. Based on samples, our knowledge of lunar compositions is limited in a number of ways. For the Apollo and Luna missions, we only have samples from nine different locations. Most of these locations are situated in or near the Th-rich PKT [3]. The range of known lunar compositions is extended by lunar meteorites, which include samples from regions such as the unsampled lunar highlands [4] and unsampled mare basalt regions [e.g., 5]. However, information from lunar meteorites is limited because the exact provenance of these samples is unknown.

A goal for future lunar missions will be to return samples from or study *in situ* previously unsampled regions. While many criteria will be used to select such locations (e.g., age of region, terrane location, geologic complexity, ease of accessibility), one criteria that should also be considered is composition. In particular, future landing sites should have a surface composition that is different from known sample abundances. Two well known locations that satisfy this criteria are South Pole-Aitken (SPA) Basin, because of a likely exposure of lower crustal material [6]; and the permanently shaded craters at the lunar poles that have anomalously high hydrogen abundances thought to be in the form of water ice [7]. While not discounting the importance of SPA Basin and the hydrogen-rich poles, we have used LP data to identify three other regions showing compositions that are significantly different from what we see in samples (see triangle that outlines sample Fe/Th abundances in Fig. 1). It should be noted that when LP data are used to interpret compositionally anomalous regions, these regions will cover a large area $\geq (60 \text{ km})^2$ because of the large LP footprint. In addition, LP measurements are more appropriately compared to regolith soil compositions than rock compositions, again because of the large footprint and because LP data measure compositions down to a depth of $\sim 30 \text{ cm}$.

Compton/Belkovich: One of the most dramatic regions identified with LP-GRS data is the Compton/Belkovich (CB) thorium anomaly [8]. Located at (60°N , 100°E), this region is unique on the Moon by having relatively high Th abundances ($5 \mu\text{g/g}$) and low FeO abundances ($\leq 5 \text{ FeO wt.}\%$). This region has recently been associated with a 20 km albedo feature [9]. If the entire Th signal seen with the LP-GRS data comes from this feature, then the surface Th abundance

could be as high as $20 \mu\text{g/g}$. As shown in Fig. 1, the Th-Fe abundances at CB (especially for $[\text{Th}] > 5 \mu\text{g/g}$) fall outside of the range of most measured soil abundances.

Western Procellarum Mare Basalts: Based on LP-GRS data, large expanses of mare basalt in western Procellarum show both FeO and Th abundances that are significantly higher than what is seen with sampled regolith soils (Fig. 1). In particular, the maximum FeO abundance of 25 wt.% is $\sim 20\%$ higher than what has been measured in regolith soil samples [10]. The Th abundances in this region are also significantly higher than what is seen for most mare basalt soil samples. While some of this high-Th material may be due to non-mare/mare mixing, in at least some locations, it is thought that the high-Th material is native to the mare basalts [e.g., 11, 12].

Highlands NW of Crisium Basin: Using newly reduced LP-GRS Mg and Al data, a large area region ($\sim 700 \text{ km}^2$) NW of Crisium basin [13] appears to show Mg# values that are significantly higher than bulk regolith soil measurements [14], but comparable to some of the highest Mg# rock measurements [e.g., 15]. Because of its expanse, this region may be a good location for a sample mission to find large amounts of Mg-rich material not seen elsewhere on the Moon.

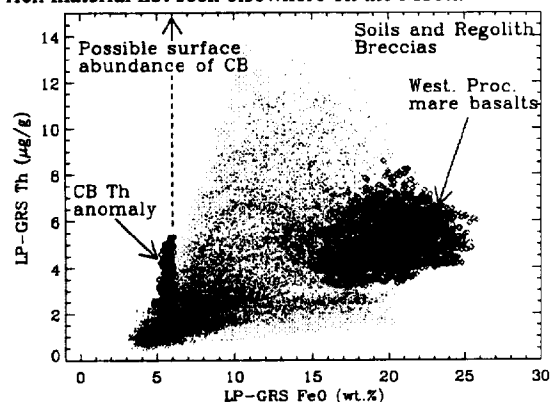


Fig. 1: Th vs. FeO abundances (small points) measured with the LP-GRS [8, 10]. Light blue triangle shows the range of abundances from soils and regolith breccias [16]. Abundances from CB and western Procellarum are also shown.

References: [1] Lucey et al., *JGR*, 105, 20297, 2000; [2] Prettyman et al., *33rd LPSC*, #2012, 2002; [3] Jolliff et al., *JGR*, 105, 4197, 2000; [4] Korotev, *30th LPSC*, #1303, 1999; [5] Fagan et al., *Met. and Plan. Sci.*, 37, 371, 2002; [6] Pieters et al., *JGR*, 106, 28001, 2001; [7] Feldman et al., *JGR*, 106, 23231, 2001; [8] Lawrence et al., *33rd LPSC*, #1970, 2002; [9] Gillis et al., *33rd LPSC*, #1967, 2002; [10] Lawrence et al., *JGR*, in press, 2002; [11] Gillis et al., *33rd LPSC*, #1934, 2002; [12] Gasnault et al., *33rd LPSC*, #2010, 2002; [13] Prettyman et al., this meeting; [14] Vaniman et al., this meeting; [15] Warren, *Ann. Rev. Earth Planet. Sci.*, 13, 201, 1985; [16] Korotev, *32nd LPSC*, #1134, 2001.

LUNAR SURFACE OUTGASSING AND ALPHA PARTICLE MEASUREMENTS. S. L. Lawson¹, W. C. Feldman¹, D. J. Lawrence¹, K. R. Moore¹, R. C. Elphic¹, S. Maurice², R. D. Belian¹, and A. B. Binder³.
¹Los Alamos National Laboratory, Los Alamos, NM; ²Observatoire Midi-Pyrénées, Toulouse, France; ³Lunar Research Institute, Tucson, AZ. (stefs@lanl.gov)

Introduction: The Lunar Prospector Alpha Particle Spectrometer (LP APS) searched for lunar surface gas release events and mapped their distribution by detecting alpha particles produced by the decay of gaseous radon-222 (5.5 MeV, 3.8 day half-life), solid polonium-218 (6.0 MeV, 3 minute half-life), and solid polonium-210 (5.3 MeV, 138 day half-life, but held up in production by the 21 year half-life of lead-210). These three nuclides are radioactive daughters from the decay of uranium-238. Radon reaches the lunar surface either at areas of high soil porosity or where fissures release the trapped gases in which radon is entrained. Once released, the radon spreads out by "bouncing" across the surface on ballistic trajectories in a random-walk process. The half-life of radon-222 allows the gas to spread out by several 100 km before it decays (depositing approximately half of the polonium-218 recoil nuclides on the lunar surface) and allows the APS to detect gas release events up to several days after they occur. The long residence time of the lead-210 precursor to polonium-210 allows the mapping of gas vents which have been active over the last approximately 60 years. Because radon and polonium are daughter products of the decay of uranium, the background level of alpha particle activity is a function of the lunar crustal uranium distribution.

Using radioactive radon and polonium as tracers, the Apollo 15 and 16 Command Module orbital alpha particle experiments obtained evidence for the release of gases at several sites beneath the orbit tracks, especially over the Aristarchus Plateau and Mare Fecunditatis [1]. Aristarchus crater had previously been identified by ground-based observers as the site of transient optical events [2]. The Apollo 17 surface mass spectrometer showed that argon-40 is released from the lunar interior every few months, apparently in concert with some of the shallow moonquakes that are believed to be of tectonic origin [3]. The latter tectonic events could be associated with very young scarps identified in the lunar highlands [4] and are believed to indicate continued global contraction. Such quakes could open fissures leading to the release of gases that are trapped below the surface. A primary goal of the APS was to map gas-release events, thus allowing both an appraisal of the current level of tectonic activity on the Moon and providing a probe of subsurface uranium concentrations.

Analysis: The APS consisted of five pairs of silicon ion-implanted detectors which were collimated

to a 45° half-angle aperture. The detectors were positioned on the five outward-pointing faces of a cube which was mounted at the tip of one of the spacecraft booms. The five analog signals sent to the electronics box were digitized using a common 8 bit ADC, spanning the nominal energy range between 4.5 MeV and 6.6 MeV (corresponding to 0.02 MeV per channel). The detector resolution was approximately 0.1 MeV. During data acquisition, LP spun at 12 RPM with its spin axis approximately perpendicular to the ecliptic. Thus, three of the APS faces swept through nadir when the spacecraft was near the equator, while the other two faces were either nadir- or zenith-pointing when the spacecraft was near the poles.

The primary lunar alpha-particle signal is from reflected interplanetary alpha particles. Therefore, we have examined only APS data acquired during periods of low interplanetary alpha particle flux. To minimize statistical uncertainties, spectra were summed over all LP mapping cycles when the instrument was turned on (approximately 229 days over 16 months).

Conclusions: The LP APS data were studied to map sites of radon release on the lunar surface. We found only a faint indication of alpha particles resulting from the decay of polonium-218. However, our radon-222 alpha particle map indicates that radon gas is presently emanating from the vicinity of craters Aristarchus and Kepler. The LP gamma-ray spectrometer, which effectively has significantly higher spatial resolution than the APS, identified thorium enrichments at these two craters [5]. Thorium and uranium are both incompatible elements whose lunar surface abundances are highly correlated; thus, it is likely that the radon-222 alpha particles measured using the LP APS originate from Kepler and Aristarchus. Our detection of radon over Aristarchus is consistent with one of the results of the Apollo 15 APS. The polonium-210 distribution mapped by the APS indicates a variability in time and space of lunar gas release events.

References: [1] Gorenstein P. (1993) in *Remote Geochemical Analysis*, C.M. Pieters and P.A.J. Englert, eds., 235. [2] Middlehurst B. (1967) *Rev. Geophys.*, 5, 173. [3] Hodges R. and J. Hofman (1975) *Proc. Lunar Sci. Conf. 6th*, 3039. [4] Schultz P. (1976) *Moon Morphology*, Univ. of Texas, Austin. [5] Lawrence D.J. *et al.* (2000) *JGR*, 105, 20307.

ANOMALOUS FADING OF STIMULATED LUMINESCENCE (TL/OSL): COMPARISONS BETWEEN LUNAR MATERIALS AND THE JSC MARS-1 SIMULANT. K. Lepper, Luminescence Geochronology Lab, Los Alamos National Laboratory, MS J495, EES-10, Los Alamos, NM 87545; lepper@lanl.gov.

Introduction: Thermoluminescence (TL) from silicate minerals has been used by planetary geoscientists to investigate a variety of topics such as; transient lunar phenomena, lunar heat flow characteristics, space radiation exposure and thermal history of meteorites, and terrestrial residence time of meteorites [1]. Recently an advanced related technique, optically stimulated luminescence (OSL), has been proposed as an age-dating method for sedimentary deposits on Mars [2]. Dating applications of TL and OSL can be complicated by a property, notably present in feldspars, known as anomalous fading. A functional definition of anomalous fading is a loss of charge from thermally stable defect sites via athermal mechanisms, resulting in a decrease in dose-related luminescence over time. Additional review of anomalous fading, its mechanisms and effects, can be found in [1,3].

Review: *Anomalous fading in lunar samples.* TL investigations were conducted on a variety of lunar samples including crystalline rocks, breccias, and surface fines (bulk samples) [4]. Reports of anomalous fading as "leakage", "drainage", and "non-thermal signal effects" are numerous [4 (and many others)]. The similarity of TL properties, including anomalous fading, among lunar samples and terrestrial feldspars was also examined [5]. Based on these observations and other aspects of TL, the method was discounted for dating lunar samples [6]. Anomalous fading aside, the age of lunar surface materials is far beyond the range accessible by TL dating.

Objective: This study utilizes three different luminescence stimulation methods to evaluate the anomalous fading characteristics of JSC Mars-1 and compares them with existing data for lunar samples.

Methods: *Evaluating anomalous fading in JSC Mars-1.* A 25g bulk sample of JSC Mars-1, a terrestrial analog for Martian surface soils [7], was given a 3.3kGy γ dose from a ^{60}Co source. At approximately logarithmic time intervals during a four-month storage period aliquots were prepared by placing loose sediment into stainless steel cups and the luminescence was measured from 8-16 aliquots for each of three stimulation methods. All measurements were conducted using a Risø DA-15 automated TL/OSL reader. Measurements were initiated by stimulation with heat (TL), visible light (OSL; 420-580nm), or infrared light (IR-OSL; 875 \pm 80nm). The resulting luminescence was monitored in the UV range (340 Δ 80nm). The mean and median signal intensity and standard deviation was determined for each data group corresponding to various measurement delay intervals. F-test statistical analysis was used to determine if the group means were significantly different.

Results/Discussion: *Anomalous fading in JSC Mars-1.* The TL and OSL signal medians and inferred population means from JSC Mars-1 decreased with increasing delay time. F-test analysis provided sufficient evidence to conclude that a difference exists among the TL and OSL group means (at 90% C.L.). Therefore, anomalous fading is indicated for these stimulation methods.

No trend was observed, however, in the IR-OSL group medians or inferred population means. Additionally, insufficient evidence was obtained from F-test analyses to conclude that a difference exists among the IRSL group means (at 90% C.L.), indicating that the means of each group are not significantly different. Therefore, fading is not suggested for the IR-OSL data as evaluated here. This result is noteworthy as evidence of anomalous fading in the IR-OSL signal of JSC Mars-1 would be anticipated based on its composition, which includes Ca-rich feldspars [7,8].

The observation of TL and OSL anomalous fading in JSC Mars-1 is consistent with similar analyses of lunar samples [4,5] and terrestrial basaltic rocks [9]. The TL and OSL results from this longer duration (10^7 s) fading analysis appear to be in contradiction to an evaluation of short-term anomalous fading ($<10^4$ s) previously reported for JSC Mars-1 [2]. However, the short-term analyses were based on measurements from one aliquot per stimulation method. Subsequent work on a larger set of aliquots suggests inhomogeneous fading within JSC Mars-1, i.e. some aliquots exhibited no OSL or IR-OSL fading while others showed up to 50% signal loss over a 2 month period [10].

Conclusion: It is clear that continued study of anomalous fading in feldspars will be required as OSL dating techniques are adapted for use on Mars. Future studies could benefit greatly from analysis of lunar samples in which anomalous fading of TL has previously been documented.

References: [1] McKeever, S. (1985) *Thermoluminescence of solids*. Cambridge Univ. Press, Cambridge UK. [2] Lepper, K. & McKeever, S. (2000) *Icarus*, 144, 295-301. [3] Aitken, M. (1998) *An introduction to optical dating*. Oxford Univ. Press, Oxford UK. [4] Dalrymple, G., & Doyle, R. (1970) *Geochem. Cosmochim. Sup.* 1(3), 2081-2092. [5] Garlick, G. et al. (1971) *Geochem. Cosmochim. Sup.* 2(3), 2277-2283. [6] Garlick, G. & Robinson, I. (1972) in *The Moon*, Reidel Pub., Dordrecht, Holland. [7] Allen, C. et al. (1998) *EOS*, 79(34), 405-409. [8] Spooner, N. (1994) *Radiat. Meas.* 23, 625-632. [9] Wintle, A.G. (1973) *Nature* 245, 143-144. [10] Banerjee, D., et al. (2002) *Radiat. Protect. Dosimetry* 100/101, in press.

POLAR NIGHT: A MISSION TO THE LUNAR POLES P. G. Lucey¹ ¹Hawaii Institute of Geophysics and Planetology, University of Hawaii at Manoa, 2525 Correa Road, Honolulu HI 96822 (lucey@higp.hawaii.edu).

The Discovery Program, through measurements by the Lunar Prospector spacecraft, established that the volatile element hydrogen is enriched in the lunar polar regions. It is virtually certain that this enrichment is due to cold trapping of hydrogen in one or more chemical states owing to the low temperatures of obliquely illuminated and permanently shadowed regions near the Moon's poles. This measurement confirms suggestions that the lunar (and mercurian) polar regions can capture and retain volatiles that encounter these surfaces. Modeling of lunar polar temperatures has indicated that water ice at shallow depths can persist for geologic time, even at high latitude regions which are not permanently shaded. Modeling of permanently shadowed craters indicates that temperatures in the shallow subsurface are low enough, as low as 40 kelvins, to retain for geologic time extremely volatile ices including carbon dioxide, methane, ammonia, sulfur dioxide. These model temperatures are also low enough to retain a host of low molecular weight organic compounds. Modeling of the Moon's obliquity over time indicates that permanently shaded regions can have persisted for 2.5 BY, exposing them to a host of potential sources of volatiles.

The confirmed existence of lunar cold traps raises the possibility that the lunar poles have trapped and retained volatile materials from sources which are central to many aspects of NASA's strategic plans. These sources include comets, asteroids, interplanetary dust particles, interstellar molecular clouds, the solar wind, and lunar volcanic and radiogenic gases.

In addition to the possible presence of volatiles originating from strategically important sources, the temperatures, energy available and plausible presence of feedstock elements captured by the cold trap raises the possibility of synthesis of organic molecules in situ on the Moon. Hydrogen is known to be present at reasonably high abundances even at the 50km scale of lunar prospector measurements. C and N may have accumulated in the form of volatile ices or at least exists as cold-trapped solar wind on grain surfaces. These elements, coupled with low temperatures and temperature cycling, have been shown to produce organic molecules when exposed to a driving energy source. The polar surfaces are illuminated by Lyman alpha and by galactic cosmic rays. While the UV is limited to the optical surface, the upper few centimeters of the regolith experience a relatively high flux of energetic protons derived from the galactic cosmic ray cascade. The lunar poles may then provide a natural

laboratory for organic synthesis on silicate grains which may mimic conditions found in interstellar space. At minimum, the lunar field conditions can enable a test of models of organic synthesis in space in a way that complements the organic rich conditions on Titan.

Despite these possibilities and plausibilities, all that is known about the lunar poles regarding this problem is that hydrogen is enriched, and that temperatures are low. There is no information on the presence of other volatiles and the temperatures and temperature variations of the coldest portions of the poles, the permanently shadowed regions, are unknown.

The Polar Night mission will conduct an inventory of volatiles and provide sufficient analysis to determine or greatly constrain the sources of polar volatiles and their nature. Polar Night will determine the chemical composition, abundance and deuterium to hydrogen ratio of volatiles cold-trapped in permanently shadowed regions of the lunar poles. These measurements will be conducted in situ using mass spectrometers, and neutron spectrometers deployed on six penetrator hard landers. The landing sites of the penetrators will be selected using remote measurements of the temperature, H-abundance at high resolution, and radar polarization properties measured from orbit during a six month remote sensing campaign.

A COMPLETE FIRST ORDER MODEL OF THE NEAR-INFRARED SPECTRAL REFLECTANCE OF THE MOON. P. G. Lucey¹, and D. Steutel¹ ¹Hawaii Institute of Geophysics and Planetology, University of Hawaii at Manoa, 2525 Correa Road, Honolulu HI 96822 (lucey@higp.hawaii.edu).

Introduction: The spectral reflectance properties of the Moon are governed by the minerals and glasses composing the lunar regolith, their physical state, and the optical effects of soil maturity. Work by Hapke and others has provided all the tools necessary to produce a model of near-IR spectra of the Moon within simplifying assumptions. We have produced such a model and are beginning to apply it to lunar science problems. Two classes of problems are amenable to immediate use: determining compositions of lunar surface regions using groundbased and Clementine data, and understanding the detection limits for minerals and rock types using existing and planned data sets.

Model: Our model is based on the equations of Hapke [1] who showed how the visible and near-IR spectra of mixtures of minerals could be computed from their optical constants at arbitrary grain sizes and relative abundances, and recently it was shown how the method of [1] could be modified to include the effects of submicroscopic particles [2].

Optical constants of all components are required for this model. An inversion of the Hapke equations was presented by [3] in order to compute optical constants from reflectance spectra. We used this inversion to compute the optical constants of anorthite from a spectrum of the mineral in the USGS Denver spectrum library. For the optical constants of olivine we used the optical constants computed by [3]. For pyroxene we applied a new methodology wherein we fit the optical constant spectra of a series of pyroxenes with Gaussians, then regressed the Gaussian parameters on composition, ignoring Gaussians we believed due to water or iron oxide contaminants. We simulated the spectrum of shocked anorthite by interpolating across the 1250 ferrous iron band of the USGS plagioclase. For native iron, no measurements of these constants exist at the spectral sampling of lunar telescopic measurements, but from 600 to 2000 nm the measurements of [4] Johnson and Christy (1974) scatter randomly about straight lines for both n and k , so we used linear fits to the Johnson and Christy data to represent the optical constants of Fe.

In the forward implementation of the model, the chemistry of minerals, grain sizes, modal abundances and abundance of submicroscopic iron are defined. From the mineral and glass chemistries optical constants are computed, which are then modified by submicroscopic iron coatings. These modified optical constants are then converted to single scattering albedo and mixed according to their modal abundances.

Results: Qualitatively, the model produces spectra which closely mimic the appearance of lunar spectra, sharing albedo, continuum slope, and spectral contrast, as well as the shape of the absorption features. Validation of the forward model is proceeding using the spectra and analyses of [5]. The validation will determine, for example, when the model prescribes a certain grain size, or grain size distribution, how this optical grain size corresponds to that measured via sieving.

An important unresolved measurement involves submicroscopic iron. Hapke showed that the optical effects of iron extend far beyond the range detected by ferromagnetic resonance. Work by Morris shows that the correlation between various small grain sizes of iron is relatively poor. Thus, measurements of Is/FeO can only weakly constrain the amount of submicroscopic iron prescribed by our model to best fit lunar spectra. Future lunar soil validation measurements should measure a wider, or additional, iron size ranges.

While the validation process is proceeding, we have applied the model to lunar science problems that do not depend critically on absolute abundances. For example, we recently showed that areas on the Moon previously interpreted to be composed of anorthosite that had its 1.25 micron band erased by shock, can plausibly be mimicked by spectra of mature crystalline anorthosite [6].

A recently introduced application of this model is to determine detection limits for minerals as a function of soil maturity and data quality (signal to noise ratio). In this process we model a particular soil composition, ensuring that the model spectrum lies within the field of measured lunar spectral properties. We then vary modal and chemical properties to determine the magnitude of the differential signal that can be detected by a remote sensor. Our preliminary results suggest that 10% differences in mineralogy can only be detected for the most immature surfaces at the 1% precision of Clementine and groundbased data. Future lunar missions should feature sensors with much higher signal to noise ratios.

References: [1] Hapke, B., *Theory of Reflectance and Emission Spectroscopy*, Cambridge Univ. Press, Cambridge, 1993, [2] Hapke, B., *J. Geophys. Res.*, 106, E5, 10,039-10,074, 2001., [3] Lucey, P.G., *J. Geophys. Res.*, 103, E1, pp1703-1714, 1998. [4] Johnson, P and R. Christy, *Phys. Rev. B*, 9, 5056-5070, 1975, [5] Taylor L. A., Pieters C. M., Keller L. P., Morris R.V., McKay D. S. (2001), *J. Geophys. Res.* 106, 27,985-27,999., [6] Lucey, P.G. GRL in press.

SEARCH FOR CORRELATIONS BETWEEN CRUSTAL MAGNETIC FIELDS AND OTHER LUNAR PROPERTIES. D. L. Mitchell¹ (*mitchell@ssl.berkeley.edu*), J. S. Halekas¹, R. P. Lin, S. Frey¹, and L. L. Hood²,
¹Space Sciences Laboratory, University of California, Berkeley, CA 94720, USA, ²Lunar and Planetary Laboratory, University of Arizona, Tucson, AZ 85721, USA.

Introduction: The correlation of surface magnetic fields with other known properties of the Moon can provide clues to the origin of the magnetization. In principle, crustal magnetization can exist anywhere from the surface down to the Curie isotherm (770 C for iron), which is at least several tens of kilometers beneath the surface. Thus, we must search for correlations of the magnetic field with both surface and subsurface properties.

The significance of any statistical analysis depends on the amount of data available. The sparse electron reflection data from the Apollo program, which was confined within ~35 degrees of the lunar equator and undersampled by a factor of ~100, made statistical analysis difficult. With the exception of a linear magnetic feature that follows Rima Sirsalis [1] and a tendency for strong anomalies to occur in association with unusual albedo markings of the Reiner Gamma class [2], no clear-cut association of surface magnetic fields with surface selenological features was found.

Lunar Prospector MAG/ER data provide global coverage and improve the sampling of the surface magnetic field by more than an order of magnitude. The power of this new data set was demonstrated in a study of the magnetic properties of lunar nearside geologic units [3], which clearly showed that Cayley deposits are associated with magnetic anomalies. Another correlation appears to exist between the surface magnetic field and thorium concentration in the region antipodal to the Imbrium basin [4]. Both of these correlations suggest that ejecta from the Imbrium impact may be a significant source of anomalies.

Surface: A systematic analysis over the entire lunar surface may reveal more such correlations. To make this practical, we have digitized 1:500,000 scale geologic maps covering the entire Moon, thus eliminating the need for laborious manual entry of geologic information. To obtain the best quantitative results, we use a Gaussian ideogram technique, wherein each data point is represented by a unit Gaussian centered at the magnetic field value, with a width corresponding to the statistical uncertainty. These Gaussians are first weighted by area (the original binning was equal-angle rather than equal-area), then added to create smooth unbiased estimates of magnetic field distributions. We can then use standard statistical tests (e.g., Kolmogorov-Smirnov) to determine the significance of observed differences in the magnetic field distributions for different terrains.

Preliminary results using this technique are promising. Apollo data showed [5], and LP data confirmed [6, 7], that the largest regions of strong magnetic fields lie on the lunar far side, diametrically opposite (antipodal) to young large impact basins. Our statistical results show that these antipodal regions are significantly more magnetic than any widespread non-antipodal terrain. The average surface magnetic field strength is 11 nT over the Nectaris, Serenitatis, and Crisium antipodes, and 34 nT over the younger Imbrium and Orientale antipodes. (These values are calculated by averaging

all data lying within one basin radius of the antipode centers.) In contrast, the average field over the entire lunar surface is 4 nT, while the average field outside the five antipodal regions is only 3 nT.

Correlation of magnetic fields with impact craters also reveals significant trends. We have taken all known craters and basins with diameters greater than 50 km whose age can be at least roughly determined (by crater counts and/or superposition relations), and searched for a relationship between crater age and the magnetic field intensity both within and surrounding the crater. We find that basins and craters of all ages are less magnetic than the surrounding ejecta blankets (and whatever lies beneath them), showing that even pre-Nectarian basins and craters may have been at least partially demagnetized. This implies that crustal magnetization must have existed in pre-Nectarian times.

Subsurface: There is no guarantee that the sources of crustal magnetic fields always lie close to the surface. Previous work has indicated that the magnetization depth is probably no more than a few tens of km [8]; however, even at this depth there might be little correlation with surface geology or composition. Therefore, we have obtained gravity and topographic data from the Clementine mission and used cluster analysis to search for relationships between these subsurface properties and the surface magnetic field.

This analysis clearly shows the correlation between the lowest magnetic fields and the gravity anomalies (mascons) associated with the major impact basins and reproduces the strongly magnetized impact basin antipodal zones. Also, apart from the impact basins, there is no correlation between crustal thickness and magnetic field, which supports the interpretation that the observable surface magnetic field arises from a relatively shallow layer.

References: [1] Anderson, K. A., et al. (1977) *Earth Planet. Sci. Lett.*, 34, 141. [2] Hood, L. L., P. J. Coleman, and D. E. Williams (1979) *Science*, 205, 53. [3] Halekas, J. S., et al. (2001) *JGR*, 106, 27841. [4] Lawrence, D. J., et al. (2000) 31st LPSC, Abs. #1856. [5] Lin, R. P., et al. (1988) *Icarus*, 74, 529. [6] Hood, L. L., et al. (2001) *JGR*, 106, 27825. [7] Mitchell, D. L., et al. (2002) submitted to *Science*. [8] Halekas, J. S., et al. (2002) *GRL* in press.

MISSION OUTLINE OF LUNAR-A. H. Mizutani¹, A. Fujimura¹, S. Tanaka¹, H. Shiraishi¹, S. Yoshida¹, and T. Nakajima¹, ¹Institute of Space and Astronautical Science, Yoshino-dai 3-1-1, Sagamihara, Kanaagawa, Japan, (e-mail address: mizutani@planeta.sci.isas.ac.jp)

Introduction: The Lunar-A mission of ISAS, Japan, will be launched in 2003 from Kagoshima Space Center using M-V launch vehicle. In this mission, two penetrators will be deployed on the near-side and the far-side of the Moon. Each penetrator contains an accelerometer, temperature sensors, thermal conductivity probes and two short-period seismometers. The seismological and heat flow data obtained by those instruments within the penetrator are first transmitted to a spacecraft orbiting at 200 km altitude and then sent back to the ground stations. The life time of the penetrator is estimated to be about one year. The seismic study will be made by observing various deep moonquakes at two widely-spaced stations. Observations of the amplitude and travel times of near-side deep moonquake event at the far-side stations offer a unique opportunity to prove or disprove the existence of a lunar core and to obtain information about its size and physical property. Data on the core size and its property are crucial to understand the bulk abundance of the siderophile elements. On the other hand, heat flow data at two sites will provide much better basis of estimating globally averaged heat flow value, which allow us to estimate the bulk abundance of refractory elements. Those cosmochemical signature derived from the penetrator experiment is essential for understanding the origin of the Moon.

Mission Profile: The lunar-A spacecraft is to be launched in summer of 2003 from the Kagoshima Space Center of ISAS, using M-V launch vehicle, which can send a spacecraft of 540 kg into a lunar transfer orbit. The spacecraft is first inserted into an elliptical lunar orbit in 2004, using complex Earth-lunar gravity-assist maneuvering for about one year. After insertion of the spacecraft into the lunar elliptical orbit whose perilune is about 40 km from the lunar surface, the penetrators will be separated from the orbiter.

After the separation of a penetrator from the orbiter, the orbital velocity of the penetrator is cancelled by a small solid-propellant motor and then the penetrator begins a free-fall from an altitude of about 25 km. The penetrator is impacted on the lunar surface at velocity of about 285 m/sec and with an attack angle less than 8 deg. According to numerous impact tests, each penetrator is predicted to come to rest in a depth of 1 to 3 m below the lunar surface[1].

The data gathered by the instrument in the penetrator are numerically compressed and stored in a data recorder within the penetrator before they are transmitted to Earth (with S-band) via the orbiting spacecraft (with UHF-band), which will pass above each penetrator about every 15 days.

Penetrator and Instruments: The Lunar-A penetrator has a missile-shaped body about 14 cm in diameter, 80 cm in length and 13 kg in mass. It contains two short-period seismometers, one for vertical motion, another for horizontal motion, 18 temperature sensors, and 5 thermal conductivity probes together with other supporting instruments, such as a tilt-meter and an accelerometer which are used to estimate the attitude and depth of the penetrator in the lunar regolith. All the instruments are powered by Li-SOCl₂ batteries with a power density of 430 Wh/kg, which limits the penetrator life time to about one year.

The Lunar-A seismometers are approximately 5 times as sensitive as either the Apollo short-period or long-period seismometers at frequencies of around 1 Hz. This high sensitivity allows us to obtain a higher S/N signals of seismic signals than Apollo data.

The heat flow probe consists of 18 temperature sensors and thermal conductivity probes, both of which are attached on the penetrator body surface. The vertical temperature gradient is obtained from the temperature sensors and the thermal conductivity of the regolith is obtained from the thermal conductivity probe, though accurate determination of the temperature gradient requires a detailed thermal model of the penetrator itself[3].

Seismic Experiment: A lunar seismic event is recorded only for a signal larger than a threshold (triggering) level in order to reduce power consumption and amount of data transfer. The recording duration depends on the size of the moonquakes, which will be judged 256 seconds after recognition of the event. Since each deep moonquake has its own characteristic waveform and an origin-time versus tidal-phase correlation[4], the focus of a deep moonquake is determined by data obtained at a single station near the Apollo 12 site. If we determine the foci of moonquakes, the amplitude and travel time of the seismic waves will provide important data on the internal structure. Particularly if we can detect a significant focusing effect of the seismic signal at a station near an antipodal point of a deep moonquake focus, it will give us a strong constraint of the lunar core size.

References: [1] Shiraishi et al. (2000) *ISAS Research Report* 677. [2] Mizutani et al. (2000) *Penetrometry in the Solar System, Verlag der Osterreichischen Akademie der Wissenschaften*, 125-136. [3] Tanaka et al. (1999) *Adv. Space Res.* 23, 1825-1828. [4] Nakamura (1978) *Proc. 9th Lunar and Planet. Sci. Conf.* 3489-3607.

SCIENTIFIC RESEARCH IN SELENE MISSION. H.Mizutani¹, S.Sasaki¹, Y.Iijima¹, K.Tanaka¹, M.Kato¹, and Y. Takizawa², ¹The Institute of Space and Astronautical Science(ISAS) (3-1-1 Yoshinodai, Sagamihara, Kanagawa 229-8510, JAPAN, sasaki@news1an.isas.ac.jp), ²National Space Development Agency of Japan(NASDA)

SELENE(Selenological and Engineering Explorer) mission is planned in 2005 for lunar science and technology development. The mission will consist of a main orbiting satellite at about 100 km altitude in the polar circular orbit and two subsatellites in the elliptical orbits with apolune at 2,400 km and 800 km. The orbiter will carry instruments for scientific investigation including mapping of lunar topography and surface composition, measurement of the magnetic fields, and observation of lunar and solar-terrestrial plasma environment.

The primary objective of the SELENE mission is to study the origin and evolution of the Moon by global mapping from the polar orbit at 100 km altitude. The element abundances are measured by x-ray and gamma-ray spectrometers. Alpha particle spectrometer is used to detect the radiation from the radon gas and polonium. The mineralogical characterization is performed by a multiband-spectrum imager at a high spatial resolution. The mineralogical composition can be identified by a spectral profiler, a continuous spectral analyzer in visible and near infrared bands. The surface topographic data are obtained by high resolution stereo cameras and a laser altimeter. The subsurface structure is probed by an rf radar sounder experiment. Doppler tracking of the orbiter via the relay satellite when the orbiter is in the far side is planned for study of gravimetry and geodesy. A magnetometer and electron detectors will provide data on the lunar surface magnetic field. Radio sources on the two subsatellites are used to conduct the differential VLBI observation from ground stations. Measurement of the lunar environment and observation of the solar-terrestrial plasma environment are also planned in the mission. The study of the lunar environment includes the measurement of high energy particles, electromagnetic field, and plasma. For the solar-terrestrial plasma observation, the orbiter carries imaging instruments to observe the dynamic structure of the earth plasma environment and the aurora. High-sensitivity wave receivers are used to detect the planetary radiation from the Jupiter and Saturn. For publicity and educational purposes, high-resolution cameras are onboard to observe the earth from the Moon orbit.

The spacecraft will be launched by the H-IIA rocket and directly injected into the lunar transfer trajectory. It takes about five days to reach the lunar orbit. The mid-course maneuver is planned twice on its way to the Moon. The spacecraft is captured by the Moon into an elliptical polar orbit with apolune at 11,300 km and perilune at 100 km. The apolune is lowered by 6 or-

bit-transfer maneuvers and finally the orbiter reaches the mission orbit at about 100 km altitude. During the orbit transition, the relay satellite and the VRAD satellite are released in the elliptical orbit with apolune at 2,400 km and 800 km, respectively. Upon arriving in the mission orbit, the main orbiter extends 4 antennas for the radar sounder experiment and a mast for the magnetometer. Remote-sensing observation of the lunar surface and observation of the lunar and solar-terrestrial plasma environment will be performed for about one year. The altitude of the main orbiter will be kept at 100 ± 30 km by orbit maintenance operation. If the fuel to control and keep the orbit is further available, the observation mission will be extended. One option is to lower the orbiter to 40-70 km altitude for precise measurement of the lunar magnetic and gravity fields. The two subsatellites have no fuel to keep their orbits, but will survive more than one year. Especially the VRAD satellite is expected to survive longer.

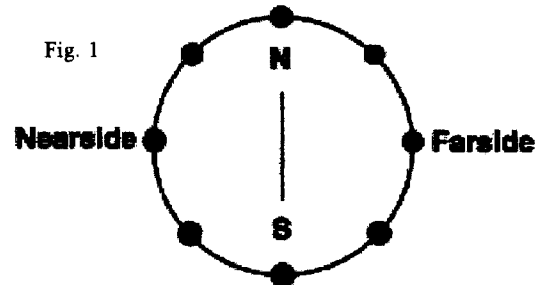
USING THE NEW VIEWS OF THE MOON INITIATIVE TO DEFINE FUTURE MISSIONS: THE LUNAR SEISMIC NETWORK. C. R. Neal, Department of Civil Engineering & Geological Sciences, University of Notre Dame, Notre Dame, IN 46556, USA; neal.1@nd.edu).

Introduction: The New Views of the Moon initiative is unprecedented in the history of lunar research because it has integrated remotely sensed and sample data in its approach to synthesizing lunar research over the last 30+ years. The integration of remotely sensed and sample data has clearly demonstrated what we know and, maybe more importantly, what we don't know about the Moon. Most significantly, it has helped to crystallize fundamental scientific questions that still need to be addressed and lessons learned from our study of the Moon provide an invaluable road map for our exploration of the inner planets. The results of the New Views initiative highlight in explicit detail just how little we know about the nature of the lunar interior. While studies of the Moon have produced the magma ocean hypothesis [e.g., 1], this cannot be fully tested until detailed seismic data are obtained and the nature of the lunar interior is fully evaluated. The existing Apollo seismic experiment data only provide us with clues about the interior of the Moon, primarily because the seismometers were set up in a relatively restricted area on the lunar nearside. Interpretations based on the limited seismic data are ambiguous. For example, the presence of garnet in the lunar mantle has been proposed by several authors to accommodate higher velocities in the middle mantle (>500 km) [e.g., 2-4]. This has been supported by geochemical evidence from some mare samples [5]. However, Nakamura et al. [6] and Nakamura [7] suggested that such velocities could be accommodated by an increased proportion of Mg-rich olivine. What has become apparent is a seismic discontinuity around 500 km, albeit somewhat heterogeneous in nature [8,9] and this has been interpreted as the maximum depth of LMO melting [7,10-12]. While innovative modeling approaches have refined the original data [e.g., 8,9], comprehensive and definitive interpretations of the lunar mantle remain elusive and fundamental questions regarding lunar origin, evolution, and structure remain unanswered. These include: What is the structure and thickness of the crust on the lunar near and far sides? Are crustal structure changes gradational or are distinct domains present? Is the ~500 km discontinuity a moon-wide phenomenon (magnasphere vs. magma ocean)? Do seismic data in the middle and deep lunar mantle define a unique garnet signature? What is the lunar core made of and how extensive is it? Are the core and mantle completely solid or do plastic zones still persist? Are nests producing Moon-quakes present on the far side?

The LUNAR-A Mission: The Japanese LUNAR-A mission is scheduled for launch in 2003 and will carry 2 penetrators, each containing heat sensors and 2 seismometers (5 times as sensitive as the Apollo seis-

mometers) [13]. One will be deployed on the nearside (between the Apollo 12 & 14 landing sites) and one on the farside of the Moon, with data being stored in the penetrator before being transmitted to Earth via an orbiter that passes overhead every 15 days [13]. The seismic experiment of LUNAR-A is designed to examine internal structure and core size and will last for one year (battery life in the penetrators).

A Possible New Frontiers Mission: In building upon the Japanese LUNAR-A mission, a seismic network is proposed for the Moon. In this mission, it is envisaged that a minimum of 8 seismometers will be deployed around the Moon (Fig. 1) to give coverage



from the nearside to the farside. An orbiting satellite will relay information back to Earth as it passes over each seismometer. The mission will last for a minimum of 2 years. A number of issues need to be addressed if this mission is to be successful. Firstly, the use of RTGs as a power supply will be essential if the mission is to last for more than ~12 months. Secondly, should the seismometers be delivered by penetrators or as soft landers? Finally, this proposed mission is intended to build upon the results of LUNAR-A and will be in cooperation with other space agencies—maximizing the science return is the goal. Planning for this mission is still in the preliminary stages, but it is hoped that this mission will be community-driven and that positive input from this workshop will help shape this into a highly successful New Frontiers mission to the Moon.

References: [1] Warren (1985) *Ann. Rev. Earth Planet. Sci.*, 13, 201-240. [2] Anderson (1975) *JGR* 80, 1555. [3] Hood (1986) in *Origin of the Moon*, 361, LPI, Houston. [4] Hood & Jones (1987) *PLPSC 17* in *JGR* 92, E396. [5] Neal (2001) *JGR* 106, 27865. [6] Nakamura et al. (1974) *GRL* 1, 137. [7] Nakamura (1983) *JGR* 88, 677. [8] Kahn et al. (2000a) *GRL* 27, 1591. [9] Kahn et al. (2000b) *LPSC XXXI* #1341. [10] Goins et al. (1981) *JGR* 86, 5061. [11] Mueller et al. (1988) *JGR* 93, 6338. [12] Hood & Zuber (2000) in *Origin of the Earth & Moon*, 397, Arizona Uni. Press. [13] Mitzutani et al. (2002) *NVM Europe*.

SIDEROPHILE ELEMENTS IN LUNAR IMPACT MELTS: IMPLICATIONS FOR THE CATACLYSM, IMPACTOR SOURCES, AND EARLY EARTH ENVIRONMENTS. M. D. Norman¹ and V. C. Bennett¹ ¹Research School of Earth Sciences, Australian National University, Canberra ACT 0200 AU (marc.norman@anu.edu.au, vickie.bennett@anu.edu.au).

Introduction: Siderophile element compositions of lunar impact melt breccias provide a primary record of the cratering history and types of impactors present in the early Solar System. In contrast to the wet and geologically active Earth, ancient impact basins on the Moon have not been reworked by weathering or tectonic events. Lunar impact breccias are, therefore, keystones for understanding such issues as the role of large meteorite impacts in the geologic evolution of terrestrial planets, and the environment in which biology and crustal structure originated on the Earth.

To improve our understanding of impact histories on the early Earth and Moon, we have studied the geochemistry of Apollo 17 poikilitic breccias which are thought to represent melt ejecta from the 3.89 Ga Serenitatis basin. Following an approach pioneered by Anders and colleagues, highly siderophile element patterns (Re, Ir, Pt, Pd, Ru) were used to image the type of impactor involved in the collision.

Impactor Discrimination: Siderophile elements are sensitive tracers of meteoritic contamination in impact melt rocks. Serenitatis impact melt breccias have W-shaped CI-normalized patterns which are enriched in Re, Ru and Pd relative to Ir and Pt, with absolute abundances ranging from ~0.5 to 4% of the CI reference values [1]. The high Pd/Pt and Re/Ir ratios of these breccias closely match the characteristics of EH-type enstatite chondrites, providing compelling evidence for the type of impactor responsible for the Serenitatis basin. As EH chondrites are thought to have formed in the inner Solar System, this precludes involvement of a comet or other outer Solar System body in this basin-forming impact event.

Was there a 3.9 Ga Cataclysmic Bombardment? On a heavily cratered body such as the Moon, cumulative meteoritic infall might lead to significant siderophile element contamination in the crust prior to formation of the late basins. The fact that projectile signatures can still be recognized in the lunar breccias shows either that the pre-impact crust was relatively free of meteoritic siderophiles, or that the impact which created these melt breccias was significantly larger than the aggregate meteorite flux prior to the basin-forming event. This argues against formation of the Nectarian and Lower Imbrian basins during a continuously declining accretionary bombardment because in that scenario the Serenitatis projectile would have impacted a crustal terrain already extensively contaminated by meteoritic siderophiles and the EH chondrite signature would be obscured. Formation of the large lunar basins during a short-lived spike in the cratering flux appears to be more consistent with the siderophile element compositions of lunar impact melt breccias.

Siderophile element signatures of pre-cataclysm lunar crust: Highly siderophile element compositions of the Apollo 17 poikilitic breccias vary systematically with concentration, from relatively constant Pd/Pt and Re/Ir ratios similar to those of EH chondrites at higher concentrations, to more fractionated compositions with high Re/Ir and Pd/Pt ratios unlike those of known meteorites at lower concentrations. These coherent trends within otherwise homogeneous breccias raise the possibility that the highly siderophile ele-

ment abundances have been modified during the impact process, and suggest a new framework for interpreting siderophile element characteristics of lunar impact melts.

The compositions of these breccias may be explained by a 2-stage impact melting process involving: (1) deep penetration of the Serenitatis impactor into meteorite-free lower crust, followed by (2) incorporation of upper crustal lithologies moderately contaminated by prior meteoritic infall into the melt sheet. This implies that the lunar crust was roughly zoned with an upper crust moderately contaminated by meteoritic infall or late accretionary veneer, grading to a meteorite-free lower crust at depth. Trends to higher Re/Ir and Pd/Ir with decreasing siderophile element concentrations may indicate an endogenous lunar crustal component, or a non-chondritic late accretionary veneer in the pre-Serenitatis upper crust.

Implications for the Early Earth: The large nearside lunar basins are coincident in age with the oldest terrestrial rocks, and are therefore relevant for considering the role of impacts in shaping the evolution of terrestrial continents and early life environments. Owing to its larger size and greater gravitational focusing, the Earth would have experienced both a significantly greater cratering rate and much larger mass accretion rate compared to the Moon. This implies that the Earth must have been hit by several large impacts during the crucial period in which the oldest preserved continental crust was forming and early life was evolving. Despite the catastrophic nature of these events, it is unlikely they were sufficiently energetic to evaporate the oceans or sterilize the Earth, and it is possible they helped establish environments conducive to the origin or evolution of life [2]. If enstatite chondrites are found to be an important population contributing to the 3.9-4.0 Ga cratering cataclysm, their fractionated siderophile element pattern may have contributed to mantle heterogeneity on Earth. The dry, reduced nature of enstatite chondrites would, however, preclude a significant contribution of these planetesimals to the volatile budget of the Earth and oxidation of the terrestrial mantle.

References: [1] Norman, Bennett and Ryder (2002) EPSL, in press [2] Ryder (2002) JGR 107, 10.1029.

CRYSTALLIZATION AGE AND IMPACT RESETTING OF ANCIENT LUNAR CRUST FROM THE DESCARTES TERRANE. M. D. Norman¹, L. E. Borg², L. E. Nyquist³, and D. D. Bogard³ ¹Research School of Earth Sciences, Australian National University, Canberra ACT 0200 AU (marc.norman@anu.edu.au) ²Institute of Meteoritics, University of New Mexico, Albuquerque NM 87131 (lborg@unm.edu) ³NASA Johnson Space Center, Mail Code SR, Houston TX 77058 USA (laurence.e.nyquist1@jsc.nasa.gov, donald.d.bogard1@jsc.nasa.gov).

Introduction: Lunar ferroan anorthosites (FANs) are relicts of an ancient, primary feldspathic crust that is widely believed to have crystallized from a global magma ocean. Compositions and ages of FANs provide fundamental information about the origin and magmatic evolution of the Moon, while the petrology and thermal history of lunar FANs illustrate the structure and impact history of the lunar crust. Here we report petrologic, geochemical, and isotopic (Nd-Sr-Ar) studies of a ferroan noritic anorthosite clast from lunar breccia 67215 to improve our understanding of the composition, age, and thermal history of the Moon.

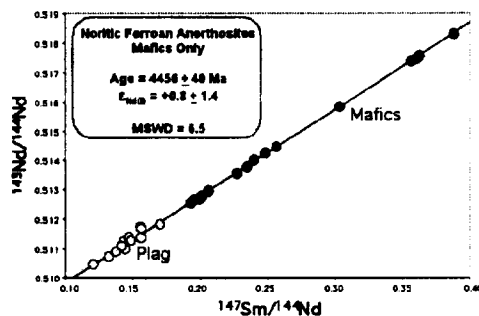
Significance of the Descartes Terrane: 67215 is a feldspathic fragmental breccia collected from the rim of North Ray Crater. These breccias have aluminous bulk compositions (28-30% Al₂O₃) that are poor in KREEP, low in meteoritic siderophiles, and lack solar wind carbon compared to lunar impact melts or regolith breccias [1]. Photogeologic and remote sensing data show that these breccias represent a regionally significant highlands unit exposed in the Descartes terrane to the north and east of the Apollo 16 landing site, and that their bulk compositions are broadly similar to those of large regions of anorthositic crust on the farside of the Moon. Descartes breccias may, therefore, provide a glimpse of a more representative region of the lunar crust than the KREEP-rich breccias which dominate the sample collection. Descartes breccias also carry ancient (>4.4 Ga) and relatively little modified crustal components that were derived from a region of the Moon distinct from the KREEPY hot-spot terranes [2, 3], making them useful for studies of early crustal genesis. Breccia 67215 consists predominantly of clasts and mineral fragments derived from a coherent suite of ferroan noritic anorthosites [2, 4], and one of these clasts is the subject of our study.

Results: The clast (designated 67215c) has an unusually well preserved, unbrecciated igneous texture. Mineral compositions combined with major and trace element characteristics show that 67215c is closely related to the ferroan anorthositic suite of lunar highlands rocks, but that it cooled more rapidly and at much shallower depths (≤ 0.5 km) compared to most other FANs (15-20 km).

¹⁴⁷Sm-¹⁴³Nd isotopic compositions of mineral separates from 67215c define an isochron age of 4.40 ± 0.11 Ga with an initial $\epsilon^{143}\text{Nd}$ of $+0.85 \pm 0.53$. ⁴⁰Ar-³⁹Ar ages of plagioclase from the clast record a post-crystallization thermal event at 3.93 ± 0.08 Ga ago, where the greatest contribution to the uncertainty in this age derives from a correction for lunar atmosphere ⁴⁰Ar. Rb-Sr isotopic systematics were severely disturbed by this event which likely dates emplacement of the Descartes feldspathic fragmental breccias, possibly as ejecta from the Nectaris basin.

Crystallization age of the lunar crust: Four ferroan noritic anorthosites have now been dated by ¹⁴⁷Sm-¹⁴³Nd mineral isochrons, producing apparent ages of 4.29-4.54 Ga. However, the Nd isotopic compositions of plagioclase in some FANs appear to have been modified by post-

crystallization exchange, whereas the mafic phases in these rocks remained resistant to this disturbance. ¹⁴⁷Sm-¹⁴³Nd isotopic compositions of mafic fractions from all four ferroan noritic anorthosites define an age of 4.456 ± 0.040 Ga which may be a robust estimate for the crystallization age of lunar ferroan anorthosites.



The best estimate for the initial ¹⁴³Nd isotopic compositions of FANs is provided by 60025 ($+0.9 \pm 0.5$; [5]) and 67215c ($+0.8 \pm 0.5$; this study). Both values are slightly higher than standard chondritic values (CHUR). An elevated initial Nd isotopic composition for the Moon might be related to early depletion of proto-lunar material by loss of small degree melts from explosively outgassed precursor planetesimals [6, 7], or accretion of the Moon from a depleted portion of a large impactor [8]. Alternatively, conventional CHUR values may not be precisely representative of material which formed the Earth and Moon.

References: [1] Norman (1981) PLPSC 12, 235-252 [2] Lindstrom and Lindstrom (1986) PLPSC 16, 263-276 [3] Alibert et al. (1994) GCA 58, 2921-2926. [4] McGee (1988) PLPSC 18, 21-31 [5] Carlson and Lugmair (1988) EPSL 90, 119-130 [6] Wilson and Keil (1991) EPSL 104, 505-512. [7] Taylor et al. (1993) Meteoritics 28, 34-52 [8] Warren (1992) EPSL 112, 101-116.

DOD TECHNOLOGIES AND CAPABILITIES OF RELEVANCE TO FUTURE LUNAR SCIENCE AND EXPLORATION OBJECTIVES. S. Nozette, Defense Advanced Research Projects Agency, 3701 N. Fairfax Ave, Arlington, VA, 22203, Email: snozette@darpa.mil, BGen S.P. Worden, USAF, US Space Command, Peterson AFB, Colorado Springs, CO, Email, Simon.Worden@PETERSON.af.mil

Currently several Department of Defense (DoD) Organizations are exploring new technologies which may be applied to future lunar science and exploration objectives. DoD launch vehicle programs currently reaching initial operational capability (e.g. Evolved Expendable Launch Vehicle), and future programs under study, can provide new capabilities for future lunar programs. These include the development of the EELV Secondary Payload Adapter (ESPA) which could allow low cost (few \$M) launch of capable (200 kg, 2 km/sec) microsattellites to Geosynchronous Transfer Orbit (GTO) or beyond. A suite of DoD developed microsattelite technologies with significant performance and reduced cost will also reach maturity in the next several years. These systems will provide comparable performance and a factor of 2 reductions in cost and mass from Clementine, developed earlier in the previous decade. Future lunar science and exploration objectives enabled by these capabilities include: astrodynamics operational verification, resource surveys, improved topographic, illumination and gravity mapping, low cost infrastructure for landers such as navigation, communications, and surface infrastructure required for future robotic and human missions. Several design concepts currently under investigation will be presented.

CAPABILITY AND DATA ANALYSIS OF THE MULTIBAND IMAGER FOR THE SELENE MISSION.
 M. Ohtake¹, H. Demura², and LISM Group ¹Lunar Mission Research Center, National Space Development Agency of Japan (NASDA) (2-1-1 Sengen, Tsukuba, Ibaraki 305-8505 Japan; E-mail: ohtake.makiko@nasda.go.jp), ²Lunar Mission Research Center, NASDA (E-mail: demura.hirohide@nasda.go.jp)

Introduction: The Lunar Imager/ SpectroMeter (LISM) is an instrument being developed for the SELENE project that will be launched in 2005. LISM consists of the three subsystems, the Terrain Camera (TC), Multiband Imager (MI), and Spectral Profiler (SP). Those systems share some components and electronics. MI is a high-resolution multiband imaging camera consisting of two visible and near infrared sensors.

Scientific Objectives: MI will observe the global mineral distribution of the lunar surface in nine band images during nominal one year SELENE mission. The spatial resolution of MI data is designed to be much higher than that of spectral images obtained by previous lunar missions. MI's high spatial resolution will enable us to investigate small but scientifically very important areas such as crater central peaks and crater walls. Investigations of such small areas are the subject of our study and will help answer current questions such as the existence, chemical composition and source of olivine at the central peaks of some craters. Main objectives of MI are as follows: 1) To search most primitive lunar crustal materials, 2) To understand horizontal and vertical structure of Mare basalt, 3) To survey outcrops of lunar mantle, 4) To understand mechanism of impact crater formation.

One of the advantages of MI data for such investi-

gation is that the topographic effect on the reflectance spectra can be corrected by an elevation model derived from TC stereo pairs and/or MI band images. Each MI band image has a slightly different tilt angle and can be used for developing elevation models.

Capability of MI: Currently flight model designing is finished [1]. To achieve scientific objectives MI is designed to have, 1) High spatial resolution (VIS: 20 m, NIR: 62 m from the 100 km SELENE orbital altitude) to understand mineralogy of small area, 2) High S/N (VIS: > 100, NIR: > 300) to classify rock types, 3) High radiance resolution, (VIS: 10 bit, NIR: 12 bit) to distinguish mare units, 4) Loss-less compression to preserve true DN value. Also to suppress stray light, masking on MI-VIS CCD surface, coating of unused band-path filters surface and coating between band-path filters are designed.

MI takes push-broom imaging data by using selected five lines for MI-VIS and four lines for MI-NIR which are selected before launch. The spectral band assignments are 415, 750, 900 and 1000 nm for visible and 1000, 1050, 1250 and 1550 nm for near infrared. On each line of the detectors, an appropriate band pass filter is mounted. Specification summary of MI is shown in Table 1.

It is confirmed from the flight model design and some measured data of already manufactured part of the flight model that the calculated S/N and other performances of MI are sufficiently satisfying our requirements for the scientific purposes.

Data analysis: We started to develop software for the analysis of LISM data (e.g., software for raw-data generation, radiometric and geometric corrections and photometric calibrations) [2]. For the data analysis we also started following studies. 1) Re-evaluation study of optical standard site on the moon to check its reliability and to estimate its error as standard of high resolution MI images. 2) Fundamental study to develop technique for estimating the abundance and chemical composition of mineral species by using reflectance spectra in our laboratory because this technique strongly affects the results of our data analysis and is especially important [3].

References: [1] Ohtake M. *et al.* (2002) *LPS XXXIII*, 1528 - 1529. [2] Hirata N. *et al.* (2002) *LPS XXXIII*, 1520 - 1521. [3] Ohtake M. *et al.* (2001) *LPS XXXII*, 1512-1513.

Table 1 Specification of MI

	VIS	NIR
Focal length	65 mm	65 mm
F number	3.7	3.7
Field of view	11 deg	11 deg
Spatial resolution	20 m	62 m
Swath width on ground	19.3 km	19.3 km
Detector	2D CCD (1024 x 1024 pixel)	2D InGaAs (320 x 240 pixel)
Pixel size	13 x 13 μm	40 x 40 μm
Detector cooler	N/A	N/A
Number of band	5	4
Band assignment	415 +/- 10 nm 750 +/- 5 nm 900 +/- 10 nm 950 +/- 15 nm 1000 +/- 20 nm	1000 +/- 15 nm 1050 +/- 15 nm 1250 +/- 15 nm 1550 +/- 25 nm
Quantization	10 bit	12 bit
S/N	> 100	> 100
MTF	> 0.2 @ Nyquist	> 0.2 @ Nyquist
Integration times	2.0, 4.1, and 8.2 msec	6.6, 13.2, and 26.4 msec
Data compression	DPCM method (loss-less)	N/A
Compression rate	< 80%	-
Solar elevation angle in operation	30-90 deg	
Data amount	49.0 Gbit/day	

ON SEARCH AND IDENTIFICATION OF SUPER HEAVY ($Z = 110 + 114$) AND SUPER SUPER HEAVY ($Z \geq 160$) COSMIC RAY NUCLEI TRACKS IN THE MOON OLIVINE CRYSTALS. V.P. Perelygin¹, I.G. Abdullaev¹, Yu.V. Bondar², Yu.T. Chuburkov¹, R.L. Fleischer³, L.I. Kravets¹, L.L. Kashkarov¹, ¹Joint Institute for Nuclear Research, Dubna, Russia, (pergam@cv.jinr.ru), ²Institute of Environmental Geochemistry, Kiev 03142, Ukraine, ³Department of Earth and Environment Science West Hall, R.P.I. Troy, New York, USA.

The main goal of the present work is the search and possible identification of relatively stable nuclei of Super Heavy ($Z = 110 - 114$) (SHE) and Super Super Heavy ($Z \approx 160$) elements (SSHE) in Galactic cosmic rays, basing on the fossil track studies of the olivine crystals from the Moon surface. Nuclei of the elements with $Z \geq 30$ up to Th - U and $Z = 110-160$ are most probably the products of Supernova explosion when freshly formed neutron star matter erupted outside (about 10% of its final mass). That neutron matter supposed to be then degraded. It is thought to be the main source of all the heaviest element in the Galaxy. The strong nonpermanent electromagnetic fields of exploding star can provide the acceleration of these freshly formed nuclei up to energies 10^6 MeV per nucleon.

It means that if the life time of these $Z \geq 110$ nuclei ranges from 10^3 to 10^7 years they can produce the long and very long tracks in extraterrestrial crystals. Our approach for the investigation of the ultra-heavy component of Galactic cosmic ray nuclei ($Z \geq 50$) has been developed since 1980. It depends on the ability of extraterrestrial nonconducting silicate crystals (olivine) to register and store during many million years the tracks due to cosmic ray nuclei with $Z \geq 22$. Our approach was based on the partial annealing of both fossil tracks and tracks due to accelerated Kr, Xe, Au, Pb and U ions and on the chemical etching of total volume track length of these nuclei in olivines [1].

Initially the olivine crystals taken from the Marjalahti and Eagle Station pallasites were annealed at 430°C during 32 hours and etched. The intercomparison of track length spectra of the fossil tracks and tracks due to the accelerated ^{238}U and ^{208}Pb nuclei proves unambiguously that the last two abundant peaks of "fossil" track length spectra (120-140 μm and 200-230 μm , first observed in 1980 in Dubna) are produced by Pt-Pb and Th-U groups of cosmic ray nuclei. During 1980-1996 more than 1600 Th-U fossil tracks were measured and 11 anomalously long tracks ($L = 340-370 \mu\text{m}$) were found.

The orientation of these anomalously long tracks in olivine crystal we recently determined with the Laue Roentgen and optical methods. We showed that 5 anomalously long fossil tracks had an angle $\geq 15^\circ$ to the main crystal planes and subsequently could be produced with $Z \geq 110$ cosmic ray nuclei [1,2].

Unfortunately due to the ablation processes, when meteorites goes trough the Earth atmosphere, more than 5cm of meteorite surface layer is lost. It contains about 90% of tracks due to $Z \geq 90$ up to $Z \approx 112$ nuclei and all the tracks due to rather short - ranged nuclei with $Z = 160$. That is why now we turn to the investigation of Moon olivine crystals, which can serve more abundant information with SHE and SSHE nuclei tracks.

In the previous study of Luna-16 and Luna-24 olivine crystals with size 0.5-1.0 mm we have got preliminarily information about Th - U nuclei tracks by annealing of these crystals at 430°C during 32 h [3]. Concerning the selection of the olivine crystals, situated very close to surface layer, we have developed the technique based on the determination of relative track density due to Fe group (VH) and $Z \geq 36$ (VVH) of cosmic ray nuclei, which allows to select the olivine crystals situated at the very surface of the Moon regolith.

The track densities for 11 lunar crystals are presented at Fig.1. It shows that the crystals for which VH track density is $\geq 10^8$ tracks/cm² had probably been at least once on the very Moon surface during their irradiation history, while the crystals which posses low track density ($\sim 10^6$ tracks/cm²) have never been on the Moon surface.

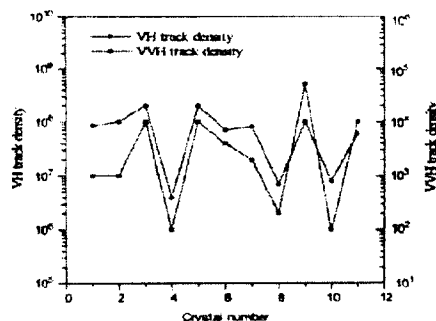


Fig.1

We point out and insist, that the fossil track studies of the Moon olivines now is only one way to discover and to identify hypothetical $Z \approx 160$ nuclei in the Nature.

[1] Perelygin V.P. (1995) *Adv.Space Res.*, 15, 15-24. [2] Perelygin et al., (1999) *Radiat.Meas.*, 32, 609-614. [3] Perelygin et al., (1997) *Radiat.meas.*, 28, 333-336.

COMPOSITIONAL UNITS ON THE MOON: THE ROLE OF SOUTH POLE-AITKEN BASIN. C. A. Peterson¹, B. R. Hawke¹, D.T. Blewett^{1,2}, D. B. J. Bussey¹, P. G. Lucey¹, G. J. Taylor¹, P. D. Spudis³, ¹Hawaii Institute of Geophysics and Planetology, University of Hawaii, Honolulu, HI 96822, ²NovaSol, 1100 Alakea Street, 23rd floor, Honolulu, HI 96813, ³Lunar and Planetary Institute, Houston, TX 77058.

Introduction: Many of the large-scale geochemical provinces found on the Moon today are strongly linked to the impact that created South Pole-Aitken (SPA) basin. This basin has a topographic rim about 2500 km in diameter, an inner shelf 400 – 600 km in width, and an irregular depressed floor at an elevation about 12 km below the rim crest [1]. Topographically high regions surround the SPA basin and are especially pronounced to the north and east; models also show very high levels of crustal thickness in those areas and relatively thin crust beneath the basin [2].

Multispectral images of the Moon were returned by the Galileo and Clementine spacecraft. Belton *et al.* [3] noted an enhancement in mafic materials in the SPA interior. Lucey *et al.* [4] derived methods that use Clementine UVVIS data to quantify the iron and titanium content of lunar surface materials and, in addition to confirming the enhanced FeO content in the basin interior, noted that regions in the far northern farside are extremely low in FeO. This indicates extensive exposures of anorthosite.

More recently, the Lunar Prospector spacecraft returned GRS data that are being used to produce elemental abundance maps [5]. Preliminary thorium maps have been produced [6], and iron maps are also being produced using techniques totally independent from those used with the Clementine data.

Method: Clementine UVVIS data cover most of the Moon between 70°N and 70°S [7]. We have used these data to produce FeO and TiO₂ maps. Elemental abundance maps derived from data returned by the Lunar Prospector mission are currently being produced. A preliminary thorium map is available for analysis.

Results and Discussion: *SPA Interior.* Apollo orbital geochemistry data were obtained for the northern portion of the SPA basin. Enhanced FeO and Th values were noted [8]. The mafic nature of the basin floor was confirmed by Galileo multispectral data [3]. Additional evidence was provided by Clementine and Lunar Prospector.

It has been suggested [9,10] that the mafic enhancement of the basin floor results from the exposure of lower crustal or perhaps even mantle material. Recent work demonstrates that neither cryptomaria nor pyroclastic deposits can account for the mafic character of the SPA interior deposits [11,12].

There have been recent suggestions that the Th (and possibly the FeO and TiO₂) enhancements in SPA are related to Imbrium ejecta deposits in the vicinity of the Imbrium antipode [13]. It seems unlikely that the mafic and Th anomalies on the interior of SPA basin can be fully attributed to Imbrium ejecta.

Enhanced FeO and TiO₂ values are seen in various portions of the SPA interior and not just in the vicinity of the antipode. In the vicinity of the antipode, several large post-Imbrium craters expose Th-rich material excavated from a depth of several km, far below the level of any reasonable thickness of Imbrium ejecta. Other large impact craters ex-

cavate Th-rich material far from the Imbrium antipode. Wicczorek and Zuber [14] suggest that Imbrium ejecta would not be concentrated at the mapped antipode because of lunar rotation during ejecta transport in ballistic trajectories.

SPA Exterior – Farside & West Limb. There is an anorthosite-rich zone on the northern farside identified by Lucey *et al.* [15]. This area exhibits extremely low FeO values. More recent work using higher resolution Clementine imaging data generally supports this interpretation [16]. Support is also provided by TiO₂ data as well as Lunar Prospector Th data. Lucey *et al.* [15] suggested that this anorthosite zone might be the surface of the plagioclase-rich flotation crust formed by the crystallization of the magma ocean.

The terrain that lies between the mafic anomaly on the interior of SPA and the “anorthosite-rich” zone exhibits intermediate FeO abundances. This intermediate terrain can be divided into inner and outer zones. The inner zone is more mafic (FeO-rich) and is located between the transient crater cavity ring and the main (outer) ring. It is covered by thick SPA ejecta. The outer zone is much less mafic and is located between inner zone and the “anorthosite-rich” zone. Small areas of very low FeO material, interpreted as pure anorthosite, occur in the outer zone. Many of these are correlated with inner rings of post-SPA basins that appear to expose anorthosite from beneath more mafic SPA ejecta deposits.

SPA Exterior – Nearside. SPA must have emplaced vast amounts of ejecta in the southern highlands and on the lunar nearside in general. We suggest that relatively mafic SPA ejecta was emplaced on top of pure anorthosite in the southern highlands. Thompkins and Pieters [17] identified two exposures of anorthosite in the central peaks of craters in the far southern nearside. No basins exist that might have exposed anorthosite in the far south, but farther north the Mutus-Vlaq and Humor basins have exposed anorthosite from beneath the more mafic surface material.

References:

- [1] Spudis, P.D. *et al.* (1994), *Science*, **266**, 1848, [2] Zuber, M.T. *et al.* (1994), *Science*, **266**, 1839, [3] Belton, M.J.S. *et al.* (1992), *Science*, **255**, 570, [4] Lucey, P.G. *et al.* (1998) *JGR*, **103**, 3679, [5] Lawrence, D.J. *et al.* (1998), *Science*, **284**, 1484, [6] Lawrence, D.J. *et al.* (2000), *JGR*, **105**, 20,307, [7] Nozette, S. *et al.* (1994), *Science*, **266**, 1835, [8] Hawke, B.R. and Spudis, P.D. (1980), *Proc. Conf. Lunar Highlands Crust*, 467, [9] Lucey, P.G. *et al.* (1998) *JGR*, **103**, 3701, [10] Pieters, C.M. *et al.* (1997), *GRL*, **24**, 1903, [11] Blewett, D.T. *et al.* (1999), *LPSC XXX*, abstract #1438, [12] Blewett, D.T. *et al.* (2000), *LPSC XXXI*, abstract #1501, [13] Has- kin, L.A. (1998), *JGR*, **103**, 1679, [14] Wicczorek, M.A. and Zuber, M.T. (2001), *JGR*, **106**, 27,853, [15] Lucey, P.G. *et al.* (1995), *Science*, **268**, 1150, [16] Peterson, C.A. *et al.* (2001), *LPSC XXXII*, abstract #1592, [17] Tompkins, S. and Pieters, C.M. (1999), *Meteoritics & Planet. Sci.*, **34**, 25.

RECONSTRUCTING THE STRATIGRAPHY OF THE ANCIENT SOUTH POLE-AITKEN BASIN INTERIOR. N. E. Petro and C. M. Pieters, Box 1846, Department of Geological Sciences, Brown University, Providence, RI 02912, USA <e-mail: Noah_Petro@Brown.edu>

Introduction: The South Pole-Aitken (SPA) basin is possibly the largest, oldest basin on the Moon. Since its formation the basin has undergone extensive modification events due largely to impacts and the limited emplacement of mare basalts. Nevertheless, albedo and geochemical data from Clementine and Lunar Prospector strongly suggest that the SPA interior contains distinct materials, which, due to the size of the basin, may be deep-seated in origin. Clearly, large and small craters have reworked materials within the basin and an unknown amount of exterior material has been transported into the basin. To confidently identify any material as representing deep-seated products requires an evaluation of the ~4Ga impact and resurfacing record. In order to identify likely components of the original SPA melt breccia and/or deep-seated material requires recognizing areas that have undergone minimum reprocessing by large craters, basins, and volcanism and the ability to reconstruct local stratigraphy.

Early Mapping of the SPA Basin: Following the Apollo missions to the Moon Stuart-Alexander [1] and Wilhelms et al. [2] first mapped the geology of the SPA basin. This mapping identified a contribution of Orientale ejecta into the basin as well as effects of smaller basins within SPA. Wilhelms et al. [2] identified SPA areas of pre-Nectarian material (i.e. not extensively modified by subsequent large impacts). A map later published by Wilhelms [3] classifies regions that contain "Interior Materials of South Pole-Aitken Basin" (Shown in Figure 1). Ancient regions may represent some of the least altered ancient materials within SPA basin.

Compositional Mapping of the Bhabha Region: Galileo, Clementine and Lunar Prospector have provided a wealth of new data [e.g. 4,5,6,7] to evaluate the ancient surfaces mapped by Wilhelms et al. [2,3] and to assess their likelihood of containing deep-seated materials. We have chosen to examine in detail a region near the crater Bhabha (Figure 1). This location is geologically significant for several reasons. Wilhelms [3] identifies materials near to Bhabha as being "Interior Materials of South Pole-Aitken Basin." Pieters et al. [5] identify a suite of rock-types in this region that may represent deep-seated material. The Bhabha region is also near a possible center of the basin [3,8].

Developing a Stratigraphy of the Bhabha Region: Relatively unaltered pre-Nectarian material mapped by Wilhelms [3] may contain a significant component of the original SPA melt breccia. We will reexamine the stratigraphy of the Bhabha region in detail using the suite of Clementine and Lunar Pros-

pector data. One aspect of this study will be assessing the redistribution of materials by large craters using scaling models of ejecta thickness [9,10,11]. All craters larger than 100 km in diameter and basins within the SPA are shown in Figure 1. We will examine all craters larger than 45 km in diameter within SPA. For the Bhabha region we will be particularly interested in determining the relative proportions of materials contributed by surrounding geologic units and assessing the contributions of melt breccia, deep-seated lithologies, cryptomare, upper crustal material, foreign (distal) material, etc. Such an analysis will help identify specific sites that may be appropriate targets for detailed study of sampling [12].

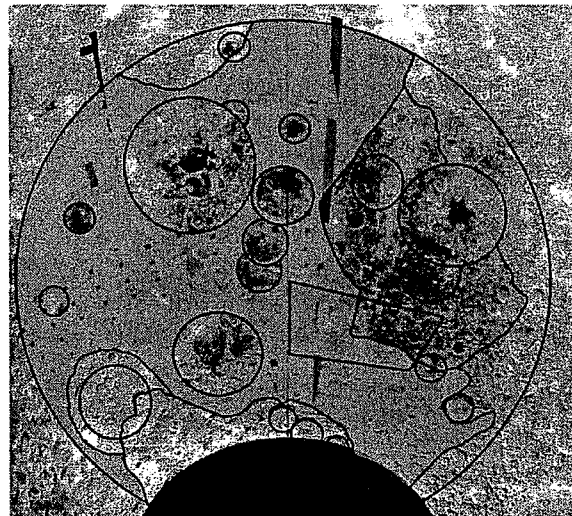
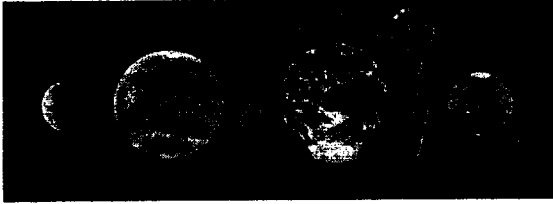


Figure 1. Orthographic view of South Pole-Aitken Basin in centered at 56°S, 180°. Craters and basins within SPA larger than 100 km are circled. The terrain identified as "Interior Materials of SPA Basin" [3] is colored gray. The Bhabha region is enclosed in the box.

References: [1] Stuart-Alexander, D.E. (1978) *USGS Misc. Inv. Series I-1047*; [2] Wilhelms, D.E. et al. (1979) *USGS Misc. Inv. Series I-1162*; [3] Wilhelms, D.E. (1987) *USGS Professional Paper 1348*; [4] Head et al. (1993) *JGR*, 98, 17,149-17,181; [5] Pieters, C.M. et al. (2001) *JGR* 106, 28,001-28,022; [6] Lawrence, D.J. et al. (2002) *LPSC* 33, #1970; [7] Prettyman, T.H. et al. (2002) *LPSC* 33, #2012; [8] Petro, N.E. and Pieters C.M. (2002) *LPSC* 33, #1848; [9] McGetchin, T.R. et al. (1973) *Earth Planet Sci. Lett.*, 20, 226-236; [10] Pike, R.J. (1974) *Earth Planet Sci. Lett.*, 23, 265-274; [11] Housen, K.R. et al. (1983) *JGR*, 88, 2,485-2,499; [12] Jolliff, B.L. et al. (2002) *LPSC* 33, #1156.

LUNAR SCIENCE MISSIONS IN CONTEXT OF THE DECADAL SOLAR SYSTEM EXPLORATION SURVEY.
 C. M. Pieters¹, M. Bullock², R. Greeley³, B. Jolliff⁴, A. Sprague⁵, and E. Stofan⁶, ¹Dept. Geological Sciences, Brown Univ. Providence, RI 02912, ²SWRI, Boulder, CO, ³Arizona State Univ., Tempe, AZ., ⁴Washington Univ., St. Louis, MO, ⁵Univ. Arizona, Tucson, AZ, ⁶Proxemy Res., VA, (pieters@mare.geo.brown.edu).



Introduction: Over the last year a broad and detailed assessment of the current status of science activities as well as research strategies for solar system exploration (SSE) was undertaken by a sub-committee of the NAS/NRC Space Studies Board. This study was requested by NASA to identify science priorities for the next decade of exploration. The report has been completed and is in the review process. This Decadal SSE Survey report is to be given to Dr. Ed Weiler, Associate Administrator for Space Science. It will be publicly released during the summer of 2002 in time for use in NASA's strategic planning.

The study consisted of individual panels charged with making recommendations for particular aspects of solar system exploration and a Steering Committee, chaired by Mike Belton, who prepared an overview of compelling solar system science and identified cross-cutting issues. The panels prepared detailed reports that were submitted to the Steering Committee. The Steering Committee, which also contained a representative from each of the panels, prioritized the diverse panel recommendations into an integrated strategy, including prioritized recommendations.

Inner Planets Panel. The Inner Planets Panel, consisting of the above authors, had responsibility for assessing the current state of knowledge about the inner planets and identifying the highest-level of scientific questions that can be realistically addressed over the next decade. In this context, we were also charged with providing the most promising avenues for flight investigations. A key aspect of this endeavor was broad input from the community throughout the study.

Although the Inner Planets Panel explored science issues pertaining to the diversity of planetary bodies inside the orbit of Jupiter, specific exploration recommendations were limited to those for Mercury, Venus, and the Moon (Mars and asteroids were treated by separate panels). The request from Ed Weiler to the NAS/NRC asked that mission recommendations only be prioritized for missions that are too large to be undertaken within the Discovery program. For objectives that could likely be met within Discovery, the Survey was asked to just list priority science goals. Although no hard guidelines exist for the number of missions likely to fly over the next decade, it is prudent to rec-

ognize the current political and economic climate.

Thus, for the Inner Planets Panel, our tasks were: 1) Interact with the scientific and engineering community to obtain as much information as possible about what has been achieved, what is desired, and what is possible for the next decade. 2) Document and describe fundamental and exciting science issues associated with the inner solar system. These provide the foundation for both intermediate-class as well as Discovery missions. 3) Identify realistic intermediate-class missions to address science issues that are compelling both for understanding the Inner Planets but also the solar system as a whole. It is clear only a handful of such missions drawn from all panels will be seriously considered over the next decade. 4) Provide ample documentation that can be successfully used to support a series of quality Discovery-class missions. After extensive deliberation, our panel was able to reach consensus on all major recommendations.

Outreach Activities. The science community was constantly probed for input throughout the period of SSE Survey deliberations. Although some of you may have tired of the repeated inquiries, the Inner Planets Panel is *most* appreciative of the extensive input received and we thank you heartily. Briefly, several means of gathering information proved to be highly productive: a) 3-hour community forums (in WDC, Chicago) with both formal and informal presentations, b) A large number of thoughtful "white papers" prepared by individuals or groups and submitted directly to the panel, c) A few more formal well integrated "Community" panel documents organized through the DPS, d) Solicited overview science presentations by leaders in the field (geophysics, atmospheres, sample analysis, particle and fields, geology, evolution), e) Solicited presentations on aspects of technology relevant to inner solar system exploration missions. We realize preparation of material for this activity takes considerable effort and each component was exceedingly important.

Recommendations. The specific recommendations of the Decadal Solar System Survey remain sequestered until the report is publicly released. By the time of The Moon Beyond 2002 meeting in Taos, NM the report should be widely available. To access the report go to the following website and click on What's New.
<http://www.nationalacademies.org/ssb/ssefrontpage.html>

It is anticipated we will have a lively discussion in Taos about the contents and implications of the report. In order to make lunar-specific recommendations a reality, it is important that the Lunar Science community focus enthusiasm and support.

CLASSIFICATION OF REGOLITH MATERIALS FROM LUNAR PROSPECTOR DATA REVEALS A MAGNESIUM-RICH HIGHLAND PROVINCE. T. H. Prettyman¹, D. J. Lawrence¹, D. T. Vaniman², R. C. Elphic¹, and W. C. Feldman¹, ¹Group NIS-1, MS D466 and ²Group EES-6, MS D462, Los Alamos National Laboratory, Los Alamos, NM 87545.

The Lunar Prospector (LP) mission returned the first global elemental maps of major elements O, Si, Al, Ti, Fe, Mg, and Ca. The maps were submitted to the Planetary Data System (PDS) archive in June of 2002. Maps are provided for all of the elements at 5 spatial resolution, corresponding to 1790 equal area pixels. This resolution is sufficient to investigate large-scale compositional variations within major lunar terranes. Further work is underway to develop 2 and 0.5 maps for a subset of these elements, which will reduce the effects of instrumental mixing and will enable more meaningful comparisons to the sample collection.

A plot of Al versus Mg' cation ratio $[Mg/(Mg+Fe)]$ is shown in Fig. 1, which contains all 1790 pixels from the 5 LP data set. This type of plot was used by Warren [1] to categorize pristine non-mare rocks. The plot is also useful for classifying regolith materials using LP data. Here, we subdivide the scatter-plot of LP data to determine the location of different types of regolith materials.

Five categories of points are shown in Fig. 1. The location of points on the lunar surface is given in the map in Fig. 2. The classification of points in the first four categories follows Vaniman, et al. [2]. Points with low Al (<72 mg/g), labeled "mare soils" in Fig. 2, are green. Note that these points occupy a contiguous region in the Procellarum basin. The red points correspond to KREEP-rich mixtures (110-72 mg/g Al and $Mg' < 0.75$), labeled "hybrid soils," are red. Points corresponding to mafic and KREEP-poor materials (157-110 mg/g Al and $Mg' < 0.75$), labeled "anorthositic gabbros," are dark blue. Points rich in Al (>157 mg/g and $Mg' < 0.75$), labeled "anorthosite," are yellow.

The final category, corresponding to $Mg' > 0.75$, is labeled "Mg rich" and colored light-blue. This category reveals contiguous regions within the highlands, including a region between Crisium and Somniorum and a region that includes the north polar highlands. The first region is near enough to the equator to be unaffected by errors caused by latitude corrections used by the data reduction algorithms. Consequently, we believe that we have discovered a highland province that may contain an abundance of Mg-rich troctolitic or noritic materials. We are investigating several possibilities for the origin of this province, one of which is the exceptional abundance of late-stage Mg-suite intrusions at a high level in the lunar crust. We will use the entire Lunar Prospector elemental data set to investigate candidate hypotheses.

References: [1] Warren P. H. (1985) *Ann. Rev. Earth Planet. Sci.*, 90, 201-240. [2] Vaniman, D. T., et al., this proceedings.

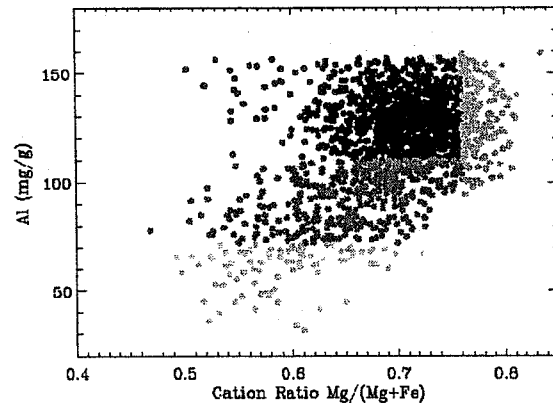


Figure 1. Scatter plot of LP data: Al versus Mg'.

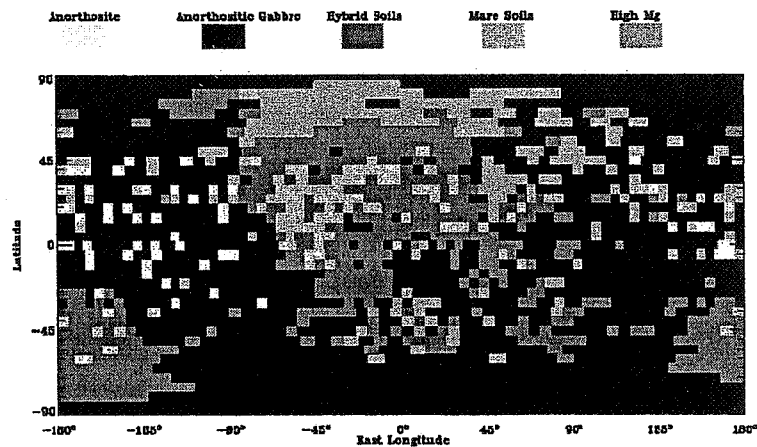


Figure 2. Global lunar map (cylindrical projection) showing the location of different categories of points.

DID THE MOON COME FROM THE IMPACTOR? SIDEROPHILE ELEMENT CONSTRAINTS. K. Righter, Lunar and Planetary Laboratory, University of Arizona, Tucson, AZ 85721 (righter@lpl.arizona.edu).

The issue of whether the Moon has a small metallic core is re-examined in light of new information: improved dynamical modelling, new geophysical constraints on core size, and high temperature and pressure metal-silicate partition coefficients. Although the Moon has similar Co and W depletions to the Earth, it has distinctly different Ni, Mo, Re, P and Ga depletions, consistent with the presence of a small metallic core. Because impact modelling predicts the Moon is made of mantle material primarily from the impactor, bulk Moon compositions are considered from "hot", "warm" and "cool" impactors and proto-Earths (deep, intermediate, and shallow melting, respectively). If the Moon is made of mantle material from either a "hot" impactor or a "warm" impactor or proto-Earth, a small metallic core (0.7 to 2 percent) is

predicted (cases 2, 3, 4; Fig. 1). If the Moon is made from mantle material from a "hot" proto-Earth, the lunar mantle would be more depleted in W or P than is observed (case 1; Fig. 1). Some have argued recently that the Moon has no metallic core; scenarios in which the Moon is made from impactor mantle material and has no core predict larger depletions of Ga, Co and W than are observed (case 5; Fig. 1). Consistency of siderophile element concentrations in the lunar mantle with an impactor bulk Moon composition eliminate previous geochemical objections to an impactor origin of the Moon. Depletions of slightly (Mn, V and Cr) and highly (Re, Au, PGE's) siderophile elements in the lunar mantle will also be considered.

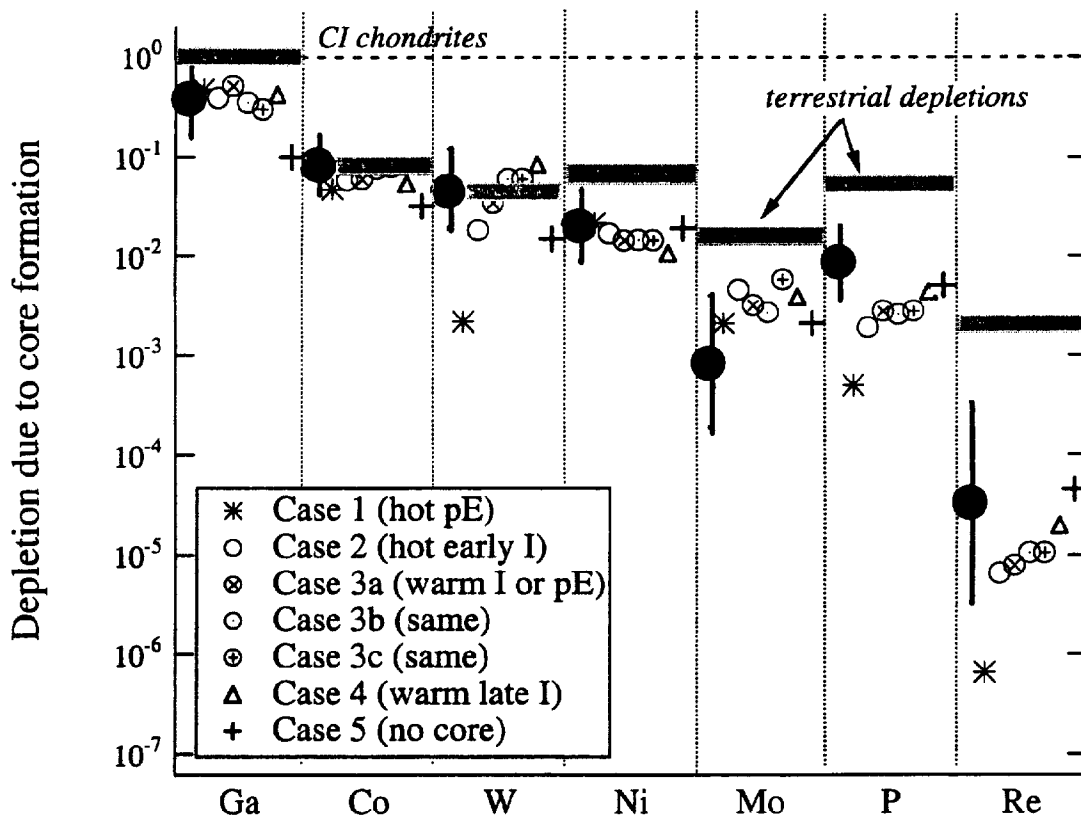


Figure 1: Depletion of siderophile elements in the lunar mantle (solid circles) normalized to chondritic values. Terrestrial mantle depletions are shown as horizontal shading.

TOPOGRAPHIC-PHOTOMETRIC CORRECTIONS APPLIED TO CLEMENTINE SPECTRAL REFLECTANCE DATA OF THE APOLLO 17 REGION. M. S. Robinson¹ and B. L. Jolliff²,

¹Northwestern University, 1847 Sheridan Road, Evanston, IL, 60208, robinson@earth.northwestern.edu,

²Washington University, St. Louis MO 63130, (blj@levee.wustl.edu).

Introduction: Recently, great strides have been made in understanding the origin and evolution of the Moon through a synthesis of Apollo sample analyses, Clementine Spectral Reflectance (CSR) data, and Lunar Prospector remotely sensed geochemical data. These studies have generally investigated regional chemical and mineralogical variations at the scale of tens to hundreds of km. More detailed studies at the sub-kilometer scale utilizing derived spectral parameters such as FeO and TiO₂ are hampered by inaccuracies in photometric corrections resulting from local slopes [1]. Detailed analysis of spectral parameters of lunar highlands and craters requires topographic data at a scale comparable to the pixel resolution of the spectral measurements, for CSR ~125-250 m/p. Unfortunately global topographic data for the Moon exist only at the scale of tens of kilometers.

Apollo 17 Area: To investigate compositional diversity of the highland massifs in the Apollo 17 area [2,3] we have combined a 10 m contour stereo-based topographic map with the CSR data to correct lighting to a uniform geometry [4]. FeO and TiO₂ concentrations were derived from these topographic-photometrically corrected CSR data: the correction indicates errors as high as 5-wt% FeO and 4-wt% TiO₂ (absolute) on uncorrected slopes of 30° (with greater changes on anti-Sun slopes). In topographically uncorrected data, such variations can lead to erroneous interpretations of rock types and rock-type diversity within highland geologic formations. The topographically corrected data and derived compositional information are used to show accurately the variation in composition of the surrounding massifs and the Sculptured Hills. We find massif compositions are consistent with mixtures of noritic impact melt and feldspathic granulitic material, plus variable amounts of high-Ti basalt on flanks at low elevations and pyroclastic deposits at high elevations, as surmised from previous studies. An unexpected enrichment in FeO at intermediate elevations in some places where massif surfaces have not been covered by mass wasting of impact-melt rich material signals an older volcanic component not previously recognized. This component may be correlative with an older, high-plains volcanic unit exposed northeast of the landing site and north of the Sculptured Hills. Downslope movement of regolith on steep slopes appears to have resulted in compositional or grain size sorting, leading to an apparent enrichment in FeO and

TiO₂ in valleys and draws. The Sculptured Hills have highly variable compositions, ranging from feldspathic patches to exposures of mafic rocks. A strong but localized mafic anomaly within the Sculptured Hills may be a small, post-basin volcanic feature consisting of very-low-Ti basalt.

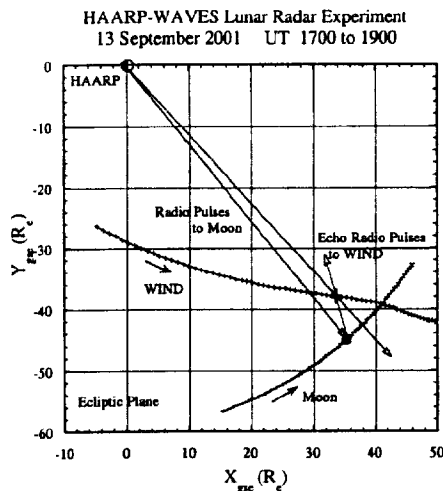
In addition to correcting for slope-related errors in compositional derivations, high-resolution digital elevation data are also useful in delimiting spatial relations of compositional units. Areas of elevated plains that are compositionally distinctive, such as the high plains formation may be correlative to compositionally similar material at similar elevations in the region, but lacking the smooth-plains morphology. In the Apollo 17 region, the compositional data suggest that these areas contain an old volcanic component and are not simply smooth plains associated with basin formation and ejecta.

Conclusions: Compositional studies of deposits that have significant local relief must be corrected topographically to enable high-resolution definition of regolith and rock units. At the Apollo 17 site, the full range of compositional variability can be determined with confidence that the feldspathic areas are not simply a result of slope-related brightening and more mafic areas, slope-related darkening. Observed variations are consistent with the occurrence of a chaotic mixture of impact melt and more feldspathic material, as indicated by massif materials brought to the edge of the valley floor by downslope mass wasting, and areas of volcanic ash deposits on the tops of the massifs and concentrated in troughs and draws by downslope movement associated with mass wasting. In order to fully exploit derived spectral parameters of lunar soils, future high-resolution color imaging of the Moon should be obtained in conjunction with stereo imaging at a resolution comparable to the spectral data (spatial resolution of derived topography is typically ~5x lower than the resolution of the stereo images from which it is derived).

References: [1] Lucey et al (1998) *JGR* 102, 3679-3699. [2] Luchitta et al. (1972) USGS Map I-800, 1:50,000 [3] Wolfe et al. (1981) *U.S. Geol. Surv. Prof. Paper 1080*, 280 pp., [4] Robinson M. S. and Jolliff B. L. (in press) *JGR*.

LUNAR RADAR CROSS SECTION AT LOW FREQUENCY. P. Rodriguez¹, E. J. Kennedy¹, P. Kossey², M. McCarrick³, M. L. Kaiser⁴, J.-L. Bougeret⁵, and Yu. V. Tokarev⁶, ¹U. S. Naval Research Laboratory, Information Technology Division, 4555 Overlook Ave., SW, Washington, DC 20375, ²U. S. Air Force Research Laboratory, Space Vehicles Directorate, 29 Randolph Rd., Hanscom AFB, MA 01731, ³Advanced Power Technologies, Inc., 1250 24th St., NW, Washington, DC 20037, ⁴NASA/Goddard Space Flight Center, Laboratory for Extraterrestrial Physics, Greenbelt, MD 20771, ⁵DESPA-DASOP, Observatoire de Paris, 5, Place Jules Janssen, 92195 Meudon Cedex, France, ⁶Radiophysical Research Institute, B. Pecherskaya St, 25, Nizhny Novgorod 603600, Russia

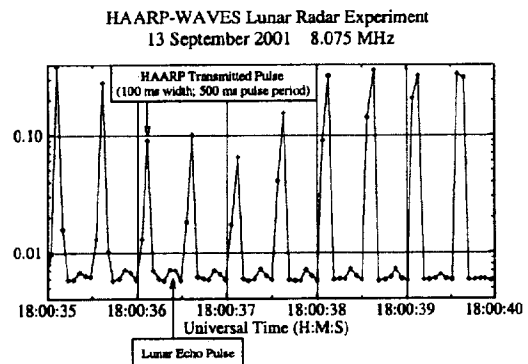
Introduction: Recent bistatic measurements of the lunar radar cross-section have extended the spectrum to long radio wavelength. We have utilized the HF Active Auroral Research Program (HAARP) radar facility near Gakona, Alaska to transmit high power pulses at 8.075 MHz to the Moon; the echo pulses were received onboard the NASA/WIND spacecraft by the WAVES HF receiver. This lunar radar experiment follows our previous use of earth-based HF radar with satellites to conduct space experiments [1]. The spacecraft was approaching the Moon for a scheduled orbit perturbation when our experiment of 13 September 2001 was conducted. During the two-hour experiment, the radial distance of the satellite from the Moon varied from 28 to 24 R_m , where R_m is in lunar radii. The figure below shows the geometry of the experiment, in the solar ecliptic plane.



Measurements: HAARP pulses with widths of 100-ms and pulse periods of 500 ms provided about 12,000 data samples of the direct and echo radiowaves integrated over 20 ms. From these pulse-echo pairs we obtain the lunar radar cross-section using the radar equation. We obtain an average cross-section of about 15% of the geometric cross-section, with maximum values of about 50%. Previous determinations [2], [3], of the lunar radar cross-section at shorter wavelengths have suggested an increase of the cross-section with

increasing wavelength. Our measurement confirms this dependence and extends the spectrum of lunar radar cross-sections to a wavelength of 37 meters.

The HAARP-WAVES experiment provided evidence of high reflectivity locations on the lunar surface that may be associated with topographical features that preferentially return an echo signal to the satellite. The motion of the spacecraft apparently changed the aspect sufficiently to allow several such regions to be sampled. The following figure illustrates a 5-second interval of data showing the direct HAARP pulses and the echo lunar pulses as received by the WAVES instrument.



Conclusion: This new technique for long wavelength radar cross-section measurement is free of scintillation effects caused by the earth's ionosphere and provides a relatively clean measurement of the lunar radar cross-section. High power long wavelength radars, such as HAARP, can enhance our methods of lunar research. We suggest that future lunar radar experiments with lunar-orbiting spacecraft can provide a new window on lunar topography and subsurface conductivity measurements.

References: [1] Rodriguez P. et al. (1998), *Geophys. Res. Lett.*, 25, 257-260; (1999), *Geophys. Res. Lett.*, 26, 2351-2354. [2] Evans J. V. and Pettengill G. H. (1963), in *The Solar System, Vol. IV, The Moon, Meteorites, and Comets*, 129-161, edited by B. M. Middlehurst and G. P. Kuiper. [3] Davis J. R. and Rohlfs D. C. (1964) *J. Geophys. Res.*, 69, 3257-3262.

A MINIATURE MINERALOGICAL INSTRUMENT FOR *IN-SITU* CHARACTERIZATION OF ICES AND HYDROUS MINERALS AT THE LUNAR POLES. P. Sarrazin¹, D. Blake¹, D. Vaniman², D. Bish², S. Chipera², S.A. Collins³, ¹NASA-ARC (MS 239-4, Moffett Field, CA 94035, dblake@mail.arc.nasa.gov), ²LANL (EES-6, Hydrology, Geochemistry, & Geology, MS D462, Los Alamos, NM 87545, vaniman@lanl.gov), ³JPL, Detector Advanced Development, (MS 300-315L, 4800 Oak Grove Dr., Pasadena, CA 91109, Stewart.A.Collins@jpl.nasa.gov).

Robotic investigation of lunar polar regolith: Lunar missions over the past few years have provided new evidence that water may be present at the lunar poles in the form of cold-trapped ice deposits [1, 2], thereby rekindling interest in sampling the polar regions. Robotic landers fitted with mineralogical instrumentation for *in-situ* analyses could provide unequivocal answers on the presence of crystalline water ice and/or hydrous minerals at the lunar poles.

Data from *Lunar Prospector* suggest that any surface exploration of the lunar poles should include the capability to drill to depths of >40 cm. Limited data on the lunar geotherm indicate temperatures of ~245-255 K at regolith depths of 40 cm, within a range where water may exist in the liquid state as brine. A relevant terrestrial analog occurs in Antarctica, where the zeolite mineral chabazite has been found at the boundary between ice-free and ice-cemented regolith horizons, and precipitation from a regolith brine is indicated [3]. Soluble halogens and sulfur in the lunar regolith could provide comparable brine chemistry in an analogous setting.

Regolith samples collected by a drilling device could be readily analyzed by CheMin, a mineralogical instrument that combines X-ray diffraction (XRD) and X-ray fluorescence (XRF) techniques to simultaneously characterize the chemical and mineralogical compositions of granular or powdered samples [4, 5]. CheMin can unambiguously determine not only the presence of hydrous alteration phases such as clays or zeolites, but it can also identify the structural variants or types of clay or zeolite present (e.g., well-ordered versus poorly ordered smectite; chabazite versus phillipsite). In addition, CheMin can readily measure the abundances of key elements that may occur in lunar minerals (Na, Mg, Al, Si, K, Ca, Fe) as well as the likely constituents of lunar brines (F, Cl, S). Finally, if coring and analysis are done during the lunar night or in permanent shadow, CheMin can provide information on the chemistry and structure of any crystalline ices that might occur in the regolith samples.

The CheMin XRD/XRF instrument: The central element of CheMin is a CCD detector capable of both spatial and energy resolution of X-ray photons. Energy discrimination is applied for XRF measurements whereas spatial discrimination is used for XRD analyses.

A proof-of-concept prototype has demonstrated capabilities for mineralogical characterization never achieved with any previous spacecraft instrument. Examples of data obtained with the prototype are shown in Figure 1. When appropriate, XRD data can be analyzed by Rietveld refinement to quantitatively determine the composition of complex mixtures.

The simple geometry and limited number of moving parts make CheMin suitable for deployment in a lightweight

lander or rover, making it particularly appropriate in the context of lunar pole exploration. The flight instrument will offer simultaneous XRF and XRD in a package expected to weigh under 1 kg with a volume smaller than 1 dm³ (Figure 2).

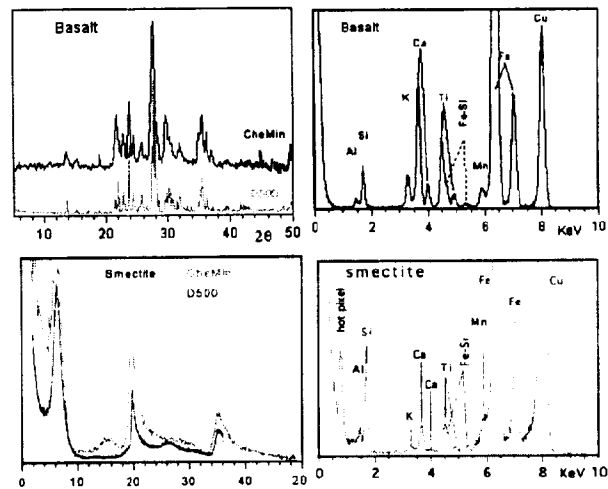


Figure 1: Example of data provided by CheMin, left: CheMin diffractogram compared with diffractogram from laboratory diffractometer (Siemens™ D500); right: CheMin XRF spectrum; top: basalt; bottom: smectite

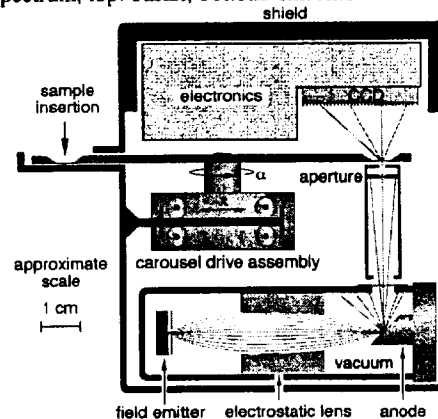


Figure 2: Schematic drawing of the spacecraft instrument fitted with low-power X-ray source and rotating carousel for sample loading.

- [1] Arnold J. R. (1979), *J. Geophys. Res.* **84**, 5659-5668. [2] Feldman, W. et al (1998), *Science* **281**, 1496-1500. [3] Dickinson W. W. and R. H. Grapes (1997), *J. Sed. Res.* **67**, 815-820. [4] Vaniman D. et al. (1998) *J. Geophys. Res.* **103**, 31,477-31,489. [5] Sarrazin P. et al. (1998). *J. Phys. IV France* **8**, 5/465-470.

FUTURE LUNAR SAMPLING MISSIONS. BIG RETURNS ON SMALL SAMPLES. C.K. Shearer, J.J. Papike, and L. Borg. Institute of Meteoritics, University of New Mexico, Albuquerque, New Mexico 87131

Introduction. The next sampling missions to the Moon will result in the return of sample mass (100g to 1 kg) substantially smaller than those returned by the Apollo missions (380 kg). Lunar samples to be returned by these missions are vital for (1) calibrating the late impact history of the inner solar system that can then be extended to other planetary surfaces, (2) deciphering the effects of catastrophic impacts on a planetary body (i.e. Aitken crater), (3) understanding the very late-stage thermal and magmatic evolution of a cooling planet, (4) exploring the interior of a planet, and (5) examining volatile reservoirs and transport on an airless planetary body. Can small lunar samples be used to answer these and other pressing questions concerning important solar system processes? Two potential problems with small, robotically collected samples are placing them in a geologic context and extracting robust planetary information. Although geologic context will always be a potential problem with any planetary sample, new lunar samples can be placed within the context of the important Apollo – Luna collections and the burgeoning planet-scale data sets for the lunar surface and interior. Here we illustrate the usefulness of applying both new or refined analytical approaches in deciphering information locked in small lunar samples.

Reconstructing the magmatic history. The Apollo 14 high-Al basalts are partially represented by a suite of small clasts (2 to = 4 mm, 10 to = 350 mg) in regolith breccia. These clasts represent the oldest period of basaltic volcanism thus far sampled from the Moon. Petrography, mineral compositions, and bulk major element compositions are similar, yet there is approximately a 8 to 10 fold increase in incompatible elements among the clasts. Are these bulk rock characteristics a product of sampling or process? Hagerty et al [1] analyzed the trace elements of individual mineral phases in these basalts using an ion microprobe capable of a 10 to 30 micron resolution. These data indicate that these clasts do not represent crystallization products of a single flow, but a series of basaltic melts produced by melting of multiple sources.

Geochemical signatures of igneous terrains. Early in the investigation of the lunar highlands, it was recognized that highland lithologies could be differentiated based on major element chemistries of individual minerals (An of plagioclase versus Mg# of mafic silicates). This approach may be ambiguous for new lunar samples (i.e. NWA 773) or individual mineral grains. Shearer et al. [2] were able to distinguish among different plutonic and volcanic lithologies using compatible (Ni, Co) and incompatible (REE, Y) trace element

characteristics of individual minerals determined by ion microprobe.

Age-dating. Several lunar studies have illustrated the current ability and future promise of deriving radiometric ages from small lunar samples [3,4,5,6]. Using fragments from a unique high-Ti basalt clast totaling = 500 mg, collaborative studies were able to produce Rb-Sr, Sm-Nd and ^{39}Ar - ^{40}Ar ages for a sample that was extensively characterized for petrography, bulk rock chemistry, and major and trace element composition of individual phases. Rb-Sr and Sm-Nd isochron ages were produced on as little as 60 mg of an Apollo 14 high-Al basalt [6].

Evolution of the Lunar Interior. In addition to dating geologic terrains, radiogenic isotopes have been critical for exploring the timing, duration, and processes of planetary differentiation. More recently, short-lived isotopic systems (Hf-W, Sm-Nd, Nb-Zr) have been developed to increase the temporal resolution for looking at these early planetary events. For the Moon, these systems have been applied to better understand the duration and timing of core formation, LMO crystallization, and mantle overturn [7,8]. These methods require < 1 gram of sample and therefore, when appropriate, can be used for the analysis of newly acquired lunar materials.

Behavior of volatiles. Airless planetary bodies such as the Moon and Mercury appear to have small volatile reservoirs in permanently shaded surface areas near their poles. The phenomenon of small-scale volatile element transport by impact was identified early in the study of Apollo samples and subsequently studied using the TEM and ion microprobe in the 1990s [9,10]. Understanding larger-scale volatile element transport and volatile reservoir formation on such planetary bodies would significantly benefit from sampling of the lunar volatile reservoirs. Ultra-sensitive analytical approaches to enhance the scientific value of volatile-rich samples and microgram- to nanogram-sized particles immersed in the volatile reservoirs have already been developed for the analysis of interstellar grains removed from meteorites [11].

References. [1] Hagerty et al. (2002) *Lunar Planet. Sci.* XXXIII, cd-rom # 1574. [2] Shearer et al. (2000) *Lunar Planet. Sci.* XXXI, cd-rom # 1643. [3] Ryder (1990) *Meteoritics* 25, 249-258. [4] Nyquist et al. (2000) *Lunar Planet. Sci.* XXXI, cd-rom # 1667. [5] Shearer et al. (2001) *Lunar Planet. Sci.* XXXII, cd-rom # 1851. [6] Dasch et al. (1987) *GCA* 51, 3241-3254. [7] Lee et al. (1997) *Science* 278, 1098-1133 [8] Shearer and Newsom (2000) *GCA*, 64, 3599-3613. [9] Keller and McKay (1992) *Proc. Lunar Planet. Sci.* 22, 137-141. [10] Papike et al., (1997) *Am. Mineral.* 82, 630-634. [11] Zolensky et al. (2000) *MAPS*, 35, 9-29.

AN IMAGING LASER ALTIMETER FOR LUNAR SCIENTIFIC EXPLORATION. D. E. Smith¹, M.T. Zuber, and J. J. Degnan, ¹Goddard Spaceflight Center, Greenbelt MD 20771.

A new approach to laser altimetry is offered by the development of micro-lasers and pixilated detectors that enable very high resolution measurement of topography and relatively wide swath observations. An imaging altimeter with a 8x8 array detector working at a probability of less than a single photon/shot could map the Moon or similar sized body in approximately 2 years and provide 5 meter horizontal resolution topography and a 10 centimeter vertical accuracy. In addition, it would provide surface roughness and surface slopes on similar length scales of 5 meters and be able to address a range of problems for which topography or lunar shape is important at the decimeter level. This includes the topography of the polar regions, where ice is thought to have been identified, and also the cratering history of the Moon which could be assessed with a dataset of uniform quality and high resolution.

SEARCHING FOR ANTIPODAL BASIN EJECTA ON THE MOON Paul D. Spudis and Brian Fessler, Lunar and Planetary Institute, 3600 Bay Area Blvd., Houston TX 77058-1113, spudis@lpi.usra.edu

Multi-ring basins are the largest impact events in lunar history and have catastrophic, global effects on the Moon (e.g., [1]). Ejecta from these events may travel over great distances, but the thickness of the ensuing debris blanket thins quickly as one goes away from the basin rim [2,3]. Because impact events tend to (more or less) eject material equidistant from the point of impact, distal ejecta converge from all directions at the basin antipodes, possibly resulting in an anomalously large accumulation of ejecta at that point [e.g., 2]. Antipodal concentrations of ejecta may have resulted in both anomalous compositional [4] and geophysical [e.g., 5] relations seen in some regions of the Moon. This hypothesis has recently been revived, with the specific proposal that anomalously high contents of Th found near the far side crater Van De Graaf are concentrations of Imbrium basin ejecta, antipodal to that impact feature [6].

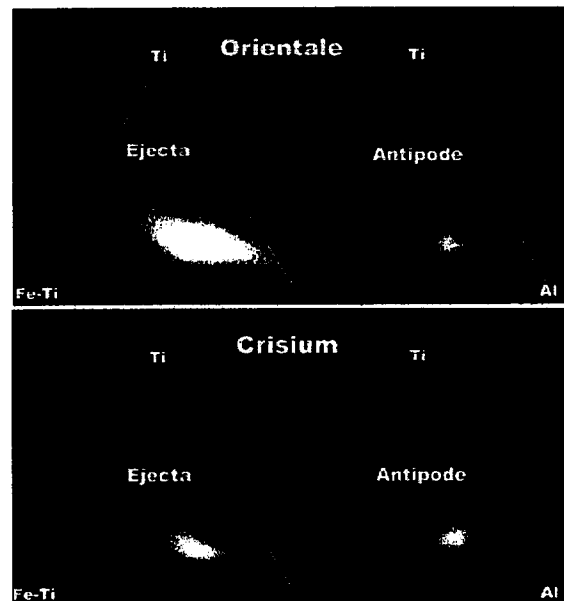
We have previously described techniques designed to map rock units on the Moon using Clementine and LP elemental data [e.g., 7,8]. These maps show how compositions vary regionally and allow us to directly compare regions distant from each other. We have used the petrologic maps of [8] to address the question of recognizable antipodal deposits of basin ejecta.

Method. As described by [9], we invert Fe data into "pseudo-aluminum" using the well-known inverse correlation between Fe and Al in lunar soils [10]. We then plot the parameters Ti, Fe-Ti, and "Al" on a ternary plot; each pixel in the Clementine image cube is assigned a value in this ternary space. The three apices are assigned the primary colors red (Ti), green (Fe-Ti), or blue ("Al"); compositions intermediate between these end members are rendered in intermediate colors. On this petrologic map, we trace the outline of areas dominated by ejecta from the Imbrium, Orientale, Nectaris, and Crisium basins. Except for Orientale, all basins are modified by other events and subsequent mare flooding [1], but recognizable deposits are extensive around these younger lunar basins. For each map of basin ejecta, a ternary plot is made, showing the composition of ejecta pixels in this space. This procedure is then repeated for the basin antipode; we drew a circle ~ 200 km in diameter, modified to avoid obvious mare deposits and other obscuring later deposits. The antipode compositions were then directly compared to the plots for the ejecta of their parent basins to determine compositional affinities.

Results. For the four basins studied, the range of compositions seen in the antipodes is much more restricted than the range seen in the near-rim deposits.

However, in each case, the antipode compositions are a subset of the basin ejecta envelope. Orientale basin, which has a very feldspathic ejecta blanket, similarly shows a feldspathic, although more restricted, composition at its antipode (Figure), near the crater Goddard, north of Mare Marginis. In contrast, the Imbrium basin has a wide-ranging ejecta composition, with most pixels being highland basalt, but a minor trend towards feldspathic lithologies. Imbrium's antipode, near Mare Ingenii, is almost completely of highland basaltic composition. The Crisium basin shows an interesting departure from this pattern, in that the antipode deposits map a trend line towards the (Fe-Ti) apex, in contrast to the trend of Crisium ejecta towards the Ti apex. Although the antipode is contained within the basin ejecta envelope of Crisium (Figure), it appears that this deposit might have a different provenance.

Conclusions. Our initial results cannot rule out the hypothesis that distal basin ejecta may concentrate at the antipodes. We plan further work to refine this mapping, including study of additional basins and other compositional data sets (e.g., Th).



References: [1] Spudis P.D. (1993) *Geology of Multi-ring Basins*, Cambridge Press, 263 pp. [2] Moore et al. (1974) *PLSC* 5, 71-100. [3] McGetchin T. et al. (1973) *EPSL* 20, 226-236. [4] Stuart-Alexander D. (1978) *USGS Map I-1047* [5] Hood L. (1979) *LPSC* 10, 2335 [6] Haskin L. (1998) *JGR* 103, 1679-1689 [7] Bussey B. et al. (1999) *New Views of the Moon*, 5 [8] Spudis P.D. et al. (2002) *LPS* 33, 1104 [9] Lucey P.G. et al. (2000) *JGR* 105, 20,297. [10] Spudis P. D. et al. (1988) *LPS* 19, 1113.

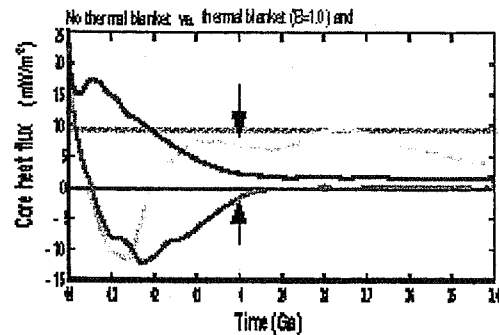
LUNAR CORE DYNAMO DRIVEN BY THERMOCHEMICAL MANTLE CONVECTION. D. R. Stegman¹, A. M. Jellinek¹, S. A. Zatman², J. R. Baumgardner³, and M. A. Richards¹, ¹Univ. California, Berkeley (Dept. Earth and Planetary Science, 307 McCone Hall, Univ. California - Berkeley, Berkeley, CA, 94720; dstegman@seismo.berkeley.edu, markj@seismo.berkeley.edu, markr@seismo.berkeley.edu), ²Washington University (Dept. Earth and Planetary Sciences, Campus Box 1169, Wilson Hall, One Brookings Drive, St. Louis, MO, 63130-4899; zatman@levee.wustl.edu), ³Los Alamos National Laboratory (Fluid Dynamics Group, Theoretical Division, Los Alamos National Laboratory, Los Alamos, NM, 87545; baumgardner@lanl.gov).

Abstract: The Moon presently has no internally generated magnetic field (i.e. core dynamo). However, an outstanding question resulting from the Apollo sample return missions is the possible existence of a lunar dynamo early in the Moon's history. Paleomagnetic data combined with radiometric ages obtained from lunar samples suggest the existence of a magnetic field from ~3.9-3.6 Ga (possibly beginning earlier), likely of comparable intensity as the Earth's present-day field¹. The implied existence of a lunar dynamo at least 500 Myr after the Moon's formation is difficult to explain. Assuming that a dynamo is driven by thermal convection in the core, the existence and duration of a dynamo correspond to periods when core heat flux exceeds the adiabatic heat flux ($Q_{\text{cmb}} > Q_{\text{ad}}$; Q_{ad} shown as grey line). Since simple thermal evolution models for the Moon yield insufficient core heat flux (blue curve) to power a dynamo at such times, we explore alternative thermal evolutions.

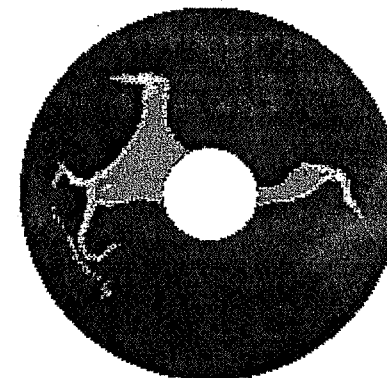
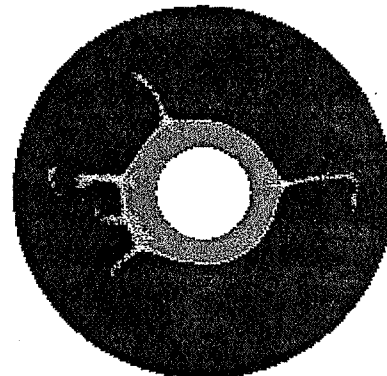
It is hypothesized that an ilmenite cumulate layer may have formed resultant to solidification of a lunar magma ocean². The layer is expected to sink and pond at the core-mantle boundary, but subsequent radioactive heating can increase the buoyancy of the layer and cause it to rise back up into the mantle. We use a 3-D spherical finite element model of mantle convection with a temperature-dependent viscosity to investigate the effect on core heat flux by removal of such a dense, radioactive-element rich layer (thermal blanket). Initially we assume a 227 km thick layer surrounding a core of radius 450 km. We assume the layer has uniform chemical density, which we vary via a dimensionless buoyancy number, $B = \Delta\rho_{\text{chem}}/\alpha_m\Delta T$. The figure shows cross-sections of the composition at 4.0 Ga for two models (marked with arrows on the red and green curves): a stably stratified model with $B=1.0$ and an unstably stratified model with $B=0.5$. With $B=1.0$, the thermal blanket is too dense to rise back into the mantle. However, a thermal blanket with $B=0.5$ becomes buoyant enough to be removed from the core, allowing for rapid core cooling.

Most reasonable parameter choices for simple layered (red curve) or unlayered models (blue curve) result in thermal evolutions with core heat fluxes a full order of magnitude below the adiabatic value (grey line) during the time which a lunar dynamo may have existed. However, dynamic coupling between mantle convection and a marginally stable, thermal blanket (green curve) may support a lunar dynamo. A key prediction of our hypothesis is a well-defined onset for the lunar magnetic field. Future sampling of magnetic paleointensity, perhaps even reanalysis of Apollo era

samples, might therefore constrain not only the history of the lunar dynamo, but also by inference the early thermal and chemical differentiation history of the Moon.



Thermal Blanket ($B=1.0$) at 4.0 Ga



References: [1] Cisowski, S. M. et al. (1983) *JGR*, 88, A691-A704. [2] Hess, P. C. and Parmentier, E. M., (1995) *Earth & Planet. Sci. Lett.*, 134, 501-514.

EFFICIENT MATERIAL MAPPING USING CLEMENTINE MULTISPECTRAL DATA. D. Steutel¹, P. G. Lucey¹, M. E. Winter¹, and S. LeMouélic², ¹Hawai'i Institute of Geophysics and Planetology, 1680 East-West Road, University of Hawai'i, Honolulu, HI 96822, dsteutel@higp.hawaii.edu. ²Institut d'Astrophysique Spatiale, Université Paris-Sud, bâtiment 121, F-91405 Orsay, France.

Introduction: Clementine UVVIS and NIR images have been used to interpret mineralogy of the lunar surface [1,2]. We have applied two algorithms to the mosaic of the Aristarchus plateau produced by [1,2] which efficiently map the regional mineralogy. This technique may be applied to the entirety of Clementine data now available.

Algorithms: First, we applied an endmember detector/linear unmixing algorithm (N-FINDR,[3]) to the multispectral data. Endmember detection is accomplished by a simplex volume expansion process which evaluates each pixel in the image. Final endmembers are spectra from the image. These endmembers are used to linearly unmix all spectra in the image.

Second, we applied a Hapke-based [4] iterative nonlinear mixture spectral analysis model to identify the modal abundance, grain size, Mg-number [5], glass abundance and composition [6], and submicroscopic iron [7].

Results: Six spectral endmembers were identified, including one endmember of mature mare with little mineralogic information. The spectral analysis model spectra converged very closely to endmember spectra. Table 1 lists the endmember compositions corresponding to the spectral analysis model. Endmember compositions were then mapped onto the linearly unmixed fraction planes to produce a mineral map. No mineralogy was mapped onto the fraction plane represented by endmember 1. The rock type [8] of each pixel was determined based on the pixel mineralogy. Figure 1 shows the rock type represented by spectral endmembers 2-6. Figure 2 shows a map of rock types. The mappable portion of the scene is dominated by olivine norite (8%), olivine gabbro (62%), and anorthositic troctolite (30%).

Conclusions: By applying automated endmember detection, spectral mixing analysis, and spectral composition analysis, mineralogic, rock type, and elemental abundance maps can be produced efficiently. The technique used can be applied to scenes such as the Aristarchus mosaic used here in just a few minutes. With planned improvements in the efficiency of the spectral composition analysis, an analysis of the entire Clementine data set could be done in days.

Future work: Most importantly, the spectral composition analysis algorithm must be validated (preliminary work on this has been done.) Also, the algorithm should be improved. We estimate that at least one order of magnitude improvement is possible. Finally,

errors in the endmember detection/linear unmixing analysis and the spectral composition analysis must be incorporated to yield an uncertainty in the final mineralogic, rock type, and elemental maps produced.

References: [1] LeMouélic, S. *et al.* (1999) *JGR*, 104, E2, 3833-3843. [2] LeMouélic, S. *et al.* (2000) *JGR*, 105, E4, 9445-9455. [3] Winter, M.E. (1999) *Proc. SPIE*, 3753, 266-275. [4] Hapke, B. (1993) *Theory of Reflectance and Emission Spectroscopy*, Cambridge Univ. Press, Cambridge. [5] Lucey, P.G. (1998) *JGR*, 103, E1, 1703-1714. [6] Lucey, P.G. *et al.* (1998) *JGR*, 103, E2, 3679-3700. [7] Hapke, B. (2001) *JGR*, 106, E5, 10,039-10,073. [8] Stöffler, D. *et al.* (1980) *Proc. Conf. Lunar Crust*, 51-70.

		Spectral Endmember						
		1	2	3	4	5	6	
Mature mare	olivine*		39.9	17.9	42.7	20.8	11.8	
	orthopyroxene*		9.6	30.1	10.4	14.1	8.0	
	clinopyroxene*		42.3	5.6	0.0	0.5	0.0	
	anorthite*		3.4	41.0	46.8	61.6	75.1	
	ilmenite*		4.8	5.4	0.1	3.1	5.2	
	minerals**		69.1	99.1	75.2	83.3	94.6	
	glass**		30.7	0.1	24.0	16.4	5.1	
	SMFe**		1.8	0.3	0.8	0.8	0.3	0.3

*Wt% of minerals present

**Wt% of minerals, glass, and SMFe

Table 1. Endmember spectra and spectral analysis model spectra.

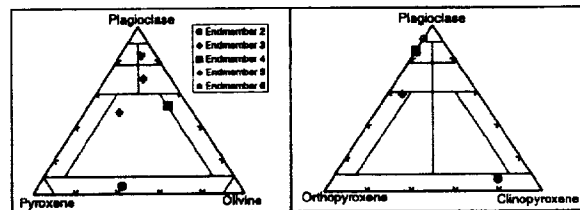


Figure 1. Rock types of spectral endmembers.

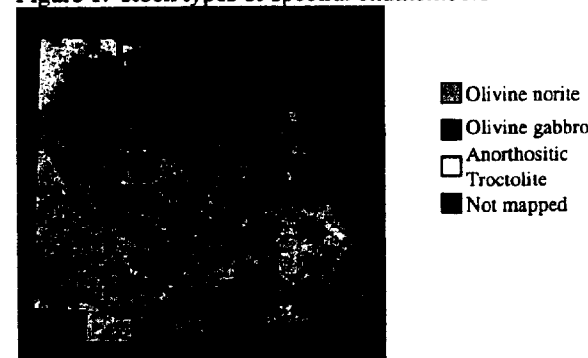


Figure 2. Three mapable rock types at Aristarchus.

CALL FOR COOPERATION BETWEEN LUNAR SCIENTISTS AND ASTRONOMERS: PROPOSING LUNAR SCIENCE MISSIONS TO ENABLE ASTRONOMY FROM THE MOON.

Y. D. Takahashi, Department of Physics & Astronomy, University of Glasgow, Glasgow, G12 8QQ, UK (yuki@astro.gla.ac.uk).

Study of the Moon for 'Science from the Moon':

Astronomers have long looked up at the Moon as a dream site to study the universe from. Observatories on the Moon have been proposed since at least the mid-1960s [1] when humans began to have access to outer space. The most seriously investigated concept has been an array of antennas on the lunar far side for very-low-frequency radio astronomy. Shielded from the terrestrial interference, such an observatory could give us new views of the universe through the completely new spectral window of 50 kHz - 30 MHz. However, in investigating astronomical observations from the Moon, I have many times needed more details about the physical characteristics of the lunar environment than are available at present. Many of these details are crucial in selecting the site, designing the instrument, and assessing the performance. Measurements at candidate sites are especially important in identifying the best site. Since the best sites are large craters on the lunar far side, geologists should hopefully share interest in such site-specific studies.

Crucial Measurements: To predict the performance of a Moon-based radio observatory, we seek answers to the following questions. It is critical to make the following measurements at our earliest opportunities: Many of these are suggested in the ESA design study of the Very Low Frequency Array on the Lunar Far Side [2]:

* *The electron density profile above the lunar surface during the day, the night, and the transition in-between.* This is probably the most wanted information as it sets the limit of the lowest possible observing frequency (the plasma frequency). After all, the ionosphere of Earth is what prevents astronomy at very low frequencies. The best data currently available is from the circumlunar plasma research by the Luna 22 spacecraft in the mid-1970s [3]. More reliable measurements, especially at altitudes below about 2km is essential.

* *Electrical permittivity and conductivity (loss tangent) of the lunar regolith at candidate sites; their variation with depth, temperature, and radio frequency.* These electrical properties of the lunar surface critically influence the antenna performance and site selection. The Lunar Sourcebook has data for limited samples [4], but more locally specific measurements are desirable.

* *Subsurface structures at candidate sites.* Dipole antennas on the lunar surface would be sensitive to any reflections from the subsurface structures. Radar sounding is required, but the Apollo Lunar Sounder Experiment was the last one.

* *Detailed topology at candidate sites.* To finalize the observatory site, we should know the topology with 0.5 m vertical resolution and 10 m grid size.

* *Level of terrestrial noise attenuation at various far-side locations.* The main attraction of the Moon is the shielding against the strong interference from Earth. We would like to know how well the terrestrial interference is attenuated on the lunar far side. Only a rough verification has been made so far by the Radio Astronomy Explorer in the 1970s [5].

* *Magnetic fields at candidate sites.* A site with low magnetic field is required.

Proposing Missions: Lunar scientists and astronomers should work together to propose missions that will maximally satisfy the common interests. Lunar locations of greatest interests to astronomers are the south polar regions (including the Malapert mountain) and the major far side craters (including Daedalus, Tsikovsky, and Aitken).

Acknowledgments: I would like to thank Dr Graham Woan for supervising me. I would also like to thank the US-UK Fulbright Commission for the Fulbright Graduate Student Award.

References: [1] Gorgolewski S. (1965) *Astronautica Acta*, 11, 2, 130-131. [2] Very Low Frequency Astronomy Study Team. (1997) *ESA report SCI(97)2*, ESA. [3] Vyshlov A. S. (1976) *Space Research*, XVI, 945-949. [4] Heiken G. et al. (1991) *Cambridge University Press*. [5] Alexander J. K. et al. (1975) *Astronomy & Astrophysics*, 40, 365-371.

LUNAR PROSPECTING. G. Jeffrey Taylor and Linda Martel, Hawai'i Institute of Geophysics and Planetology, University of Hawai'i, 2525 Correa Rd., Honolulu, HI 96822 (gjtaylor@hawaii.edu).

Space resources are essential for space settlement: Large space settlements on the Moon or Mars will require use of indigenous resources to build and maintain the infrastructure and generate products for export. Prospecting for these resources on the Moon is a crucial step in human migration to space and needs to begin before the establishment of industrial complexes. We are devising a multi-faceted approach to prospect for resources that involves planetary research, technology development, human workforce training, and education. Our work builds on previous studies [e.g., 1,2].

Methodology for planetary prospecting:

Economics of planetary ore deposits. We will develop models that define what ore deposits are on other planets. By definition [3], ores are "rocks or minerals that can be mined, processed, and delivered to the marketplace or to technology at a profit." The planetary context tosses in some interesting twists to this definition. First, the costs are compared to getting materials or products from the Earth or another planetary body, a very different case than for terrestrial ores to be used on Earth. Second, we must consider the cost of delivering extraction equipment to the Moon; these costs are much higher than delivering mining equipment to a location on Earth. The cost of extraction equipment becomes less important as a settlement grows, eventually becoming moot when local planetary industry can manufacture all equipment needed. Martian development may depend on lunar resources. For example, the cost effectiveness of extraction of some Martian resources will have to be judged against their production on the Moon and shipment to Mars. This may be particularly pertinent during the early phases of Martian settlement.

Theoretical Assessment of Potential Ore Deposits. A basic framework for understanding how ores form and in what geologic settings they occur guides the search for ore deposits on Earth. This will form the basis of our theoretical study of economic deposits on the Moon and Mars. However, our understanding of the compositions, geological histories, and geological processes on those bodies will lead to significant differences in how we assess extraterrestrial ores. For example, the bone-dry nature of the Moon (except possibly at the poles) eliminates all ore deposits associated with aqueous fluids. On the other hand, ore-forming processes might have operated on the Moon, but not on Earth. For example, solar wind (H, He, C, N) deposited in the lunar regolith may be a crucial resource for lunar oxygen production, agriculture, and ³He production.

Similarly, ice deposits at the poles could be crucial for Martian development. Thus, it will be important to develop a new classification for ore deposits for both the Moon and Mars, beginning with Guilbert and Park's [3] modification (their Table 8-4) of the classic Lindgren [3] classification of ore deposits. Without such a guide, it will be difficult to organize the search for resources on the Moon and Mars.

Search for resources using current lunar data. Prospecting can begin immediately. We have a good collection of remote sensing data for the Moon. In addition, we have a good sampling of the Moon by the Apollo and Luna missions, now supplemented by lunar meteorites. We can target specific types of deposits already identified (e.g. lunar pyroclastics) and look for other geological settings that might have produced ores and other materials of economic value. Another approach we will take is to examine all data available to look for anomalies. Examples are unusual spectral properties, large disagreements between independent techniques that measure the same property, or simply apparent exceptional properties such as elemental abundances much larger than anywhere else in a region.

Developing a strategy for prospecting. We are developing a strategy that represents a comprehensive, integrated program to prospect for resources throughout the solar system. The plan involves a hierarchy of surface exploration techniques. At the base is a huge swarm (thousands to millions) of microrobots equipped with sensors to identify targeted resources (e.g., water ice, phosphorus, rare earths). The tiny robots work in consort with orbiters and sophisticated all-terrain rovers that serve as communication links and make detailed observations at promising locations identified by the microrobots.

Training the planetary economic geologists of the future: Effective and comprehensive resource exploration and prospecting on other planets will require the expertise of specially trained planetary economic geologists. Our plan includes developing a curriculum in planetary economic geology that will include hands-on exploration projects using available data.

References: [1] McKay, M. F. et al. (1992) *Space Resources*. NASA SP-509. [2] Lewis, J. et al. (1993) *Resources of Near-Earth Space*, U. Ariz. Press. [3] Guilbert, J. M. and Park, C. F., Jr. (1986) *The Geology of Ore Deposits*. Freeman, 985 pp. [4] Lindgren, W. (1933) *Mineral Deposits*. McGraw Hill, N.Y., 930 pp.

BULK COMPOSITION OF THE MOON: IMPORTANCE, UNCERTAINTIES, AND WHAT WE NEED TO KNOW. G. Jeffrey Taylor¹, B. Ray Hawke¹, and Paul D. Spudis² ¹Planetary Geosciences, HIGP, Univ. of Hawaii, 2525 Correa Rd., Honolulu, HI 96822 (gjtaylor@hawaii.edu). ²Lunar and Planetary Institute, 3600 Bay Area Blvd., Houston, TX 77058.

Introduction: The bulk composition of the Moon is important to test models for how the Moon formed and to understand how the terrestrial planets accreted. Models of the accretion of the terrestrial planets from a disk of lunar to Mars-sized embryos [1] indicate widespread mixing of the embryos and their fragments, so that each terrestrial planet formed from material originally located throughout the inner solar system (0.5 to 2.5 AU). Such a process would erase any initial radial chemical variations in the compositions of the planetesimals and in the final assembled planets. However, Robinson and Taylor [2] suggest that a distinct compositional gradient remains as shown by the FeO contents of the terrestrial planets: Mercury (3 wt%), Venus and Earth (8 wt%), and Mars (18 wt%). Drake and Righter [3] discuss the unique composition of the Earth and also conclude that planets accreted mostly from narrow feeding zones. Knowing the composition of the Moon will help us understand the full extent of the Earth's accretion zone. We examine what we know about the composition of the Moon, with emphasis on elements that can be determined by remote sensing techniques (FeO, Al₂O₃, and Th).

The Complex Structure and Composition of the Crust: The Clementine and Prospector missions have revolutionized our view of the lunar crust, but numerous uncertainties remain. For example, Jolliff et al. [4] identified several compositionally distinct terranes on the Moon. The compositions of the terranes are reasonably well established, but the volumes they occupy are not known very well. Using their nominal values for volumes and Th contents, and our measurements of FeO and Al₂O₃, we infer that the crust contributes 0.11 ppm Th, 0.6 wt% FeO, and 2.9 wt% Al₂O₃ to the lunar bulk composition. In contrast, we [5-7] have presented a somewhat different view of the crust. We suggest that it is layered with an upper mixed, somewhat mafic zone, underlain by an anorthosite zone, which overlies a more mafic lower crust. Using the volumes given by Taylor et al. [6], but with Jolliff's Procellarum KREEP terrain added as a separate unit, we calculate the following contributions to the lunar bulk composition: Th, 0.14 ppm; FeO, 0.7 wt%; Al₂O₃, 2.7 wt%. Both estimates indicate Th higher than in the nominal primitive terrestrial mantle (0.08 ppm [e.g., 8]). On the other hand, a reinterpretation of the lunar seismic data [9, 10] suggests that the crust might be only 40-50 km thick, much thinner than previous estimates. If correct, this will lower Th and Al₂O₃ in the calculated bulk Moon.

Mantle Composition: We know even less about

the mantle. We can use the compositions of mare basalts to estimate the composition, but there are great uncertainties in Th, because magmas likely assimilated KREEP as they migrated to the surface. One could assume that Th concentrated almost completely in the crust during initial lunar differentiation, leaving essentially none in the mantle, but we do not know if all lunar material participated in the primary differentiation. Experiments on mare basalts suggest derivation from olivine-pyroxene sources with FeO around 18 wt%, which would contribute 16.5 wt% FeO to the lunar bulk composition (if the mantle is 89.8 wt% of the Moon). The experiments also indicate that aluminous phases were exhausted, so Al₂O₃ might have been about 0.4 wt% in the mare basalt source regions. However, as Warren [11] has noted, mare basalts may come from an atypical region of the mantle. More magnesian and feldspathic rocks, such as the parent magmas of the Mg-suite rocks, would come from less FeO-rich (about 7 wt% if the parent was something like the HON composition [12]) and more aluminous (1-2 wt%). If 90% of the mantle was like this composition the lunar bulk FeO would be the same as the terrestrial bulk FeO (8 wt% [e.g., 8]; Al₂O₃ would be about 4 wt%, not too different from Earth (4.4 wt% [8])).

Data Needed: It is essential to determine the detailed structure of the crust and mantle. This requires emplacement of a global seismic network, preferably using a long-lived power source for extended operation over the course of at least 3-5 years. We also need to know the MgO and Al₂O₃ contents of the crust (the values for Al₂O₃ in the crust discussed above are inferred from the FeO content and the well established inverse relationship between FeO and Al₂O₃). This would give us a firmer handle on the abundance and nature of magnesian rocks in the crust. These elements can be measured from orbit with x-ray spectrometry.

References: [1] Wetherill G.W. (1994) *GCA* **58**, 4513-4520. [2] Robinson, M. S. and Taylor, G. J. (2001) *MAPS* **36**, 841-847. [3] Drake, M. J. and Righter, K. (2002) *Nature* **416**, 39-44. [4] Jolliff, B. L. et al. (2000) *J. Geophys. Res.* **105**, 4197-4216. [5] Spudis P.D. et al. (1996) *LPS XXVII*, 1255. [6] Taylor, G. J. et al. (1998) In *Origin of the Earth and Moon*, LPI Contrib. No. 957, 44-45. [7] Hawke, B. R. (2002) *J. Geophys. Res.-Planets*, in press. [8] McDonough, W. F. and Sun, S.-s. (1995) *Chem. Geol.* **120**, 223-253. [9] Khan, A. et al. (2000) *Geophys. Res. Lett.* **27**, 1591-1594. [10] Khan, A. and Mosegaard, K. (2001) *Geophys. Res. Lett.* **28**, 1791-1794. [11] Warren, P. W. (1986) In *Origin of the Moon*, 279-310. [12] Korotev, R. L. (1981) *PLPSC* **12**, 577-605.

ORIGIN OF NANOPHASE Fe^0 IN AGGLUTINATES: A RADICAL NEW CONCEPT

Lawrence A. Taylor (lataylor@utk.edu); Planetary Geosciences Institute, Department of Geological Sciences, University of Tennessee, Knoxville, TN 37996.

Introduction: It has become accepted lore that the myriad of grains of nanophase Fe^0 (abbrev. np Fe^0) in lunar agglutinates are the result of “auto-reduction of impact-melted lunar soil in the presence of solar-wind hydrogen” [1]. However, recent studies have demonstrated other sources of np Fe^0 in lunar soils [2-3], as present in thin patinas (~0.1 μm) on the surfaces of most soil particles [4]. The major portion of this np Fe^0 formed by deposition of vapor produced by abundant micrometeorite impacts, as documented by the presence of multiple and overlapping patinas. It would appear that the presence of np Fe^0 in the vapor-deposited patinas (rims) on virtually all grains of a mature soil [6] provides an additional and abundant source for the greatly increased I_s/FeO values observed as grain size decreases [7], with some of these results having been predicted by Hapke [8].

Agglutinates by Auto-reduction of FeO :

The reaction that supposedly occurs involves in the auto-reduction paradigm is $\text{FeO}_{(l)} + 2\text{H}^+ = \text{Fe}^0 + \text{H}_2\text{O}$. There should be distinct remnants of the water trapped within the glass. Yet, detailed FTIR studies by Taylor et al. [9] failed to detect any traces (>5 ppm) of water in numerous agglutinitic glasses. This observation casts suspicion on the hydrogen auto-reduction theory.

Surface-Related np Fe^0 : The Lunar Soil Characterization Consortium [e.g., 10] has produced hard data on the finest fractions of numerous lunar soils (<45 μm), and have come to the following conclusions: 1) the abundances of agglutinitic glass and the I_s/FeO values increase with decreasing grain size; 2) if the increase in I_s/FeO that is attributable to the increase in agglutinitic glass is accounted for in each change in grain size, the “residual” is the possible surface-correlated I_s/FeO contribution; and

3) on average, there is ~100% increase in I_s/FeO value between the finest two size fractions, with only about 10% increase in agglutinitic glass. These general large increases in I_s/FeO versus nominal increases in agglutinitic glass contents are particularly well demonstrated in the <10 μm [7].

Origin of Agglutinitic Glass: It has been demonstrated conclusively by the research of the LSCC [7] that it is the fusion of the finest fraction [F^3 model; 11] of lunar soil that forms the majority of the agglutinitic glass. But, it is exactly this <10 μm fraction that also contains the vast majority of the surface-correlated np Fe^0 .

A Outrageous Hypothesis: *It is considered entirely possible that most of the np Fe^0 in the “agglutinitic glass” had its ultimate origin as vapor-deposited np Fe^0 in patinas on soil particles, which were subsequently melted and became part of the overall glass component.*

Effectively, as the <10 μm fraction contains the most vapor-deposited np Fe^0 , this is melted and incorporated into impact glass. The average size of the np Fe^0 in this recycled glass (agglutinate) increases. This correlates with the data of Keller et al. [12] and James et al [13], where the average grain size np Fe^0 in “agglutinitic glass” is larger than in vapor-deposited np Fe^0 .

References: [1] Housley *et al.*, 1973, PLSC 4; [2] Keller & McKay, 1993, Science; [3] Keller & McKay, 1997, GCA; [4] Wentworth *et al.*, 1999, MaPS; [5] Bernatowicz *et al.*, 1994, LPSC XXV; [6] Keller *et al.*, 1999, New Views II; [7] Taylor *et al.*, 2001, MaPS; [8] Hapke, B., 2001, JGR-P; [9] Taylor *et al.*, 1995, LPSC XXVI; [10] Taylor *et al.*, 2001, JGR-P; [11] Papike *et al.*, 1981, PLPSC12; [12] Keller *et al.*, 2000, LPSC XXXI; [13] James *et al.*, 2002, LPSC XXXIII; [14] Anand *et al.*, 2002, LPSC XXXIII..

CONTOURED DATA FROM LUNAR PROSPECTOR INDICATE A MAJOR ROLE FOR MINOR SAMPLES. D. T. Vaniman¹, T. H. Prettyman², D. J. Lawrence², R. C. Elphic², and W. C. Feldman². ¹Group EES-6, MS D462 and ²Group NIS-1, MS D466, Los Alamos National Laboratory, Los Alamos, NM 87545.

Introduction: Lunar Prospector (LP) γ -ray data are now available for most major elements to cover the Moon at a resolution of 5°. At this resolution, full lunar coverage is 1790 data points. Although precision and accuracy of LP γ -ray data are still being evaluated, data available show the range and diversity of lunar surface composition at this resolution.

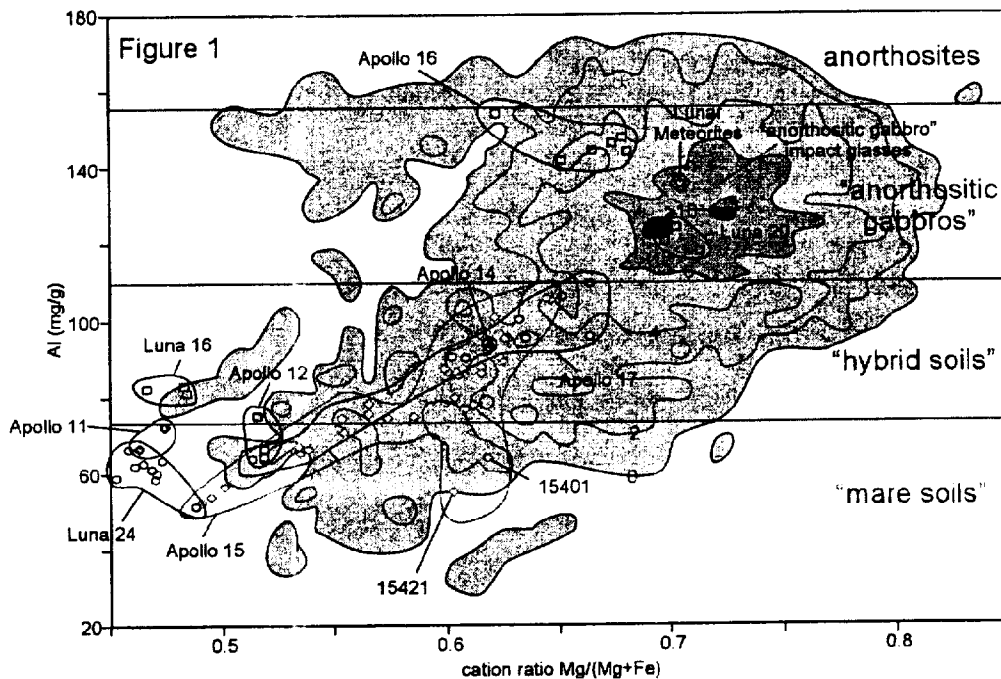
Figure 1 shows LP coverage of the Moon in Al weight abundance and Mg' cation ratio [Mg/(Mg+Fe)]. This figure is based on a plot used to display the compositional range of pristine lunar rocks [1]. Although this plot is typically used only for pristine rocks, we find it useful for regolith data. Colored fields show distribution of LP compositional points in Al-Mg' space as log contours of point density (contours increase in densities of <2, 2, 4, 8, and >16 points within bins of 4 mg/g Al by 0.01 Mg'). Also shown are individual data points and ranges for lunar soils from the literature. Purple horizontal lines mark off regions where soil compositions are anorthositic (>157 mg/g Al, equivalent to >85% An96), more mafic yet KREEP poor (157-110 mg/g Al "anorthositic gabbros"), KREEP-rich mixtures (110-72 mg/g Al "hybrid soils"), and low in Al (<72 mg/g Al "mare soils").

Assessment: Several mare regoliths (Apollo 11, Apollo 15, and Luna 24) are outside the range of Al-

problems in accuracy of LP γ -ray data. However, the greatest concentrations of LP data points are maxima in the range 120-132 mg/g Al and Mg' 0.69-0.74, equivalent to a common composition among regolith impact glasses ("anorthositic gabbro" impact glasses). Overlap with this composition suggests that LP Al-Mg' data are fairly accurate. Discounting inaccuracy, the explanation for lack of LP data points comparable to low-Mg' mare soils may be the absence of such soils in areas big enough to be seen at 5° resolution. Low-Mg' Apollo 15 mare soils, if imaged with soils containing high-Mg' pyroclastic glass (15401, 15421), would produce an intermediate-Mg' composition represented in the LP data. Pyroclastics are not abundant among mare lithologies, but at 5° orbital resolution shallow, widespread pyroclastic deposits may be very important.

Figure 1 also shows a lack of Apollo soil compositions near the most common LP data points (orange and red contours). Closest to this common composition are relatively minor components of the lunar sample suite - Luna 20 regolith and lunar meteorites. As others have noted [2,3], some of these rarer samples may be most relevant to understanding the lunar crust.

References: [1] Warren P. H. (1985) *Ann. Rev. Earth Planet. Sci.*, 90, 201-240. [2] Palme H. et al. (1991) *Geochim. Cosmochim. Acta.*, 55, 3105-3122.



Mg' mapped by LP. In part this mismatch may reflect

[3] Korotev R. (2002) *LPS XXXIII*, #1224.

STUDY TOWARDS HUMAN AIDED CONSTRUCTION OF LARGE LUNAR TELESCOPES.

P. J. van Susante¹, ¹Colorado School of Mines, faculty of Engineering, paulvans@mines.edu / tel. (303)-216-0632

Introduction: On the Moon, unique situations exist for observing the universe. The Polar areas contain permanently shadowed areas, which are among the coldest places in our solar system, within which the infrared background radiation that can disturb measurements is very low. Also disturbances generated on Earth are mostly out of view and thus the measurements can be much more sensitive in all wavelengths.

The South Pole offers a good location for building such an observatory. Clementine mission data indicate That permanently shadowed areas are located within a few kilometers of a areas that are almost permanently lit by the sun. [1] By placing a communication relay on one of the lunar mountains it is also possible to have a communications link for periods in which these shadowed areas can not be seen directly from Earth. The South Polar region of the Moon is also interesting geologically because it is located inside the largest basin on the moon (South Pole - Aitken Basin) as well as the possibility that ice may exist there.

Shackleton Crater is suggested as a site for the placement and construction of the Lunar South Pole Infrared Telescope together with a communication relay lander at Malapert Mountain and another communication relay and energy supply lander at the Peak of Eternal Light, located near the rim of Shackleton.

A near infrared telescope has been designed for emplacement in Shackleton that appears to have the same capabilities as the Next Generation Space Telescope except for sky coverage, which will be limited by the location and orientation. [2] The telescope has a diameter of 8 meters and is an altitude-azimuth design. The bearings will be made of superconducting magnets that use fluxpinning to stabilise themselves while at the same time they are very energy-efficient. [3] The foundation will be dug and constructed in-situ using robots and telepresence together with virtual reality and local laser rangefinders. If all goes well the telescope would have settlement no greater than 0,03 mm during operation. It would be possible for astronauts to maintain, repair and upgrade the telescope much in the same way that the Hubble Space Telescope has been maintained.

When the telescope is built, an infrastructure will also have been created for energy supply and communications that can be used in subsequent missions. The total mission can be achieved by launching 3 Ariane 5 rockets in the year 2006 configuration that can launch 20,000 kg into GTO.

New studies of the construction of even larger telescopes have also been undertaken.. One additional aspect that will be very important is the synergy between humans and robots and their role in transport, construction, operation, maintenance, etc. is addressed in these new studies. Also an attempt will be made to make a parametric cost model for different scenario's as well as the technology readiness levels for the techniques necessary to build a telescope with the capacity of the "planet finder", equivalent up to 1000 m² of photon collecting surface.

Part of the scenario definition and conceptual design of a large lunar telescope has also been done in the lunar base design workshop, held from 10-21 of June at ESTEC, NL. After the conceptual phase there will be a more engineering oriented workshop, which will be held in the concurrent design facility at ESTEC. This paper includes discussion of recent progress on these studies.

References: [1] Kruijff M. (2000) The Peaks of Eternal Light on the Lunar South Pole : How they were found and what they look like, ESA, SP-462, Pp 333-336. [2] Van Susante P.J. (2002) Scenario Description of the construction of a Lunar South Pole Infrared Telescope (LSPIRT), Space 2002 proceedings, ASCE. [3] www.issu.uh.edu/publications/A9798/chu1.htm
www.issu.uh.edu/publications/A9697/9697-5.html

A MANNED LUNAR BASE FOR DETERMINING THE THREE-DIMENSIONAL MAKE-UP OF A LUNAR MARE. J.L. Whitford-Stark, Department of Earth and Physical Sciences, Sul Ross State University, Alpine, TX, 79832. jlwhstark@overland.net

Introduction: I think no one would disagree that the next stage of lunar exploration has to be a manned lunar base. The criteria for its establishment and the missions and professional qualifications of its inhabitants are largely constrained by subjective political and economic considerations. The Apollo and Luna missions demonstrated what could be achieved with thirty year old technology. The communications and miniaturization strides made in the intervening time frame allow for exploration and experimental techniques inconceivable to the earlier mission planners.

Mare Geology: Apart from drill core samples of the lunar regolith, limited seismic and Lunar Sounder data, together with extrapolated information from the distribution of impact crater ejecta we have little idea as to the nature of materials in the vertical dimension. Particularly in the lunar maria where there is a paucity of large post-eruption, completely mare-penetrating impacts. Analysis of earth-based and orbital imagery, together with supplemental information from morphological and crater-counting techniques enabled the creation of a stratigraphy for Oceanus Procellarum (1). The later acquisition of more detailed imagery by the Clementine mission led to a reanalysis (2) of the same area, confirming parts of the original analysis, refining other parts, and presenting alternative explanations for the remainder. The now classic article by Pieters (3) presented a spectral classification scheme for the entirety of lunar maria on the near side of the Moon, however, in spite of its many virtues, it also suffers from being purely two-dimensional. In more or less the same way that a very thin widespread layer of tephra can produce a uniquely definable timeline (employed in the technique of tephrochronology pioneered by Sigurdur Thorarinsson), a very thin layer of lava can totally skew the age and compositional characteristics of a particular mare basin. The only incontrovertible conclusion that can be drawn from such data is that of the age and composition of the youngest material occupying that particular area of the lunar surface. Clearly, to more realistically understand the volumetric compositional and chronological variations within the individual mare it will be necessary to accurately determine the make-up of the third dimension.

Digging Holes: Few, if any, of the lunar samples returned by the Apollo and Luna missions were acquired *in situ*. The closest approach to such a situation was obtained at the edge of Hadley Rille during the Apollo 15 mission where the astronauts were able to observe the layering of the lava flows on the far wall of the rille.

Information concerning the thickness and density variations of inhomogeneous subsurface strata can be obtained via seismic profiling. Apart from superposition relationships, such data provide no information on absolute age nor anything other than bulk chemistry other than whether or not it has the characteristics of basalt. To obtain samples, it is necessary to have a hole, a deep hole. Obviously there are two options; either a natural hole or a man-made hole. The latter is totally unrealistic, barring the application of a thermonuclear device, in and of itself totally unrealistic since it would never get into Earth orbit, let alone to the Moon. Conventional excavation techniques would require equipment far too bulky and labor intensive to make them feasible alternatives, at least for the initial site. This leaves natural holes, of which there are essentially two types, impact craters and rilles. Impact craters have two major drawbacks; there aren't many large ones of post-mare age and the impact event variably alters the radiometric and geochemical characteristics of the impactee.

Ideally, a potential lunar permanent site should have as wide a range of geology as can be sampled within a short distance. The Apollo 15 landing site has many such attributes but a major disadvantage, in the eyes of many, in that it has been already sampled. The Aristarchus Plateau has a number of advantageous characteristics; it is Earth-facing (not essential, but cheaper and more convenient), it has a rille wider and deeper than Hadley, it has lava flows, pyroclastic materials and volcanic edifices, it has a chemistry in places distinct from the surrounding mare, and it has a large young crater. The choice of such a location is not new (e.g., 4) but is logical. A location on the extrapolated rim of the Imbrium basin adds to its merit.

If such samples are obtained, how are they to be analysed; on the spot or returned to Earth on a regular basis? The former would require the transport of sophisticated and robust equipment plus experienced operators.

References:

- [1] Whitford-Stark, J.L. and Head, J.W. (1980) *JGR*, 85, 6579-6609.
- [2] Hiesinger, H. et al. (2000) *LPSC XXXI*.
- [3] Pieters, C.M. (1978) *Proc. Lunar Sci. Conf^{9th}*, 2825-2849.
- [4] Coombs, C.R. et al. (1998) *Proc. 6th Int. Conf. & Expos. on Engin., Construct. & Operations in Space*, 608-615.

REGOLITH THICKNESS, DISTRIBUTION, AND PROCESSES EXAMINED AT SUB-METER RESOLUTION. B. B. Wilcox¹, M. S. Robinson¹, P. C. Thomas², ¹Northwestern University 1847 Sheridan Rd. Evanston, IL 60208, ²Cornell University, Ithaca, NY 14853.

Introduction: We have utilized very high resolution (60-200 cm/p) Lunar Orbiter frames to investigate regolith thickness, distribution, and processes in both mare and highland areas. Previous studies have proposed that the depth to an interface between the regolith and a coherent substrate controls crater interior morphology (Q&O craters) and block distributions in and around host craters [1,2,3]. To test this hypothesis we have mapped the distribution of these key morphologic indicators over mare and highland regions. Our data show that the block populations and Q&O crater populations are generally consistent with this idea. However, we have noted some important deviations, namely that the indicators are irregularly distributed and thus seem to imply a highly variable regolith thickness in a local area. Another important result of our data is the documentation that at small sizes the mare contain greater numbers of craters.

Crater Distribution: To quantify the frequency of blocky craters and Q&O craters and their distribution we identified, mapped, and classified (from most to least blocky) all craters with diameters larger than ~50 m in both mare and highland areas. Our mare study area (~1°S to 4°S, 42°W to 45°W) is contained within the large (~50 km diam) mare flooded crater Flamsteed Ring. From 12 images we identified 549 craters with diameters between 50 and 1400 m (average 124 m) in a total area of 119 km². From 7 highland images we identified 155 craters between 50 and 753 m (average 114 m) in a total area of 48 km².

Q&O populations: Craters showing morphologic evidence of strength discontinuities in the mare are randomly distributed on a local scale and compose ~8% of the population. Wherever these Q&O craters appear, normal-geometry craters as large and larger appear nearby, which begs the question: why aren't all craters of a comparable size in a region Q&O craters? We propose that the flat bottomed and concentric geometry (Q&O) craters degrade relatively quickly to more normal bowl-shaped geometry through impact degradation and seismic shaking over time. Such degradation is consistent with the erosion rate of 5 ± 3 cm/m.y. for loose material [4]. It also explains the commonly observed presence of angular to sub-angular blocks found on degraded craters; blocks erode 20-80x slower (~1 mm/m.y.) [e.g. 5] than loose regolith.

Blocky crater populations: Because blocky craters indicate the presence of a coherent substrate, we find it significant that 68% of mare craters and 97% of high-

land craters have no blocks. Craters with abundant blocks are rare (~1%) in both the highlands and the mare. While these craters cover only 3% of the mare area of study, the craters plus their blocky ejecta (2 crater radii from the center) cover 12% of the area. Blocky craters are rare in number, but they cover a significant fraction of the surface. Thus many of the blocks on the lunar surface have been produced from only a small portion of the total craters. We note that the LO images were selected on the criteria that they had craters with blocks, thus our results represent an upper limit for the distribution of blocky craters. Because of the key role resolution plays in the detection of blocks, our results are limited to the case of ~1 m/p.

Blocky craters were randomly distributed in our area of study, which again brings up the question: why are some craters blocky while other seemingly similar nearby craters are not? Although this indicates heterogeneities in the coherence of the impacted material, the cause of these heterogeneities is not clear. Differences in fragmentation and jointing of the subsurface is one possibility. Cumulative size-frequency slopes for blocks in and around craters in the mare ranged from -2.8 to -5.1; steeper slopes represent more heavily fragmented materials [6]. At this time, with only 7 blocky craters analyzed, the significance of these results is not yet clear.

Crater Frequency: At small sizes (50-1400 m) the mare contain 43% more craters than the highlands in our areas of study (size range 50-200 m there are ~45% more craters in the mare). This can be explained by the fact that the highlands have no near-surface coherent substrate and are thus composed of a thicker layer of regolith allowing these smaller craters to be erased relatively rapidly, possibly enhanced by steeper slopes.

Implications for Other Airless Bodies: The Moon provides the only data comparable to those for asteroid 433 Eros. The complete absence of Q&O craters and the paucity of small craters on Eros are evidence of a thick and mobile regolith. That nearly all of the blocks on the surface of Eros came from one crater and other craters did not produce abundant block populations [7] is consistent with the lunar example. The slopes of cumulative size-frequency histograms for blocks on Eros [7] fall within nearly the same range as the lunar slopes, indicating that fracturing mechanics are similar on different airless bodies, despite gross variations in gravity and impact velocity.

References: [1] Quaide and Oberbeck (1968) *JGR*, 73, 5247-5270. [2] Shoemaker and Morris (1968) *JPL Tech Rept* 32-1265, 86-103. [3] Cintala and McBride (1995) *NASA Tech Memo* 104804, 41pp. [4] Arvidson et al. (1975) *The Moon*, 13, 67-79. [5] Crozaz et al. (1971) *Proc 2nd Lunar Sci Conf*, 2543-2558. [6] Hartmann (1969) *Icarus*, 10, 201-213. [7] Thomas et al. (2001) *Nature*, 413, 394-396.

CURRENT AND FUTURE LUNAR SCIENCE FROM LASER RANGING. J. G. Williams¹, D. H. Boggs¹, J. T. Ratcliff¹, J. O. Dickey¹, and T. W. Murphy², ¹Jet Propulsion Laboratory, California Institute of Technology, Pasadena, CA, 91109 (e-mail James.G.Williams@jpl.nasa.gov), ²University of Washington, Seattle, WA, 98195.

Introduction: The interior properties of the Moon influence lunar tides and rotation. Three-axis rotation and tides are sensed by tracking lunar landers. The Lunar Laser Ranging (LLR) experiment has acquired three decades of accurate ranges from observatories on the Earth to four corner-cube retroreflector arrays on the Moon. Lunar Laser Ranging is reviewed in [1].

Lunar Science Questions: What is the deep interior structure and properties? What are the core properties? Is there an inner core? What causes strong tidal dissipation? What roles did tidal and core dissipation play in the dynamical and thermal evolution? What stimulates free librations?

Moment of Inertia: Analyzing tracking data on orbiting spacecraft gives the second-degree gravity harmonics J_2 and C_{22} . From LLR one obtains the moment of inertia combinations $(C-A)/B$ and $(B-A)/C$. Combining the two sets gives C/MR^2 , the polar moment normalized with the mass M and radius R [2].

Elastic Tides: Elastic tidal displacements are characterized by the lunar (second-degree) Love numbers h_2 and l_2 . Tidal distortion of the second-degree gravity potential and moment of inertia depends on the Love number k_2 . Love numbers depend on the elastic properties of the interior including the deeper zones where the seismic information is weakest. LLR detects tidal displacements [3], but more accurate is the determination of $k_2 = 0.0266 \pm 0.0027$ through rotation [4]. The orbiting spacecraft determination through variation of gravity field is $k_2 = 0.026 \pm 0.003$ [5]. Simple model values of k_2 are lower than both determinations and a partial melt above the core and below the deep moonquakes, previously suspected from the seismic data [6], would improve agreement [4].

Tidal Dissipation: The tidal dissipation Q is a bulk property which depends on the radial distribution of the material Q_s . LLR detects four dissipation terms and infers a weak dependence of tidal Q on frequency [3]. The tidal Q_s are surprisingly low, but LLR does not distinguish the location of the low- Q material. At seismic frequencies low- Q material, suspected of being a partial melt, was found for the zone above the core.

Dissipation at a Liquid-Core/Solid-Mantle Interface: A fluid core does not share the rotation axis of the solid mantle. While the lunar equator precesses, a fluid core can only weakly mimic this motion. The resulting velocity difference at the core-mantle boundary causes a torque and dissipates energy. Several dissipation terms are considered in the LLR analysis in order to separate core and tidal dissipation. Applying Yoder's turbulent boundary layer theory [7] yields 1-sigma upper limits for the core radius of 352 km for molten iron and 374 km for the Fe-FeS eutectic [3].

Inner Core: A solid inner core might exist inside the fluid core. Gravitational interactions between an inner core and the mantle could reveal its presence.

Evolution and Heating: Both tidal and core-mantle dissipation would have significantly heated the Moon when it was closer to the Earth [3,8]. Early dynamical heating could

have approached radiogenic heating helping to promote convection and a dynamo.

Core Ellipticity: A fluid core also exerts torques if the core-mantle boundary (CMB) is elliptical. LLR detection of elliptical effects is marginal. Core ellipticity influences solutions for the Love number and the above k_2 value has a preliminary ellipticity correction.

Free Librations: Lunar free libration modes are subject to damping so the observed amplitudes imply active or geologically recent stimulation [9]. If the mode analogous to Chandler wobble is stimulated by eddies at the CMB [10] then such activity might be revealed as irregularities in the path of polar wobble.

Site Positions: The moon-centered locations of four retroreflectors are known with submeter accuracy [11]. These positions are available as control points for current [12,13] and future networks.

Future: Important time scales for lunar science observations span 1/2 month to decades and continued accurate tracking of multiple lunar retroreflectors will give further results. A ranging system with improved accuracy and sensitivity is being assembled [14] which will improve results. It will allow ranging to single corner-cube reflectors which even small landers could carry. A wider spread of reflector locations would improve the determination of rotation and tides so reflectors on future landers would benefit lunar science.

References: [1] Dickey et al. (1994) *Science*, 265, 482-490. [2] Konopliv A. S. et al. (1998) *Science*, 281, 1476-1480. [3] Williams J G et al. (2001) *J. Geophys. Res. Planets*, 106, 27933-27968. [4] Williams J G et al. (2002) Abs. No. 2033 of *Lunar and Planetary Sci. Conf. XXXIII*. [5] Konopliv A. S. et al. (2001) *Icarus*, 150, 1-18. [6] Nakamura Y. et al. (1974) *Proc. Lunar and Planetary Sci. Conf. 13th*, Part 1, *J. Geophys. Res.*, 87, Suppl., A117-A123. [7] Yoder C. F. (1995) *Icarus*, 117, 250-286. [8] Williams J G et al. (2000) Abs. No. 2018 of *Lunar and Planetary Sci. Conf. XXXI*. [9] Newhall X X, and Williams J G (1997) *Celestial Mechanics and Dynamical Astron.*, 66, 21-30. [10] Yoder C. F. (1981) *Phil. Trans. R. Soc. London A*, 303, 327-338. [11] Williams J G et al. (1996) *Planet. and Space Sci.*, 44, 1077-1080. [12] Davies M E et al. (1994) *J. Geophys. Res.*, 99, 23211-23214. [13] Davies M E and Colvin T R (2000) *J. Geophys. Res.*, 105, 20277-20280. [14] Murphy T W et al. (2002) Proc. of 12th International Workshop on Laser Ranging, Matera, Italy, in press.

GRAND OBSERVATORY. Eric W. Young, NASA Goddard Space Flight Center, Code 551, Greenbelt, MD 20771

Various concepts have been recently presented for a 100 m class astronomical observatory. The science virtues of such an observatory are many: resolving planets orbiting around other stars, resolving the surface features of other stars, extending our temporal reach back toward the beginning (at and before stellar and galactic development), improving on the Next Generation Space Telescope, and other (perhaps as yet) undiscovered purposes. This observatory would be a general facility instrument with wide spectral range from at least the near ultraviolet to the mid infrared. The concept espoused here is based on a practical, modular design located in a place where temperatures remain (and instruments could operate) within several degrees of absolute zero with no shielding or cooling. This location is the bottom of a crater located near the north or south pole of the moon, most probably the South Polar Depression. In such a location the telescope would never see the sun or the earth, hence the profound cold and absence of stray light. The ideal nature of this location is elaborated herein. It is envisioned that this observatory would be assembled and maintained remotely thru the use of expert robotic systems. A base station would be located above the crater rim with (at least occasional) direct line-of-sight access to the earth. Certainly it would be advantageous, but not absolutely essential, to have humans travel to the site to deal with unexpected contingencies. Further, observers and their teams could eventually travel there for extended observational campaigns. Educational activities, in general, could be furthered thru extended human presence. Even recreational visitors and long term habitation might follow.